

Award Number: W81XWH-11-1-0492

TITLE: Protective Role of Ets1 in SLE

PRINCIPAL INVESTIGATOR: I-Cheng Ho

CONTRACTING ORGANIZATION: Brigham and Women's Hospital, Inc.
Boston, MA 02115-6110

REPORT DATE: July 2014

TYPE OF REPORT: Final

PREPARED FOR: U.S. Army Medical Research and Materiel Command
Fort Detrick, Maryland 21702-5012

DISTRIBUTION STATEMENT: Approved for Public Release;
Distribution Unlimited

The views, opinions and/or findings contained in this report are those of the author(s) and should not be construed as an official Department of the Army position, policy or decision unless so designated by other documentation.

REPORT DOCUMENTATION PAGE			<i>Form Approved</i> <i>OMB No. 0704-0188</i>		
Public reporting burden for this collection of information is estimated to average 1 hour per response, including the time for reviewing instructions, searching existing data sources, gathering and maintaining the data needed, and completing and reviewing this collection of information. Send comments regarding this burden estimate or any other aspect of this collection of information, including suggestions for reducing this burden to Department of Defense, Washington Headquarters Services, Directorate for Information Operations and Reports (0704-0188), 1215 Jefferson Davis Highway, Suite 1204, Arlington, VA 22202-4302. Respondents should be aware that notwithstanding any other provision of law, no person shall be subject to any penalty for failing to comply with a collection of information if it does not display a currently valid OMB control number. PLEASE DO NOT RETURN YOUR FORM TO THE ABOVE ADDRESS.					
1. REPORT DATE July 2014		2. REPORT TYPE Final		3. DATES COVERED 1 July 2011 - 30 June 2014	
4. TITLE AND SUBTITLE Protective Role of Ets1 in SLE			5a. CONTRACT NUMBER		
			5b. GRANT NUMBER W81XWH-11-1-0492		
			5c. PROGRAM ELEMENT NUMBER		
6. AUTHOR(S) I-Cheng Ho E-Mail: iho@partners.org			5d. PROJECT NUMBER		
			5e. TASK NUMBER		
			5f. WORK UNIT NUMBER		
7. PERFORMING ORGANIZATION NAME(S) AND ADDRESS(ES) Brigham and Women's Hospital, Inc. Boston, MA 02115-6110			8. PERFORMING ORGANIZATION REPORT NUMBER		
9. SPONSORING / MONITORING AGENCY NAME(S) AND ADDRESS(ES) U.S. Army Medical Research and Materiel Command Fort Detrick, Maryland 21702-5012			10. SPONSOR/MONITOR'S ACRONYM(S)		
			11. SPONSOR/MONITOR'S REPORT NUMBER(S)		
12. DISTRIBUTION / AVAILABILITY STATEMENT Approved for Public Release; Distribution Unlimited					
13. SUPPLEMENTARY NOTES					
14. ABSTRACT Single nucleotide polymorphisms (SNP) at ets1 locus have been shown to increase the risk of SLE. Ets1-deficient mice display a few autoimmune features similar to SLE and their T cells produce an abnormally high level of IL-10 and a low level of IL-2, two features reminiscent of those of T cells of lupus patients. Ets1 directly binds to the il10 gene and recruited histone deacetylase, thereby suppressing the expression of IL-10. In contrast, Ets1 promotes IL-2 expression by an NFAT-dependent mechanism. We further found that the level of Ets1 in peripheral blood was negatively correlated with the level of anti-dsDNA. Our preliminary data suggest that Ets1 acts synergistically with FcγIIbR in counteracting the autoimmune process of SLE. Future direction is to investigate the molecular mechanism mediating the synergistic effect between Ets1 and FcγIIbR.					
15. SUBJECT TERMS Ets1, IL-10, IL-2, Fcgr2b, lupus					
16. SECURITY CLASSIFICATION OF:			17. LIMITATION OF ABSTRACT	18. NUMBER OF PAGES	19a. NAME OF RESPONSIBLE PERSON USAMRMC
a. REPORT U	b. ABSTRACT U	c. THIS PAGE U			19b. TELEPHONE NUMBER (include area code)
			UU	65	

Table of Contents

	<u>Page</u>
Introduction.....	4
Body.....	4-21
Key Research Accomplishments.....	21
Reportable Outcomes.....	22
Conclusion.....	22-23
Personnel.....	23
References.....	24-26
Appendix 1-4	

Introduction

SLE is an autoimmune disease of unknown etiology. Despite the recent advances in the diagnosis of lupus, there is still no effective treatment or cure for this life-threatening disease. The lack of progress in developing new treatments for lupus is mainly due to poor understanding of the autoimmune process of this disease. Recent genome wide association (GWA) studies have identified genetic variations (single nucleotide polymorphism or SNP) in several genes that are associated with an increased risk of lupus. However, how these SNPs influence the function of the lupus-associated genes and how these genes interact with one another are largely unknown. Addressing these two important questions will be the first step toward understanding the pathogenesis of lupus. A genetic variation with the gene *ets1* was recently shown to increase the risk of SLE. The goal of this project is to elucidate the regulatory role of *ets1* in SLE

Body

Ets1 protein, encoded by the *ets1* gene, is the prototype of the ETS family of transcription factors (1). Previous studies have demonstrated that its activity can be regulated by its level, differential phosphorylation, alternative splicing, and nuclear/cytoplasmic translocation. Two independent GWA studies have identified two SNPs (rs6590330 and rs1128334) that are associated with a higher risk of SLE (2, 3). These findings are consistent with the observation that Ets1-deficient (KO) mice spontaneously develop a lupus-like autoimmune disease (4). This phenotype is probably mediated by both Ets1KO B and T cells.

Published data have connected Ets1 with several other lupus-associated genes, including IL-2, IL-10, IL-17, BAFF, and Blimp1, and strongly suggest that Ets1 can counteract the autoimmune process of lupus in several ways. It promotes the expression of IL-2 but inhibits the expression of IL-10 and Th17 differentiation in Th cells. It also keeps Blimp1 in check in B cells, dampening plasma cell differentiation. We postulate that the **Ets1-mediated counteracting mechanism is weakened in lupus patients due to attenuated Ets1 activity and/or the presence of lupus-prone *il10* SNPs** and that **attenuated Ets1 activity can act together with other pathogenic pathways to induce lupus**. The ultimate goal of this project is to test these hypotheses.

This project contains three original specific aims:

Aim 1. Examining the interactions between Ets1 and lupus-prone *il10* SNPs in regulating the expression of IL-10 in Th cells

Aim 2. Investigating the role of Ets1 in human lupus

Aim 3. Investigating the role of Ets1 in animal models of lupus

Each aim is divided into several tasks and we will address our progress in each task. For the purpose of continuity, new progress is highlighted in yellow and added to the progress report of 2013.

Task 1. Examining the interactions between Ets1 and lupus-prone *il10* SNPs in regulating the expression of IL-10 in Th cells

Ia. A composite human IL-10 reporter construct will be generated and examined in Th1 and Th2 cells (Time frame: months 1-12): completed and reported in 2012

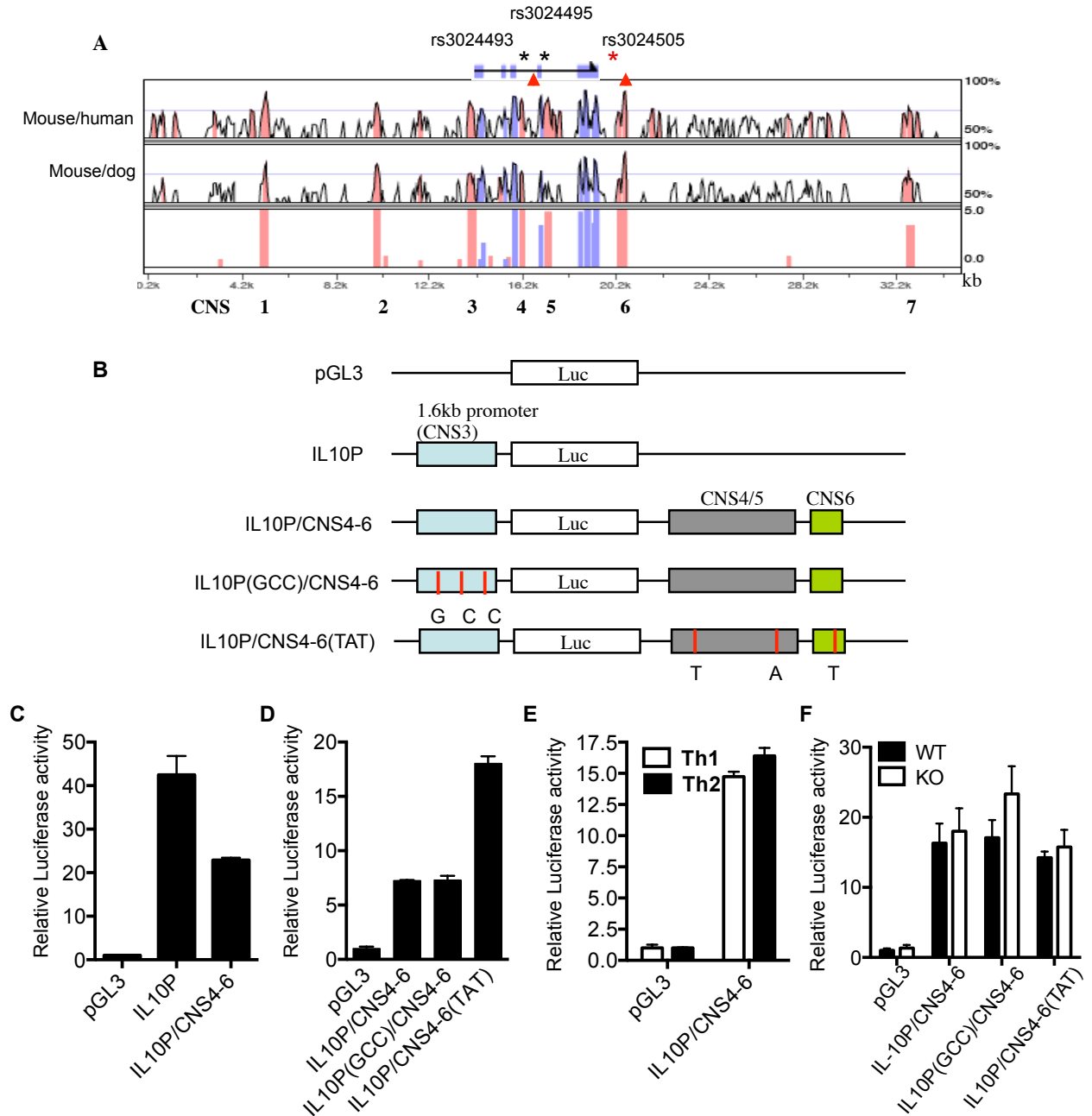


Figure 1. Impacts of SNPs on the activity of IL-10 promoter. **A.** Sequence comparison of the *il10* locus among human, mouse, and dog. The blue columns indicate exons and the pink columns indicate conserved non-coding sequences (CNS), which are numbered. The * indicates SNP and the red arrow heads represent potential Ets1 binding sites. **B.** Schematic diagrams of IL-10 luciferase reporter constructs. The red lines indicate SNPs. The nucleotides of the minor alleles are listed. **C-F.** Bjab cells (**C**), EL4 cells (**D**), primary WT Th1 and Th2 cells (**E**), and WT and Ets1KO Th1 cells (**F**) were transfected with indicated reporters, and stimulated with PMA/ionomycin for 24 hours. Luciferase activity was measured with Dual-Luciferase™ Reporter Assay System (Promega, Madison, WI). The luciferase activity thus obtained was adjusted for transfection efficiency. The adjusted luciferase activity of pGL3 was then arbitrarily set as 1. Data shown are cumulative results of at least three independent experiments.

Human IL-10 gene contains several conserved non-coding sequences (CNS) (Figure 1A). The CNS6

contains a conserved Ets1 binding site and a SNP (rs3024505 C/T) that is associated with a higher risk of SLE. This SNP is tagged with two SNPs (rs3024493 G/T and rs3024495 G/A) located within CNS4 and 5, respectively. In addition, the promoter (CNS3) contains three SNPs (-1087A/G, -819T/C, and -592A/C). The all-minor GCC haplotype of the promoter is supposed to be more potent than other haplotypes and is associated with a higher risk of SLE. We have made several human IL-10 luciferase reporter constructs, which contains the promoter alone (IL10P) or in combination with CNS4+5 and CNS6 (IL10P/CNS4-6, Figure 1B). We first tested the constructs in human Jurkat T cells but got very little activity mainly because Jurkat cells expressed very little IL-10 (data not shown). We then tested the constructs in human Bjab B cells, which do produce IL-10, and found that the activity of IL10P/CNS4-6 was slightly weaker than IL10P (Figure 1C). This was probably due to the large size of IL10P/CNS4-6 plasmid and less robust transfection efficiency. IL10P/CNS4-6 was also active in mouse EL4 T cells (Figure 1D), which also express IL-10, but was not as potent as in Bjab B cells. We then compared the activity of IL10P/CNS4-6 in murine primary Th1 and Th2 cells. Somewhat unexpectedly, we found the activity of IL10P/CNS4-6 was very comparable between Th1 and Th2 cells (Figure 1E). Our data collectively suggest that although IL10P/CNS4-6 reflects the ability of producing IL-10, additional cis-acting elements are probably needed for the preferential expression of IL-10 in Th2 cells compared to Th1 cells.

1b. Mutations corresponding to the lupus-prone SNPs of the il10 gene will be introduced into the composite IL-10 reporter. The impact of these SNPs on the activity of the composite IL-10 reporter will be examined. (Time frame: months 12-24)-completed and reported in 2012

We have examined the effect of two sets of SNP on IL10P/CNS4-6. The first set of SNPs includes -1087A/G, -819T/C, and -592A/C, which are located within the IL-10 promoter. The minor alleles of these three SNPs (G/C/C) were introduced into the wild type IL10P/CNS4-6 reporter through site-directed mutagenesis (Figure 1B). We found that the GCC haplotype, namely IL10P(GCC)/CNS4-6, was as active as wild type reporter in EL4 cells (Figure 1D). The second set of SNP includes rs3024493 G/T, rs3024495 G/A, and rs3024505 C/T. The minor T allele of SNP rs3024505 is associated with a higher risk of SLE and is tagged by rs3024493 and rs3024495. As the minor alleles of these three SNPs are tagged, it is logical to introduce them all together into IL10P/CNS4-6 reporter. We have thus far examined the effect of these three minor alleles on the activity of IL10P/CNS4-6 reporter in EL4 cells and found that the all-minor TAT version, namely IL10P/CNS4-6(TAT), was almost twice more active than the wild type version (Figure 1D), suggesting that these three SNPs can modulate the expression of IL-10.

1c. Th cells will be purified from control or Ets-1-deficient mice with Miltenyi magnetic beads or through cell sorting at our Cell Sorting Core. The purified Th cells will be activated in vitro. (Time frame: months 1-12)-completed and reported in 2012

We have established this task as a routine procedure according to a published protocol (5). We routinely started with 1-2 Ets1KO mice and an equal number of control mice. Approximately 10-12 millions Th cells were obtained from each mouse. The purified Th cells were activated in vitro under Th1 polarizing conditions. The phenotype of differentiated Th1 cells was confirmed by the production of cytokines, which were measured with ELISA or intracellular staining. The result of a representative experiment was shown in Figure 3 of the original grant application and will not be shown here again.

1d. The activated Th cells will be subjected to chromatin immunoprecipitation (ChIP) with Ets1 antibody to identify potential Ets1 binding site in the IL-10 locus (Time frame: months 1-12)-completed and reported in 2012

We have used rVista 2.0 program to search for conserved Ets1 binding site within the *il10* locus and identified two potential sites: one located within CNS4/5 and one within CNS6 (Figure 1A). We found no conserved Ets1 site within the promoter of the *il10* gene. We have performed chromatin immunoprecipitation with anti-Ets1 antibody on murine primary Th cells according to a published protocol (reference 5) to examine in vivo recruitment of Ets1 to the two putative Ets1 bindings sites. We found that Ets1 was recruited to CNS6 of the *il10* gene as strongly as to a known Ets1 binding site within the CD127 gene (Figure 2). In contrast, we detected no recruitment of Ets1 to CNS4/5, which also contains a putative Ets1 binding site.

1e. DNase I hypersensitivity assay and ChIP with anti-acetylated H3 and H4 will be performed in wild type and Ets1-deficient Th cells to characterize the epigenetic landscape of the IL-10 locus in the presence or absence of Ets1. (Time frame: month 12-24)-completed and reported in 2012

We have collaborated with Dr. Sin-Hyeog Im in examining the epigenetic landscape of the IL-10 locus in both wild type and Ets1KO Th cells. We performed chromatin immunoprecipitation with anti-acetylated histone 3 (H3Ac), a mark of active transcription. We found that acetylated histones were recruited to the promoter (CNS3) and CNS4/5, but not CNS6, in wild type Th2 but not Th1 cells, a finding consistent with the fact that IL-10 is actively expressed in Th2 cells. Interestingly, Ets1KO Th1 cells actually display a pattern of H3Ac recruitment almost identical to that of wild type Th2 cells. This finding was recently published in *The Journal of Immunology* (Figure 3A and 3B of appendix 1). This collaborative effort also demonstrated that Ets1 recruited HDAC1 to the *il10* locus, thereby suppressing the transcription of IL-10.

1f. The function of putative Ets1 binding site or Ets1 response element in the context of the composite IL-10 reporter will be examined. (Time frame: months 12-24)-completed and reported in 2013

We have compared the activity of IL10P/CNS4-6, IL10P(GCC)/CNS4-6, and IL10P/CNS4-6(TAT) in wild type primary Th1 cells. Although IL10P/CNS4-6(TAT) was more active than the other two reporters in EL4 cells, we detected no significant difference among these three reporters in primary Th1 cells (Figure 1F).

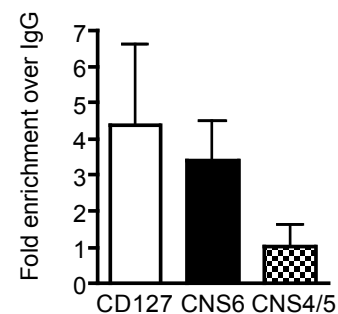


Figure 2. Ets1 is recruited to the CNS6 of the *il10* locus. Primary mouse Th1 cells were subjected to chromatin immunoprecipitation with anti-Ets1 or control IgG. The precipitated chromatin was subjected to real-time PCR using primers targeting a known Ets1 binding site within the CD127 promoter and potential Ets1 binding sites within CNS6 and CNS4/5 of the *il10* gene. The fold enrichment with anti-Ets1 over control IgG was calculated. The mean and range of triplicate from one of two independent experiments were shown.

1g. The interaction between *Ets1* and the lupus-prone SNP of the *IL-10* gene in the context of the composite *IL-10* reporter will be examined. (Time frame: months 12-24)-completed and reported in 2013

We also compared the activity of IL10P/CNS4-6, IL10P(GCC)/CNS4-6, and IL10P/CNS4-6(TAT) between WT and *Ets1*KO Th1 cells. We saw no difference between WT and *Ets1*KO Th1 cells (Figure 1F). Taken all together, our data suggest that all the SNPs included in our reporters had very little impact on the transcription of *IL-10* gene in primary Th1 cells. In addition, the suppressive effect of *Ets1* on the expression of *IL-10* most likely is not mediated by these SNPs.

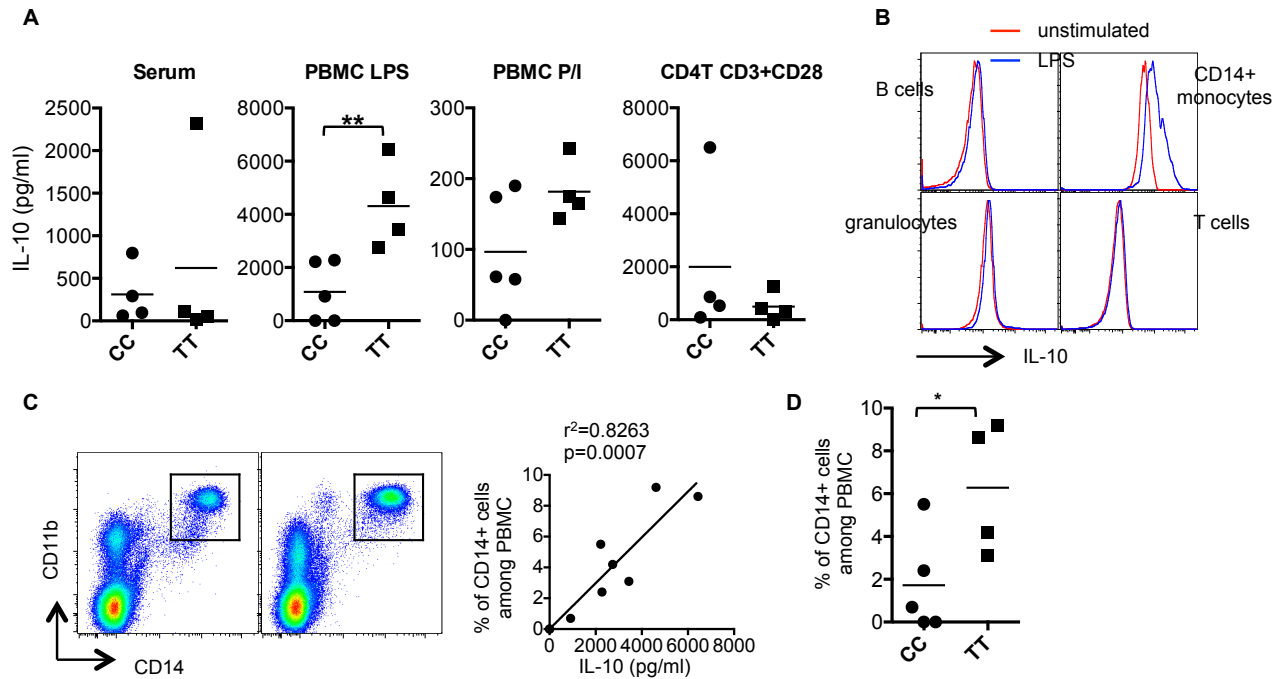


Figure 3. The minor T allele of rs3024505 is associated with heightened production of IL-10 by PBMC in response to LPS and a higher percentage of CD14+CD11b+ monocytes among PBMC. **A.** Serum, PBMC, and CD4+Th cells were harvested from 4 healthy donors who are homozygous for the T allele of rs3024505 and 5 healthy age and gender matched donors homozygous for the C allele. PBMC were stimulated with LPS and PMA/ionomycin, and CD4+T cells were stimulated with anti-CD3/anti-CD28. The level of IL-10 in serum or supernatant of stimulated PBMC and CD4+T cells were quantified with ELISA. **B.** Intracellular IL-10 staining was performed on the LPS-stimulated PBMC. Histograms of IL-10 of indicated population were overlaid with those of corresponding un-stimulated populations. **C.** Peripheral blood monocytes were identified as CD14+CD11b+ cells. Representative FACS plots from one CC and one TT donor are shown in the left panel. The level of IL-10 produced by PBMC in response to LPS was plotted against the percentage of CD14+ monocytes among PBMC of corresponding donors. Statistical analysis was performed with linear regression. **D.** The percentage of CD14+ monocytes among PBMC of 4 TT and 5 CC donors are shown. Statistical analysis was performed with Student's t test.

New development since the 2013 report

To further elucidate the role of rs3024505 in the regulation of *IL-10* expression, we obtain blood samples from five healthy donors, who are homozygous for the protective C allele of the SNP, and four age- and gender-matched healthy donors, who are homozygous for the risk T allele. We found that serum *IL-10* level was comparable between these two groups (Figure 3A). However, PBMC from the TT donors produced more *IL-10* in response to LPS stimulation. A similar trend was observed in PMA/ionomycin-stimulated PBMC. Interestingly, we detected no difference in *IL-10* production in T

cells stimulated with anti-CD3/anti-CD28. We subsequently performed intracellular IL-10 staining and found that CD14⁺ monocytes but not B cells, T cells, or granulocytes were the main source of LPS-induced IL-10 (Figure 3B). In addition, the level of LPS-induced IL-10 was positively correlated with the percentage of CD11b⁺CD14⁺ monocytes among PBMC (Figure 3C). Thus, TT donors as a group had a higher percentage of CD14⁺ monocytes than CC donors (Figure 3D). This unexpected but intriguing result suggests that rs3024505 is associated with the percentage of CD14⁺ monocytes in PBMC. Additional funding will be needed to confirm this association and to investigate its molecular mechanism.

Research activities related to Aim 1

In addition to over-producing of IL-10, Th cells of lupus patients also express a low level of IL-2 (6, 7), a feature also seen in Ets1KO Th1 cells. Understanding how Ets1 promotes the expression of IL-2 will shed light on the mechanism of action of Ets1 and the pathogenesis of SLE. Ets1 is known to suppress the differentiation of plasma cells by counteracting the activity of Blimp1 (8), a transcription factor that is also associated with SLE. Blimp1 is known to promote IL-10 but suppress IL-2 production in Th cells (9-11). These observations raise the possibility that Ets-1 indirectly regulates the expression of IL-10 and IL-2 by suppressing the activity or expression of Blimp1. We have tested this hypothesis and made the following exciting findings.

1. Ets1 is also required for the expression of IL-2 in human primary Th cells.
2. Ets1 indeed suppresses the expression of Blimp1 in Th1 cells but not vice versa.
3. However, Th1 cells deficient in both Ets1 and Blimp1 still express an abnormally high level of IL-10 and a low level of IL-2, indicating that Ets1 regulates the expression of IL-10 and IL-2 in a Blimp1-independent manner.
4. Instead, Ets1 acts synergistically with NFAT in transactivating the IL-2 gene.
5. Ets1 is present in both the nucleus and cytoplasm of resting Th cells. Nuclear Ets1 is quickly translocated to the cytoplasm in response to calcium signals. The nuclear exit of Ets1 follows a kinetics different from that of nuclear entry of NFAT.
6. Cytoplasmic Ets1 physically interacts with NRON complex, which traps NFAT in the cytoplasm in resting Th cells (12, 13).
7. Deficiency of Ets1 attenuates the nuclear entry of NFAT proteins and their recruitment to the IL-2 promoter.

A manuscript describing these results has been published in *The Proceedings of National Academy of Sciences* (2013, 110:15776) and is attached as appendix 2.

Original Task 2. Investigating the role of Ets1 in human lupus

Revision of Aim 2

While we were recruiting new lupus patients for tasks 2a-2c and designing experiments to understand the molecular mechanism mediating the negative correlation between the level of Ets1 and anti-dsDNA, a paper was published confirming our data shown in Figure 5B and 5C (14). This paper further suggests that DNA-containing immune complexes induce the expression of micro-RNA155 through the TLR4-Myd88 pathway. This induction of micro-RNA also requires the presence of HMGB1 (high mobility group box1) with the immune complexes. Micro-RNA155 once induced then targets Ets1, resulting in a reduction in the level of Ets1. As this paper demonstrated what we set out to test in the original Task 2, we were given the permission by DOD to revise Aim 2, which will be described latter.

2a. PBMC, Th, and B cells will be purified from peripheral blood of SLE patients with Miltenyi magnetic beads or through a cell sorter at our Cell Sorting Core based on pre-selected surface markers. (Time frame: months 1-30)-**incomplete due to the revision of Task 2 described above**

2b. cDNA, nuclear and cytoplasmic protein extract will be harvested from the purified PBMC, Th and B cells. (Time frame: months 1-30): **not started due to the revision of Task 2 described above**

2c. Real-time PCR will be performed to quantify the transcript level of *Ets1*, IL-10, IL-17, and BAFF in Th and B cells. Cytoplasmic and nuclear protein extract will be subjected to Western analysis using *Ets1*-specific antibodies. (Time frame: month 1-30)-**not started due the revision of Task 2 described above**

2d. ELISA will be perform to quantify the level of IL-10, IL-17, and BAFF in serum or supernatant of cultured cells. (Time frame: 1-30 months)-**completed and reported in 2013**

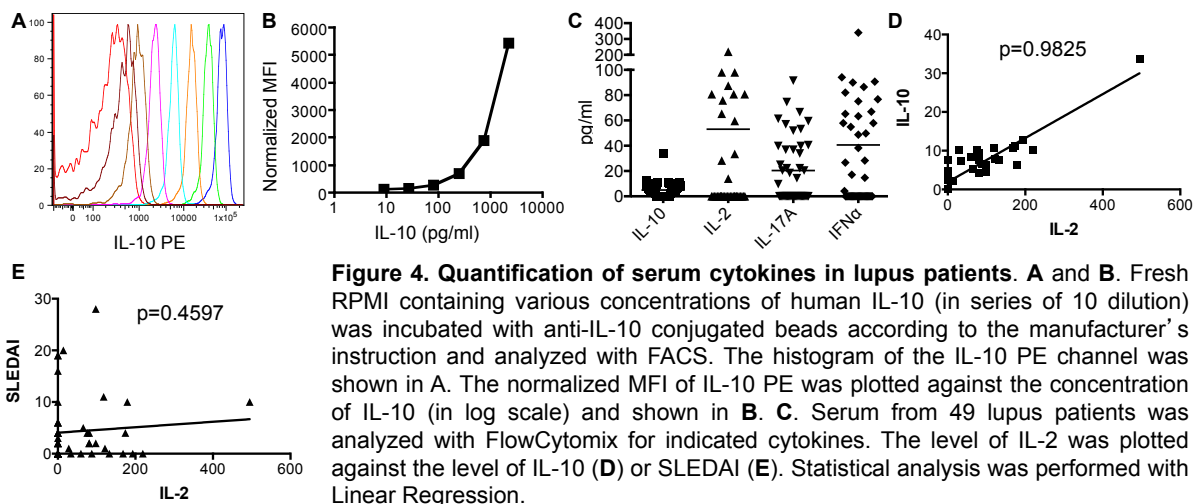


Figure 4. Quantification of serum cytokines in lupus patients. **A** and **B**. Fresh RPMI containing various concentrations of human IL-10 (in series of 10 dilution) was incubated with anti-IL-10 conjugated beads according to the manufacturer's instruction and analyzed with FACS. The histogram of the IL-10 PE channel was shown in **A**. The normalized MFI of IL-10 PE was plotted against the concentration of IL-10 (in log scale) and shown in **B**. **C**. Serum from 49 lupus patients was analyzed with FlowCytomix for indicated cytokines. The level of IL-2 was plotted against the level of IL-10 (**D**) or SLEDAI (**E**). Statistical analysis was performed with Linear Regression.

Although we are unable to obtain PBMC from lupus patients, we were able to measure cytokines in the serum received from BWH Lupus Biobank. We chose to use FlowCytomix™ of eBioscience, which allows us to quantify the level of several cytokines in a small volume of serum. An example of standardization of IL-10 was shown in Figure 4A and 4B. We have thus far examined serum of 49 lupus patients. The demographic characteristics of study subjects are shown in Table 1. Overall, the level of cytokines including IL-10, IL-2, IL-17A, and IFN α was low and was detectable in only a half of the samples (Figure 4C). There was no reverse correlation between IL-2 and IL-10 or IL-17A (Figure 4D), a pattern different from what one would expect from *Ets1* deficiency. In addition, there was no correlation between the level of any of the cytokines and various parameters of SLE activity including SLEDAI, SLICC, ANA level, and dsDNA level (Figure 4E and data not shown). Our results suggest that the abnormal cytokine profile seen in SLE patients is not solely due to *Ets1* deficiency. However, we felt that the levels of various cytokines in serum were too low to be reliably detected and that this approach was unlikely to yield a conclusive result. We therefore decided not to pursue this approach further.

2e. Medical records of lupus patients expressing normal or abnormal levels of *Ets1* will be reviewed and statistical analyses will be performed to identify clinical features that are associated with abnormal levels of *Ets1*. (Time frame: months 30-36)-**incomplete due to the revision of Task 2 described above**

Table 1: Demographic characteristics of study subjects

	Healthy	SLE
Number and gender	15 F	53 F and 2 M
Age (years)	46.2 ± 5.2	48.8 ± 12.5
Ethnicity	9 Caucasians, 4 African Americas, 1 Asians, and 1 Asian/Caucasian	42 Caucasians, 4 blacks, 4 Asians, and 5 Hispanics

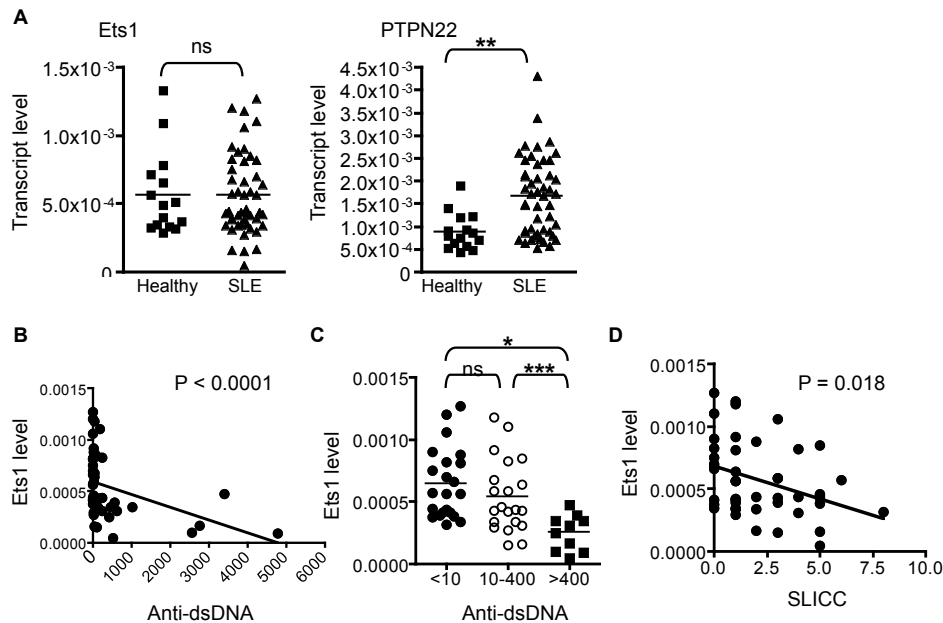


Figure 5. The level of Ets1 in peripheral blood negatively correlates with the level of anti-dsDNA in lupus. **A.** The transcript levels of Ets1 and PTPN22 in peripheral blood of lupus patients (N=55) and healthy donor (N=15) were measured with real time PCR. The transcript level thus obtained was normalized against that of actin from the same sample. Statistical analysis was performed with Student's t test (**p < 0.005; ns not significant). **B.** Correlation between Ets1 and anti-dsDNA in lupus patients was calculated with non-parametric Spearman test. **C.** The lupus patients were divided into three groups based on the level of anti-dsDNA and their levels of Ets1 were compared with One-Way ANOVA test followed by Tukey's Multiple Comparison test (*p<0.05; ***p<0.0001) **D.** Correlation between Ets1 and SLICC score was calculated with non-parametric Spearman test.

Lupus Biobank has also stored peripheral blood in PaxGene tubes, which are designed to preserve RNA of peripheral blood for long periods of time. We found that the RNA thus purified from the PaxGene tubes of Lupus Biobank was of good quality, enabling us to quantify the transcript level of Ets1 in peripheral blood of lupus patients. We have measured the Ets1 level in peripheral blood of 55 lupus patients and reviewed their clinical features, which were provided by the BHW Lupus Biobank. We also simultaneously measured the transcript level of PTPN22, which was used as a control gene. PTPN22 was chosen because a SNP located at position 1858 of its cDNA is also associated with a higher risk of SLE (15, 16). Lupus Biobank does not have blood samples from healthy donors. We therefore obtained peripheral blood of 15 age- and gender-matched healthy donors recruited from BWH PhenoGenetic project, and measured the transcript level of Ets1 and PTPN22 in their peripheral blood. The

demographic characteristics of healthy and lupus population were shown in Table 1. We have made two very interesting findings.

1. We found that the level of Ets1 in peripheral blood was very comparable between healthy donors and lupus patients, however the level of PTPN22 was 2-3 higher in lupus group than in healthy group (Figure 5A). **A manuscript describing this interesting finding has been published and is attached as appendix 3.**
2. We found a strong but reverse correlation between the level of Ets1, but not PTPN22, and the titer of anti-double stranded DNA (dsDNA) (Figure 5B and 5C). There was also a modest reverse correlation between Ets1 level and Systemic Lupus International Collaborative Clinics damage index (SLICC) (Figure 5D). In contrast, we found no correlation of Ets1 level with SLEDAI, level of ANA, or age (data not shown). Although the sample size was still small, the p value for the negative correlation between Ets1 level and anti-dsDNA was very significant ($p < 0.0001$).

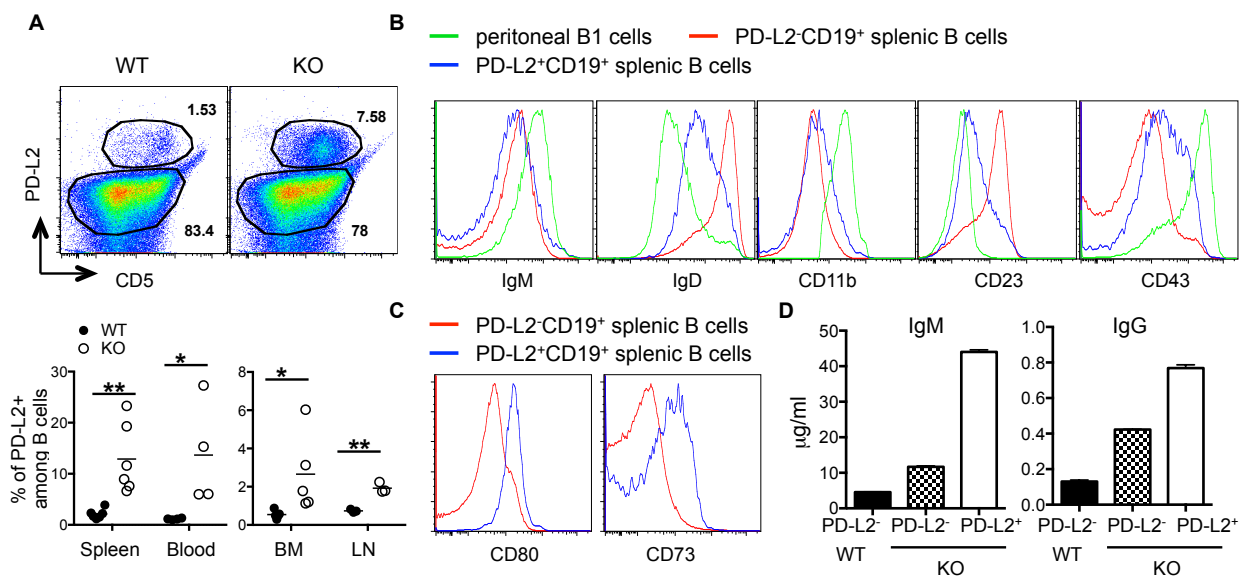


Figure 6. Ets1 regulates the homeostasis of PD-L2⁺ memory B cells. **A.** Splenic CD19⁺ B cells of WT and Ets1KO mice were analyzed for the expression of CD5 and PD-L2. **B.** The percentages of PD-L2⁺ cells among CD19⁺ B cells in indicated organs of WT and Ets1KO mice were enumerated. Each circle represents one mouse. BM and LN stand for bone marrow and lymph node, respectively. **C** and **D.** Ets1KO PD-L2⁺ and PD-L2⁻ B cells gated in **A** were analyzed for their expression of indicated surface markers. WT peritoneal B1 cells were also included in **C** for comparison. **E.** WT PD-L2⁻ B cells and Ets1KO PD-L2⁻ and PD-L2⁺ B cells were stimulated with for 6 days. The level of IgM and IgG in supernatant was quantified with ELISA. The data shown are the average and range of two experiments.

Revised Task 2. Determining whether the abnormal expansion of memory B cells in Ets1KO mice is a cell-autonomous phenomenon

Revised 2a. Memory and naive B cells in WT mice will be identified based on the expression of PD-L2, CD80, and CD73. (Time frame: months 20-24)-completed and reported in 2013

Ets1KO mice have an increase in the number of PD-L2⁺ B cells in their spleens, lymph nodes, bone marrow, and peripheral blood (Figure 6A). A recent publication suggests that murine PD-L2⁺ B1 cells preferentially produce anti-dsDNA (17). This unique population of B cells is expanded in lupus mice. Although human counterparts of PD-L2⁺ B1 cells have yet to be identified, we postulate that expansion of equivalents of PD-L2⁺ B1 cells caused by Ets1 deficiency is the reason why the level of Ets1 is negatively correlated with the level of anti-dsDNA (Figure 5B and 5C). We therefore set to determine

the identity and function of the PD-L2⁺ B cells seen in Ets1KO mice. Although the PD-L2⁺ B cells also express a medium level of CD5, they are negative for CD11b, IgM, and CD43, a profile not consistent with that of classical B1 cells (Figure 6B). They also have a relative low level of CD23 and surface IgD compared to PD-L2⁻ B2 cells, most of which are naive B cells. Instead, they express CD80 and CD73 (Figure 6C), a phenotype bearing striking similarity to that of memory B cells (18). In addition, the Ets1KO PD-L2⁺ B cells produced a higher level of anti-dsDNA in response to stimulation compared to Ets1KO or WT PD-L2⁻ B2 cells (Figure 6D), a feature consistent with that of memory B cells. Murine memory B cells are usually present in a very low number even after immunization, and very little is known regarding the transcription factors regulating their homeostasis. Our data strongly suggests that Ets1 negatively regulates the homeostasis of memory B cells. The expansion of PD-L2⁺ B cells is not observed in FF/CD19cre (data not shown), indicating that PNT domain of Ets1 is not required to regulate the homeostasis of memory B cells.

Revised 2b. The number of memory B cells in WT and Ets1KO young (3 weeks of age) and adult (6-8 weeks of age) mice will be quantified. (Time frame: months 24-36)-completed

We found that 3-week-old WT and Ets1KO mice contained very few PD-L2⁺ B cells in their spleens. This population of B cells slowly expanded along with age in WT mice (Figure 7A). In contrast, the PD-L2⁺ B cells rapidly expanded in Ets1KO mice and reached a peak of approximately 15-25% of splenic B cells 12-15 weeks after birth. Although the percentage of splenic PD-L2⁺ B cells in Ets1KO mice remained unchanged after week 15, their number continued to increase due to splenomegaly. Thus the absolute number of splenic PD-L2⁺ B cells of 34-week-old Ets1KO mice was much higher than that of 15-week-old mice (Figure 7B).

Revised 2c. Naive B cells will be sorted from WT and Ets1KO mice and then adoptively transfer to Ets1KO and WT mice, respectively. Three weeks after the transfer, donor cells will be harvested and their expression of memory markers will be examined with FACS. (Time frame: months 24-36)-completed

We have transferred naive (PD-L2⁻) B cells

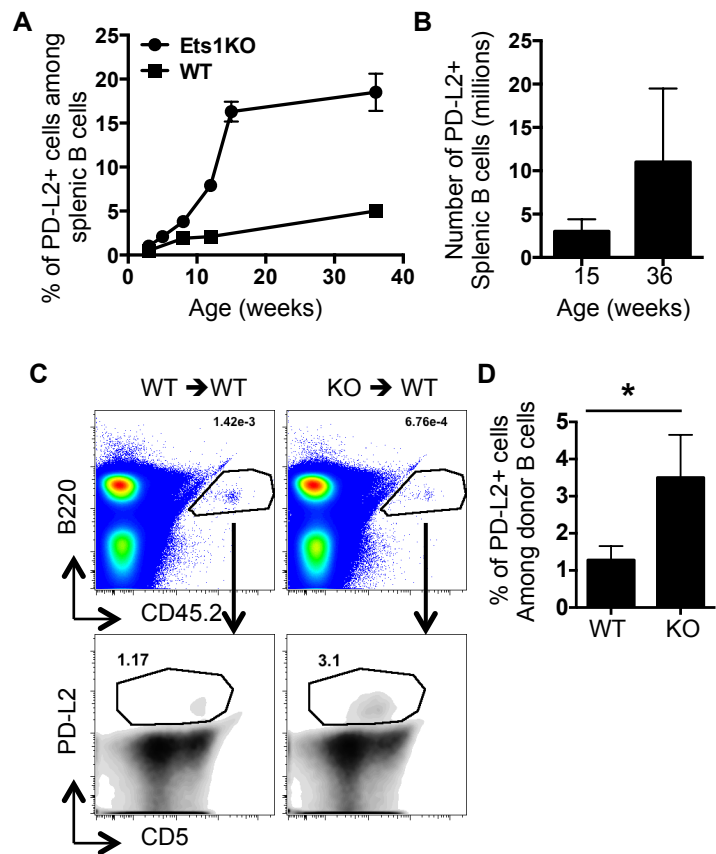


Figure 7. Cell-intrinsic expansion of PD-L2⁺ B cells in Ets1KO mice. A&B. Splenic PD-L2⁺ B cells were identified with FACS in WT and Ets1KO mice of indicated ages. Their percentage among splenic B cells was calculated and is shown in A. The absolute numbers of PD-L2⁺ splenic B cells from 15-week-old and 36-week-old Ets1KO mice are shown in B. C & D. Two millions of WT and Ets1KO PD-L2⁻ B cells were sorted and transferred into congenic CD45.1⁺ WT mice. Three weeks after the transfer, donor cells in host spleens were identified and their expression of PD-L2 and CD5 was examined with FACS. Representative FACS plots are shown in C and the percentage of PD-L2⁺ cells among donor B cells from three pairs of mice are shown in D.

from WT and Ets1KO mice into congenic WT mice. Approximately 1% of WT donor B cells became positive for PD-L2, whereas 3% of Ets1KO donor B cells expressed PD-L2. (Figure 7C and 7D). Ets1KO mice were born in a very low frequency (one KO mice in 3 litters from Ets1Het x Ets1KO mating), and we were not able to obtain an enough number of Ets1KO mice to serve as hosts of WT naive B cells. Regardless, our results strongly suggest that the abnormal homeostasis of memory B cells in the absence of Ets1 is mediated by a cell-intrinsic mechanism. In order to identify the target genes of Ets1 that regulate the homeostasis of memory B cells, we have performed in silico gene expression analyses, which will be described in Task 3b.

Task 3. Investigating the role of Ets1 in animal models of lupus

This task requires 20 mice from the following strains: FF/CD4cre, FF/CD19Cre, FF/LysCre, Ets1-deficient, Ets1-deficient/ FcγIIbR^{+/−}, Ets1-deficient/ FcγIIbR^{−/−}, FcγIIbR^{−/−}, and wild type C57BL/6.

3a. The following mouse strains will be created: FF/CD4Cre, FF/CD19Cre, FF/LysCre (Time frame: months 1-12)-completed and reported in 2013

We have created these strains of mice, which are at N12 C57BL/6 background.

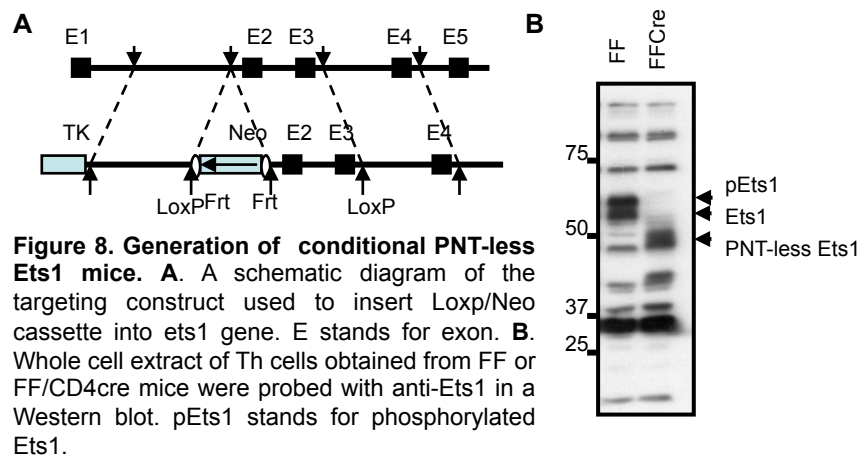
3b. The phenotype of FF/CD4Cre, FF/CD19Cre, and FF/LysCre will be characterized. (Time frame: months 12-24)-completed and reported in 2013, **new update**

We have made significant progress in this task. The floxed Ets1 allele contains two loxp site flanking exon 2 and 3 (Figure 8A). When the exon 2 and 3 was deleted with the CD4cre transgene, we saw no detectable full length Ets1 protein. However, a new protein with a molecular weight of 50 kD was detected with anti-Ets1 antibody in T cells of FF/CD4cre mice (Figure 8B).

We subsequently confirmed that this new protein was a truncated Ets1 protein missing the Pointed (PNT) domain, which is encoded by exon 2 and 3. It is the product of an in-frame splicing between exon 1 and 4. We have since called this truncated protein PNT-less Ets1. This result, albeit unexpected, actually provided us with a great opportunity to investigate PNT domain dependent and independent function of Ets1. We have made the following discoveries.

1. FF/CD4cre and FF/CD19cre mice were born at an expected frequency and grossly healthy up to 6 months after birth.

2. Although Ets1KO (germline Ets1-deficient) mice have a defect in thymocyte development and lacks NKT cells (19-21), FF/CD4cre have normal thymocyte development and a normal number of NKT cells (Figure 9A and 9B). These data indicate that the PNT domain is not required for the development of thymocytes and NKT cells.



3. The PNT domain is also required for normal production of Th cytokines including IL-2 and IL-10. In addition, FF/CD4cre Th17 cells still produce IL-17A and IL-17F as high as or even higher than Ets1KO Th17 cells (Figure 9C).

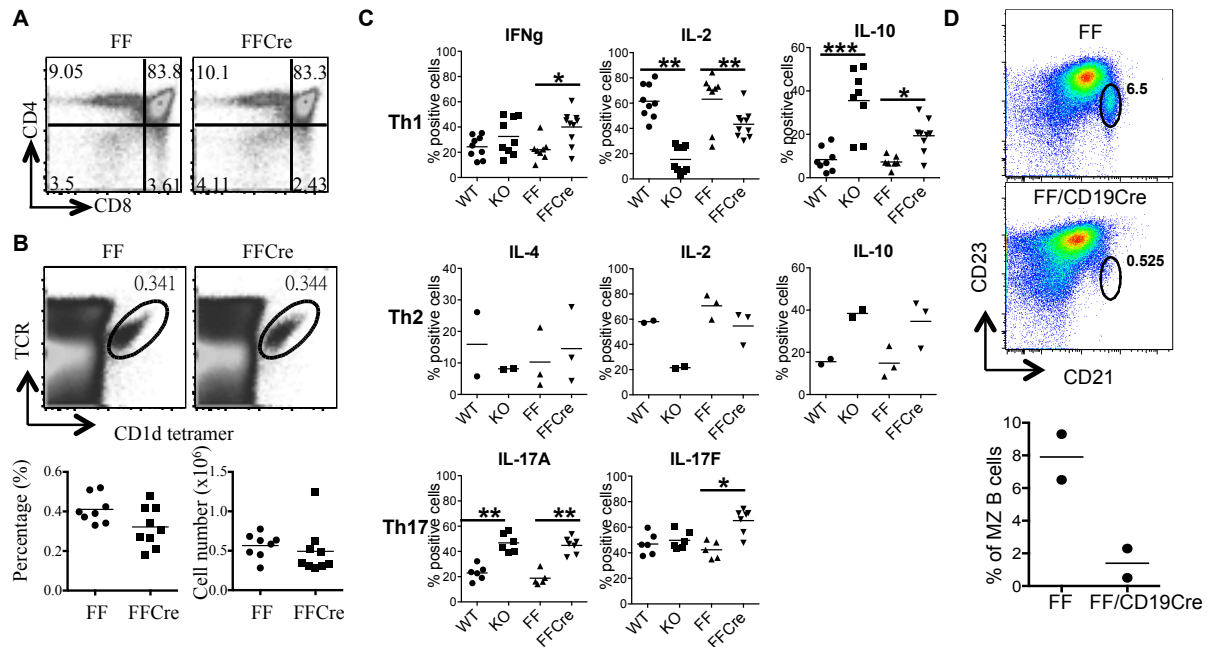


Figure 9. PNT domain-dependent and independent function of Ets1. **A.** Thymocytes from FF and FF/CD4cre (FFCre) mice were analyzed for their expression of CD4 and CD8. **B.** NKT cells of FF and FFCre mice were identified with TCR and CD1d tetramer. Representative FACS plots are shown in the top panels. The percentages and absolute number of NKT cells in the thymus of 8 FF and 9 FFCre mice are shown. **C.** Th cells from WT, Ets1KO, FF, FFCre mice were differentiated into Th1, Th2, and Th17 cells in vitro, and restimulated with PMA/ionomycin. The expression of indicated cytokines was examined with intracellular cytokine staining. Each symbol represents one mouse. **D.** Splenic B220+ cells of FF and FF/CD19cre mice were analyzed for their expression of CD21 and CD23. Representative FACS plots are shown in the top two panel. Cumulative results from two experiments are shown in the bottom panel.

4. Despite our results, the downstream genes mediating the effect of Ets1 are largely unknown. We believe that identification of Ets1 target genes will greatly advance our understanding of the mechanism of action of Ets1 and the pathogenesis of SLE. However, the budget agreement of this grant does not allow us to perform extensive gene chip analysis. We therefore carried out in silico gene expression analyses. One striking feature of Ets1 deficiency in T cells is virtual absence of NKT cells (21). As Ets1 very likely regulates the same genes in NKT cells and conventional T cells, we used the Population Comparison tool in Immgen (<http://www.immgen.org>) to identify genes that are up-regulated during the transition from pre-selected DP thymocytes to NKT cells. Among 1000 genes thus identified, we searched for genes that are bound by Ets1 within 500 bp of their transcriptional start site according to an Ets1 ChIP-seq database generated from Jurkat T cells (22). We further narrowed down the list by using rVista program (<http://rvista.dcode.org>) to look for genes that contain conserved ETS binding sites within their promoters. This sequence of analyses yields 55 genes (Figure 10A and appendix 4). We were able to confirm the differential expression between WT and Ets1KO thymocytes in 4 of 5 randomly selected genes including *cxcr3*, *dusp2*, *gmfg*, and *chd7*, validating our in silico approach (Figure 10B). These 55 genes include the known Ets1 target IL7R (CD127) and two lupus-associated genes PTPN22 and UBE2I3. Fortuitously, we also discovered that the induction of ICOS, also a lupus-associated gene, was impaired in Ets1KO Th cells and that Ets1 was recruited to the promoter of ICOS

(Figure 10C and 10D). Thus, our in silico approach has established molecular links among several lupus-prone genes. A manuscript describing the in silico gene analyses is now under preparation .

5. Germline deficiency of Ets-1 results in a marked reduction in the number of CD21⁺CD23^{lo} marginal zone (MZ) B cells (23). This feature is still present in FF/CD19cre mice (Figure 9D), indicating that the PNT domain is required for the development of MZ B cells.

6. We have also applied the in silico gene analysis described above to B cells. There is no gene chip data on memory B cells in Immgen. We therefore compared the gene expression between marginal zone B cells, which are missing in Ets1KO mice, and follicular B cells. We then looked for genes that are also expressed at a high level in B1 cells, which are also missing in Ets1KO mice, and contain conserved ETS binding sites in their promoters. This sequence of analyses yields Myof, Fcrl5, PTPN14, and Pik3r4. We are in the process of validating the role of Ets1 in regulating the expression of these genes.

7. Deficiency of Ets1 has little impact on the homeostasis and function of myeloid cells including macrophages and neutrophils (data not shown).

A manuscript reporting some of the findings described above is under preparation.

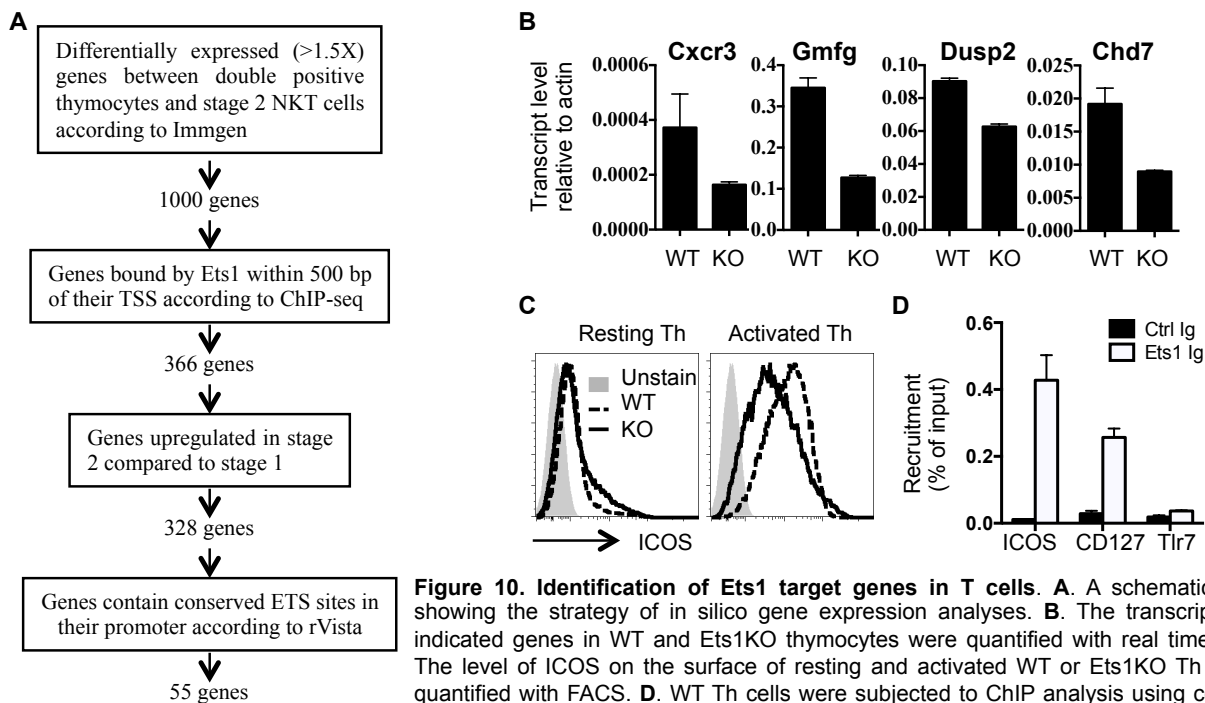


Figure 10. Identification of Ets1 target genes in T cells. **A.** A schematic diagram showing the strategy of in silico gene expression analyses. **B.** The transcript level of indicated genes in WT and Ets1KO thymocytes were quantified with real time PCR. **C.** The level of ICOS on the surface of resting and activated WT or Ets1KO Th cells was quantified with FACS. **D.** WT Th cells were subjected to ChIP analysis using control IgG or anti-Ets1. The recruitment of Ets1 to ICOS, CD127 (positive control), or Tlr7 (negative control) was quantified with real time PCR.

3c. Ets-deficient/FcγIIbR^{-/-} mice will be created (Time frame: months 12-24)-completed and reported in 2013, new update

We have backcrossed Ets1Het/FcγIIbR^{+/-} mice to N12 C57BL/6 genetic background. Our original hypothesis was that double haplo-insufficiency of Ets1 and FcγIIbR would result in lupus features. However, Ets1Het/FcγIIbR^{+/-} mice remained healthy up to 38 weeks of age and did not have any weight loss or sign of autoimmunity (Figure 11A data not shown). Two of three FcγIIbRKO mice died unexpectedly before developing any weight loss or sign of stress; their cause of death is still unclear. We therefore decided to terminate this line.

Instead, we have created Ets1KO/ FcγIIbRKO (DKO) mice of N4 C57BL/6 genetic background. We decided to create and examine N4 DKO for the following reasons. Ets1KO mice are still viable at N4 generations and N4 FcγIIbRKO mice are healthy and free of lupus-like disease. Thus N4 DKO mice allow us to compare the contribution of Ets1 deficiency and FcγIIbR deficiency in the development of lupus like disease. **Given the low frequency of DKO mice, we have so far analyzed 5 DKO female mice,**

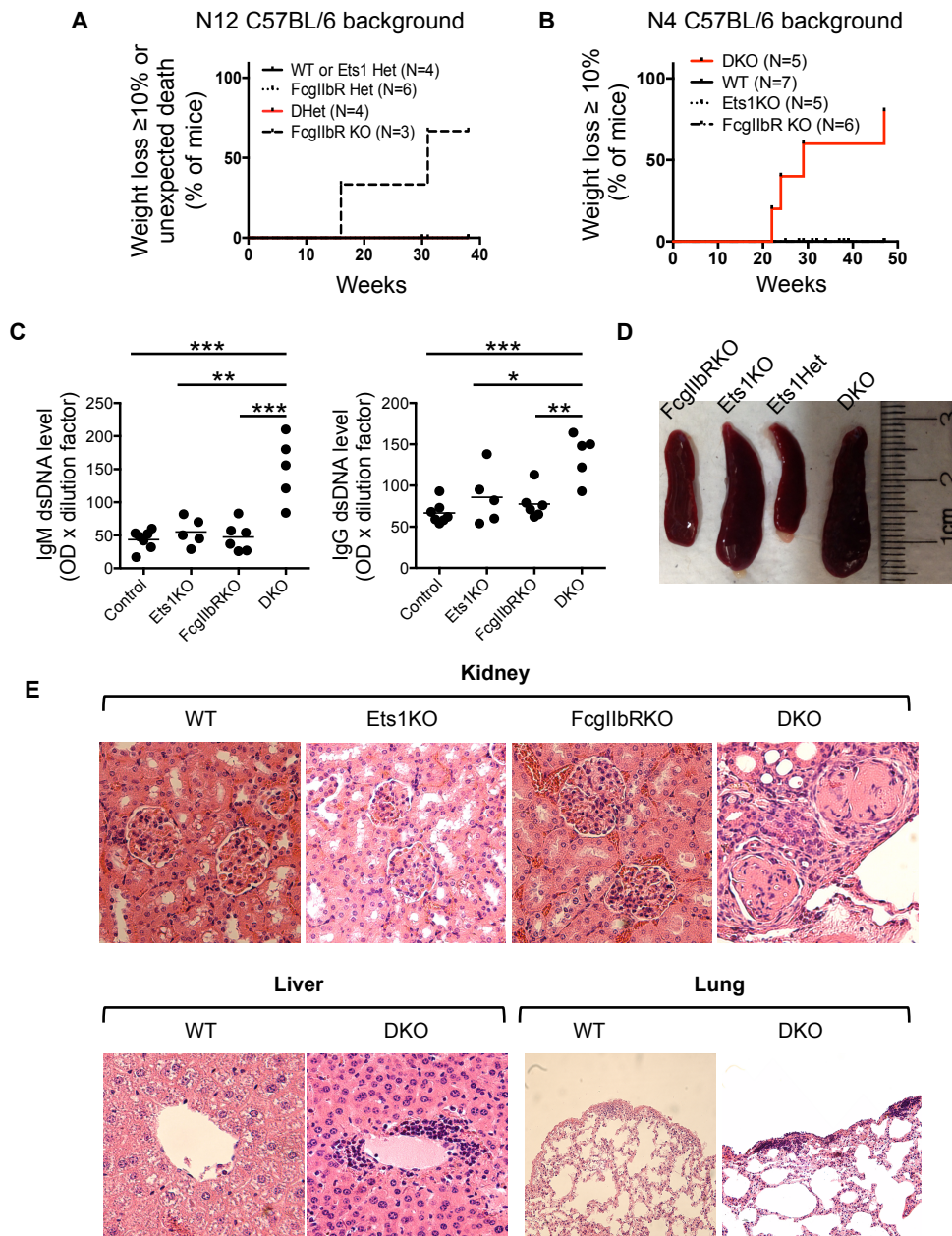


Figure 11. Potential synergy between Ets1 and FcγIIbR in suppressing autoimmunity. A&B. Survival curve of N12 C57BL/6 (A) or N4 C57BL/6 (B) mice of indicated genotypes. Mice were weighed at week 14 and then twice a month. The data shown are percentage of mice with weight loss reaching 10% of the starting weight or died unexpectedly. **C.** Serum levels of IgM and IgG anti-dsDNA of N4 C57BL/6 mice shown in B was measured with ELISA and are shown. Statistical analyses were performed with one-way ANOVA followed by Tukey's multiple comparisons test. **D.** Splens from N4 C57BL/6 mice of indicated genotypes are shown. **E.** H&E staining of the kidney, liver, and lung from N4 C57BL/6 mice of indicated genotypes are shown. Only data from female mice are shown in A-E.

performed the tasks described in 3d-3f, and have made the following exciting discoveries.

1. The control mice (WT, Ets1KO and/or FcγIIbRKO) and male DKO mice stayed healthy and steadily gained weight through the whole course (Figure 11B), though deficiency in Ets1 resulted in a low average weight probably due to congenital cardiac defects. Female DKO mice started to lose weight around week 29, and 4 of 5 DKO female mice had weight loss reach 10% of their starting weight (measured 14 weeks after birth).
2. All female DKO mice developed proteinuria detected by Dipstick about the same time when they started to lose weight (Table 2). Ets1KO mouse had equivocal proteinuria, whereas male DKO mice and control mice had no detectable proteinuria.
3. The level of serum anti-dsDNA (either IgM or IgG) in FcγIIbRKO and Ets1KO mice was very comparable to that of control mice, whereas female DKO mice had a statistically significant higher titer of anti-dsDNA (both IgM and IgG) (Figure 11C).
4. All female DKO mice and Ets1KO mouse had splenomegaly at the time of euthanasia (Figure 11D and data not shown). We have so far analyzed the histology in 3 female DKO mice, which all showed evidence of chronic glomerulonephritis including sclerosis, crescent formation, and accumulation of proteinaceous material in tubules (Figure 11E). There was also lymphocytic infiltration in periportal areas of liver and sub-pleural region of lung, but no obvious lymphadenopathy. In contrast, male DKO mice (N=2), Ets1KO (N=3) and FcγIIbRKO (N=3) mice, and control mice (N=4) showed no histological evidence of glomerulonephritis or lymphocytic infiltration.

Table 2. Summary of the phenotype of DKO mice

Genotype	Control	FcγIIbRKO	Ets1KO	male DKO	female DKO
Weight loss	no	no	no	no	starting at 25 wks
proteinuria	no	no	+/-	no	+++
splenomegaly	no	mild	yes	yes	yes
Lymphoma	no	no	no	no	1 out of 5
Glomerulonephritis on H&E	no	no	no	no	yes
serum dsDNA	no	no	no	+/-	+++
increase in CD11b+Gr1+ cells	no	no	modest	yes	strong in 4 out of 5
increase in CD11b-Gr1- cells	no	no	no	yes	strong in 4 out of 5

5. Unexpectedly, one female DKO developed T cell lymphoma made out of monoclonal Vb14⁺CD4⁺CD8⁺ T cells (data not shown).

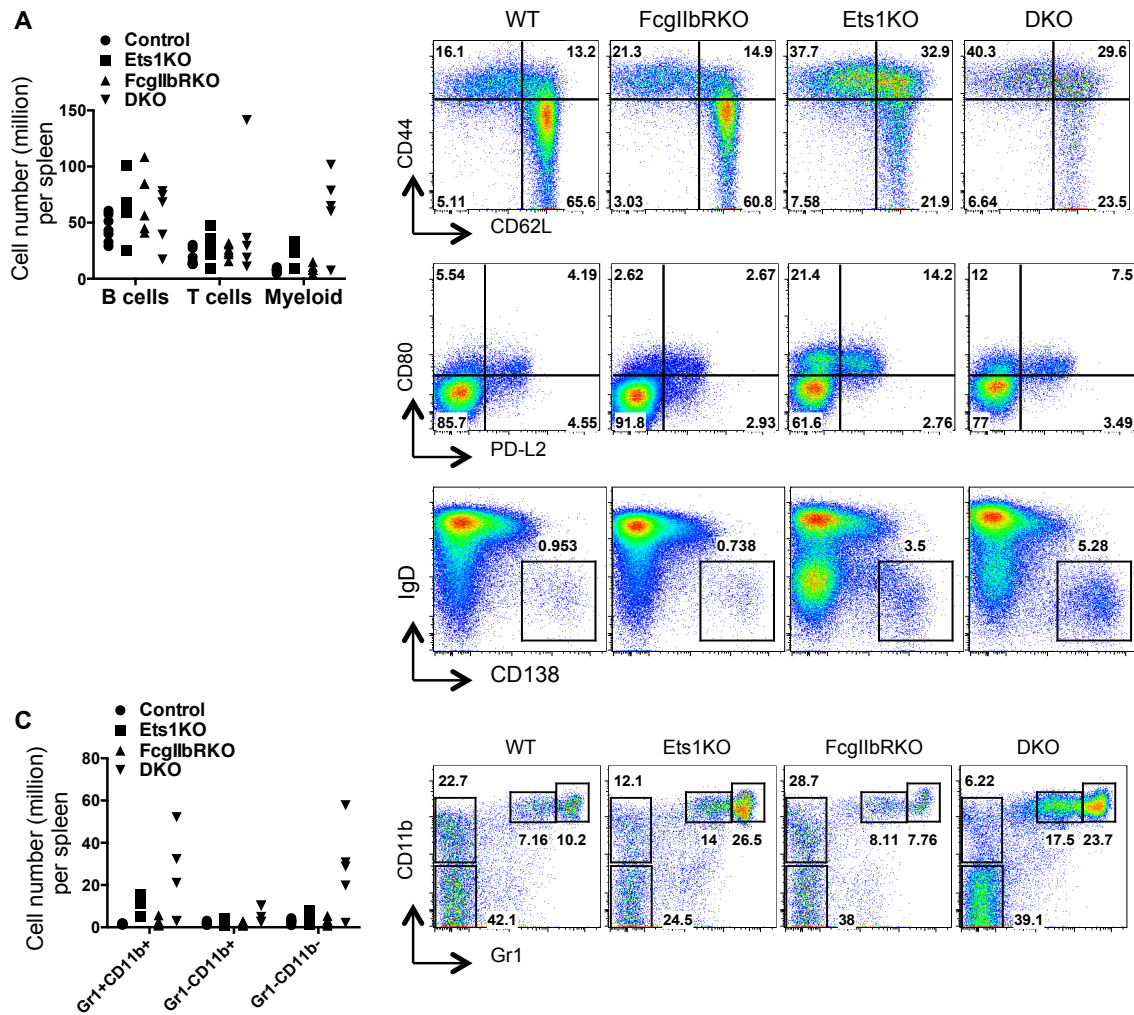


Figure 12. Abnormal cellular composition of DKO mice. **A** The numbers of splenic B, T, and myeloid cells from mice of indicated genotype were enumerated and shown. **B**. Splenic CD4⁺Th cells (the top row) and B cells (the middle and bottom rows) were analyzed for their expression of indicated surface markers. Representative FACS plots are shown. **C**. Splenic non-T, non-B cells of indicated genotypes were analyzed for their expression of Gr1 and CD11b. Representative FACS plots are shown in the right panels. The cell number of indicated subsets of splenic non-T, non-B cells of all mice were enumerated. The cumulative results are shown in the left panel. Only data from female mice are shown in **A-C**.

6. The other female DKO mice, however, had a near normal number of lymphocytes including B and T cells (Figure 12A). Their T cells exhibited a phenotype (CD44⁺) of activated/memory cells. Deficiency of Ets1 alone led to an increase in the percentages of memory B cells (PD-L2⁺, CD80⁺, and/or CD73⁺) and plasma cells (IgD⁻CD138⁺), and double deficiency of Ets1 and FcγIIbR resulted in a further increase in the percentage of plasma cells but not memory B cells (Figure 12B).

7. Interestingly, All DKO mice except one had a marked increase in the number of non-T/non-B myeloid cells (Figure 12A). These excessive non-T/non-B cells were made up of two major populations (Figure 12C). The first population is CD11b⁺Gr1⁺, which are most likely granulocytes. A modest increase in the number of granulocytes was also seen in Ets1KO mice. The second population is CD11b⁻Gr1⁻. This finding was unique to DKO mice and was detected even in the male DKO mouse, which had very no glomerulonephritis. Thus, the increase in CD11b⁻Gr1⁻ cells is not the result of glomerulonephritis. We subsequently found that the CD11b⁻Gr1⁻ non-T/non-B population consisted of

NK cells, innate lymphocytes, γ/δ T cells, and mast cells (data now shown) and was not dominated by any of the sub-populations.

Our preliminary findings indicate that deficiency of Ets1 and Fc γ IIbR synergistically hasten the development of lupus-like autoimmune disease, which preferentially attack female. As Ets1 deficiency has little impact on myeloid cells, we believe the development of autoimmune features in DKO mice is dependent on adaptive immune cells. One advantage of DKO mice as a lupus model is that both Ets1 and Fc γ IIbR are associated with lupus in genome-wide association studies. Thus, this model is highly relevant to human lupus. However, the disadvantages of this model are late onset of disease and low frequency of DKO mice, rendering it very difficult to carry out any large study requiring a high number of mice. The former hurdle can be remedied by providing additional lupus-inducing stimuli, such as a small dose of topical TLR7 ligand, which has been shown to induce lupus in all strains of mice in a few weeks (24). The latter hurdle can be overcome by moving DKO mice from N4 C57BL/6 genetic background to earlier backcrosses, such as N3 C57BL/6, in which the perinatal fatality caused by Ets1 deficiency is less of an issue. We plan to try both remedies in the near future.

*3d. Urine collected from mice thus created in this task will be monitored for the presence of protein by urine dipstick (Time frame: 24-36)-**completed, see task 3c***

*3e. Serum obtained from mice thus created in this task will be subjected to ELISA assays to quantify the level of immunoglobulin and anti-nucleus antibodies (Time frame: 24-36)-**completed, see task 3c***

*3f. All mice created in this task will be sacrificed and various organs, including skin, lung, liver, heart, and kidney will be harvested and subjected to histological and immunohistochemical analyses looking for signs of inflammation, cellular infiltration, and deposition of immune complex (Time frame: 24-36)-**partly completed, see also task 3c***

We still need to complete histological analyses in all experimental mice.

Milestones of the first funding period:

Aim 1:

- a. construction and functional characterization of a compound IL-10 reporter: **reached**
- b. screening the IL-10 locus with Ets1 ChIP: **reached.**

Aim 2:

- a. examining Ets1 level/activity and quantifying the level of IL-10, IL-17, and BAFF in blood samples from 30 lupus patients and 10 healthy individuals: **reached.**

Aim 3: crossing CD4Cre, CD19Cre, and LysCre to FF mice: **reached.**

At the end of the second funding period:

Aim 1: Introducing mutations corresponding to the lupus-prone SNPs to the compound IL-10 reporter and examining their impact on the promoter activity; examining the influence of Ets1 on the epigenetic landscape of the IL-10 locus; determining the interaction between Ets1 and the lupus-prone *il10* SNPs: **reached**

Aim 2: Examining Ets1 activity and quantifying the level of IL-10, IL-17, and BAFF in blood samples from additional 40 lupus patients and 30 healthy individuals: **reached**

Aim 3: Initial phenotypic characterization of FF/CD4Cre, FF/CD19Cre, and FF/LysCre mice; breeding Ets1KO mice to Fc γ IIbR $-/-$ mice: **reached**

At the end of the third funding period:

Aim 2: Enumerating the number of memory B cells in WT and Ets1KO mice, completing adoptive transfer of naive B cells into host mice: **reached**

Aim 3: Screening for autoimmune features in FF/CD4Cre, FF/CD19Cre, FF/LysCre, and Ets1-deficient/FcγIIbR^{-/-} mice: **partially reached**

Key Research Accomplishments in year 3

1. The T allele of rs3024505 is potentially associated with a higher percentage of CD14⁺ monocytes among PBMC and a higher level of IL-10 produced by LPS-stimulated PBMC.
2. Ets1 negatively regulates the homeostasis of memory B cells partly by a cell-intrinsic mechanism.
2. We have defined PNT domain-dependent and independent function of Ets1. The PNT domain of Ets1 is dispensable for the development of thymocytes, NKT cells, and B1 cells, and the homeostasis of memory B cells, but critically regulates the cytokine production by Th cells and NKT cells, and the development of MZ B cells.
3. Our data indicate that Ets1 and FcγIIbR synergistically maintain self-tolerance and prevent autoimmunity. Although double haplo-insufficiency of Ets1 and FcγIIbR did not cause autoimmunity, deficiency of both Ets1 and FcγIIbR led to the development of several features of autoimmunity even in mice not of N12 C57BL/6 genetic background, and may increase the risk of lymphoma. We have thus established a new mouse model of lupus that is highly relevant to human SLE.
4. Ets1 regulates the expression of several lupus-associated genes, including ICOS, PTPN22, and UBE2I3.

Reportable Outcome

Publications

The following paper has been published.

1. Lee, C. G., H. K. Kwon, A. Sahoo, W. Hwang, J. S. So, J. S. Hwang, C. S. Chae, G. C. Kim, J. E. Kim, H. S. So, E. S. Hwang, R. Grenningloh, I. C. Ho, and S. H. Im. Interaction of Ets-1 with HDAC1 represses IL-10 expression in Th1 cells. *J Immunol.* 2012; 188:2244-2253.
2. Tsao, H. W., T. S. Tai, W. Tseng, R. Grenningloh, S. C. Miaw, and I. C. Ho. Ets-1 facilitates nuclear entry of NFAT proteins and their recruitment to the IL-2 promoter. *Proc Natl Acad Sci USA.* 2013; 110:15776.
3. Chang, H. H., W. Tseng, K. Costenbader, and I. C. Ho. Altered expression of PTPN22 isoforms in SLE. *Arthritis Res Ther.* 2014 (Epub ahead of print)

The following manuscript is in preparation.

1. Tai, T. Z., H. W. Tsao, R. Grenningloh, P. Oettgen, and I. C. Ho. Ets1 controls the expression of ICOS and regulates the maturation, activation, and peripheral homeostasis of NKT cells.

Abstract presentations

1. Tsao, H. W., T. S. Tai, W. Tseng, I. C. Ho, and S. C. Miaw. Ets1 interacts with NRON complex and facilitates the nuclear entry of NFAT. American Association of Immunologists Annual Meeting 2013, Hawaii, USA

Degree obtained

1. Hsiao-Wei Tsao, PhD from Graduate Institute of Immunology, College of Medicine, National Taiwan University, October, 2013.

Animal models created

1. Ets1/FcγIIbR DKO mice: a new animal model of human lupus

Employment received

1. Tzong-Shyuan Tai: Research Associate, E-Da University Hospital, Taiwan; September, 2013

Conclusion

Aim 1

1. Ets1 suppresses the expression of IL-10 by recruiting HDA to the il10 locus (Figure 13).
2. This effect of Ets1 is independent of the genotype of rs3024505, rs3024493 and rs3024495.
3. However, the T allele of rs3024505 is potentially associated with a higher level of IL-10 by LPS-stimulated PBMC. The main producers of LPS-induced IL-10 are CD14+ monocytes.
4. The T allele of rs3024505 is potentially associated with a higher percentage of CD14+ monocytes in PBMC.
5. Ets1 promotes the expression of IL-2, which is down-regulated in T cells of lupus patients, by an NFAT-dependent mechanism. Ets1 is translocated to the cytoplasm in response to calcium signals and interacts with NRON complex, thereby disrupting the complex and releasing NFAT into the nucleus. In addition, the residual nuclear Ets1 recruits NFAT to the promoter of the IL-2 gene; these two proteins then synergistically transactivate IL-2.

Aim 2

1. The transcript level of Ets1 in peripheral blood is negatively correlated with the level of anti-dsDNA in lupus patients.
2. Ets1 suppresses the expansion of PD-L2+ B cells in a cell-intrinsic manner.
3. The PD-L2+ B cells very likely represent memory B cells and produce more anti-dsDNA than PD-L2- B cells.
4. The abnormal expansion of the PD-L2+ cells provides an attractive explanation for the negative correlation between the levels of Ets1 and anti-dsDNA.

Aim 3

1. Ets1 regulates the development and function of lymphocytes by both PNT domain-dependent and independent mechanisms.
2. Deficiency of both Ets1 and FcγIIbR, but not either gene, leads to lupus-like features in mice of N5 C57BL/6 genetic background and possibly a higher risk of lymphoma.
3. The high incidence of lupus features can be contributed to a high number of plasma cells and memory B cells.
4. Ets1 regulates the expression of several other lupus-associated genes, including ICOS, PTPN22, and UBE2I3. Dysregulation of these putative Ets1 target genes probably contribute to the development of lupus-like features.

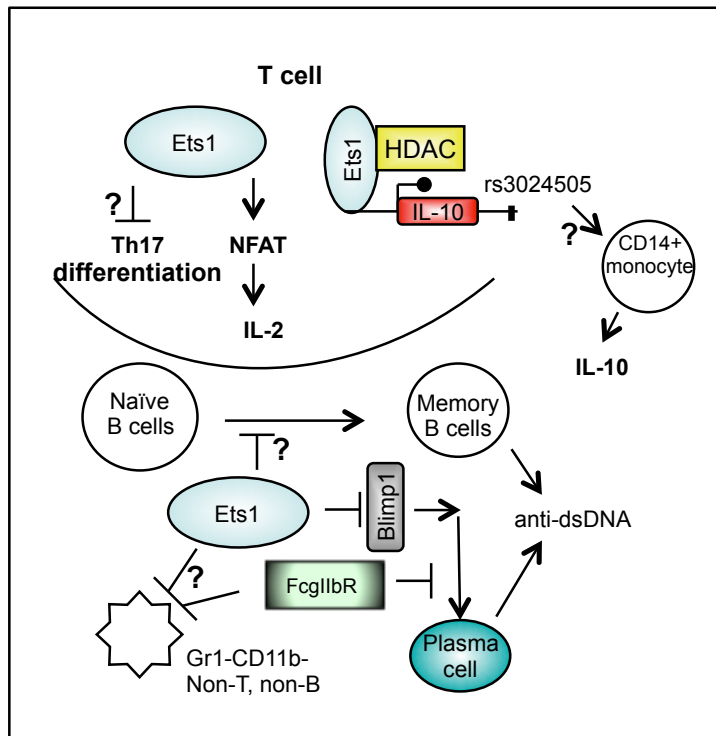


Figure 13. Ets1 counteracts the immune mechanism of SLE in many ways. In Th cells, Ets1 recruits HDAC to the *il10* locus, thereby suppressing the expression of IL-10. Its effect on IL-10 is not mediated through rs3024505 SNP. However, the T allele of this SNP is associated with a higher percentage of CD14⁺ monocytes in peripheral blood and a higher level of LPS-induced production of IL-10 in PBMC. Ets1 also facilitates the nuclear entry of NFAT proteins and their recruitment to the IL-2 promoter. How Ets1 inhibits the differentiation of Th17 cells is still not fully understood. In B cells, Ets1 negatively regulates the differentiation of plasma cells by suppressing the expression of Blimp1. Ets1 also inhibits the expansion of memory B cells by a cell-intrinsic and PNT domain-independent mechanism. Furthermore, Ets1 and FcγIIbR synergistically maintain self-tolerance and suppress the expansion of a novel non-T, non-B, Gr1⁻ and CD11b⁻ population. The identity and pathogenic role of this population of cells is unknown.

Personnel

1. I-Cheng Ho, MD, PhD: principal investigator
2. Hui-Hsin Chang, PhD: postdoctoral fellow
3. Tzong-Shyuan Tai, PhD: postdoctoral fellow
4. William Tseng: research assistant
5. Hsiao-Wei Tsao: graduate student

References

1. Sharrocks, A. D. 2001. The ETS-domain transcription factor family. *Nat Rev Mol Cell Biol* 2: 827-837.
2. Han, J. W., H. F. Zheng, Y. Cui, L. D. Sun, D. Q. Ye, Z. Hu, J. H. Xu, Z. M. Cai, W. Huang, G. P. Zhao, H. F. Xie, H. Fang, Q. J. Lu, J. H. Xu, X. P. Li, Y. F. Pan, D. Q. Deng, F. Q. Zeng, Z. Z. Ye, X. Y. Zhang, Q. W. Wang, F. Hao, L. Ma, X. B. Zuo, F. S. Zhou, W. H. Du, Y. L. Cheng, J. Q. Yang, S. K. Shen, J. Li, Y. J. Sheng, X. X. Zuo, W. F. Zhu, F. Gao, P. L. Zhang, Q. Guo, B. Li, M. Gao, F. L. Xiao, C. Quan, C. Zhang, Z. Zhang, K. J. Zhu, Y. Li, D. Y. Hu, W. S. Lu, J. L. Huang, S. X. Liu, H. Li, Y. Q. Ren, Z. X. Wang, C. J. Yang, P. G. Wang, W. M. Zhou, Y. M. Lv, A. P. Zhang, S. Q. Zhang, D. Lin, Y. Li, H. Q. Low, M. Shen, Z. F. Zhai, Y. Wang, F. Y. Zhang, S. Yang, J. J. Liu, and X. J. Zhang. 2009. Genome-wide association study in a Chinese Han population identifies nine new susceptibility loci for systemic lupus erythematosus. *Nat Genet* 41: 1234-1237.
3. Yang, W., N. Shen, D. Q. Ye, Q. Liu, Y. Zhang, X. X. Qian, N. Hirankarn, D. Ying, H. F. Pan, C. C. Mok, T. M. Chan, R. W. Wong, K. W. Lee, M. Y. Mok, S. N. Wong, A. M. Leung, X. P. Li, Y. Avihingsanon, C. M. Wong, T. L. Lee, M. H. Ho, P. P. Lee, Y. K. Chang, P. H. Li, R. J. Li, L. Zhang, W. H. Wong, I. O. Ng, C. S. Lau, P. C. Sham, and Y. L. Lau. 2010. Genome-wide association study in Asian populations identifies variants in ETS1 and WDFY4 associated with systemic lupus erythematosus. *PLoS genetics* 6: e1000841.
4. Wang, D., S. A. John, J. L. Clements, D. H. Percy, K. P. Barton, and L. A. Garrett-Sinha. 2005. Ets-1 deficiency leads to altered B cell differentiation, hyperresponsiveness to TLR9 and autoimmune disease. *International immunology* 17: 1179-1191.
5. Grenningloh, R., B. Y. Kang, and I. C. Ho. 2005. Ets-1, a functional cofactor of T-bet, is essential for Th1 inflammatory responses. *J Exp Med* 201: 615-626.
6. Alcocer-Varela, J., and D. Alarcon-Segovia. 1982. Decreased production of and response to interleukin-2 by cultured lymphocytes from patients with systemic lupus erythematosus. *J Clin Invest* 69: 1388-1392.
7. Crispin, J. C., and G. C. Tsokos. 2009. Transcriptional regulation of IL-2 in health and autoimmunity. *Autoimmunity reviews* 8: 190-195.
8. John, S. A., J. L. Clements, L. M. Russell, and L. A. Garrett-Sinha. 2008. Ets-1 regulates plasma cell differentiation by interfering with the activity of the transcription factor blimp-1. *J Biol Chem* 283: 951-962.
9. Martins, G. A., L. Cimmino, M. Shapiro-Shelef, M. Szabolcs, A. Herron, E. Magnusdottir, and K. Calame. 2006. Transcriptional repressor Blimp-1 regulates T cell homeostasis and function. *Nat Immunol* 7: 457-465.
10. Gateva, V., J. K. Sandling, G. Hom, K. E. Taylor, S. A. Chung, X. Sun, W. Ortmann, R. Kosoy, R. C. Ferreira, G. Nordmark, I. Gunnarsson, E. Svenungsson, L. Padyukov, G. Sturfelt, A. Jonsen, A. A. Bengtsson, S. Rantapaa-Dahlqvist, E. C. Baechler, E. E. Brown, G. S. Alarcon, J. C. Edberg, R. Ramsey-Goldman, G. McGwin, Jr., J. D. Reveille, L. M. Vila, R. P. Kimberly, S. Manzi, M. A. Petri, A. Lee, P. K. Gregersen, M. F. Seldin, L. Ronnblom, L. A. Criswell, A. C. Syvanen, T. W. Behrens, and R. R. Graham. 2009. A large-scale replication study identifies

- TNIP1, PRDM1, JAZF1, UHRF1BP1 and IL10 as risk loci for systemic lupus erythematosus. *Nat Genet* 41: 1228-1233.
11. Panchanathan, R., H. Liu, H. Liu, C. M. Fang, L. D. Erickson, P. M. Pitha, and D. Choubey. 2012. Distinct regulation of murine lupus susceptibility genes by the IRF5/Blimp-1 axis. *J Immunol* 188: 270-278.
 12. Willingham, A. T., A. P. Orth, S. Batalov, E. C. Peters, B. G. Wen, P. Aza-Blanc, J. B. Hogenesch, and P. G. Schultz. 2005. A strategy for probing the function of noncoding RNAs finds a repressor of NFAT. *Science* 309: 1570-1573.
 13. Sharma, S., G. M. Findlay, H. S. Bandukwala, S. Oberdoerffer, B. Baust, Z. Li, V. Schmidt, P. G. Hogan, D. B. Sacks, and A. Rao. 2011. Dephosphorylation of the nuclear factor of activated T cells (NFAT) transcription factor is regulated by an RNA-protein scaffold complex. *Proc Natl Acad Sci U S A* 108: 11381-11386.
 14. Wen, Z., L. Xu, X. Chen, W. Xu, Z. Yin, X. Gao, and S. Xiong. 2013. Autoantibody Induction by DNA-Containing Immune Complexes Requires HMGB1 with the TLR2/MicroRNA-155 Pathway. *J Immunol* 190: 5411-5422.
 15. Kyogoku, C., C. D. Langefeld, W. A. Ortmann, A. Lee, S. Selby, V. E. Carlton, M. Chang, P. Ramos, E. C. Baechler, F. M. Batliwalla, J. Novitzke, A. H. Williams, C. Gillett, P. Rodine, R. R. Graham, K. G. Ardlie, P. M. Gaffney, K. L. Moser, M. Petri, A. B. Begovich, P. K. Gregersen, and T. W. Behrens. 2004. Genetic association of the R620W polymorphism of protein tyrosine phosphatase PTPN22 with human SLE. *American journal of human genetics* 75: 504-507.
 16. Orozco, G., E. Sanchez, M. A. Gonzalez-Gay, M. A. Lopez-Nevot, B. Torres, R. Caliz, N. Ortego-Centeno, J. Jimenez-Alonso, D. Pascual-Salcedo, A. Balsa, R. de Pablo, A. Nunez-Roldan, M. F. Gonzalez-Escribano, and J. Martin. 2005. Association of a functional single-nucleotide polymorphism of PTPN22, encoding lymphoid protein phosphatase, with rheumatoid arthritis and systemic lupus erythematosus. *Arthritis and rheumatism* 52: 219-224.
 17. Zhong, X., S. Lau, C. Bai, N. Degauque, N. E. Holodick, S. J. Steven, J. Tumang, W. Gao, and T. L. Rothstein. 2009. A novel subpopulation of B-1 cells is enriched with autoreactivity in normal and lupus-prone mice. *Arthritis Rheum* 60: 3734-3743.
 18. Tomayko, M. M., N. C. Steinel, S. M. Anderson, and M. J. Shlomchik. 2010. Cutting edge: Hierarchy of maturity of murine memory B cell subsets. *J Immunol* 185: 7146-7150.
 19. Zamisch, M., L. Tian, R. Grenningloh, Y. Xiong, K. F. Wildt, M. Ehlers, I. C. Ho, and R. Bosselut. 2009. The transcription factor Ets1 is important for CD4 repression and Runx3 up-regulation during CD8 T cell differentiation in the thymus. *J Exp Med* 206: 2685-2699.
 20. Clements, J. L., S. A. John, and L. A. Garrett-Sinha. 2006. Impaired generation of CD8+ thymocytes in Ets-1-deficient mice. *J Immunol* 177: 905-912.
 21. Walunas, T. L., B. Wang, C. R. Wang, and J. M. Leiden. 2000. Cutting edge: the Ets1 transcription factor is required for the development of NK T cells in mice. *J Immunol* 164: 2857-2860.
 22. Hollenhorst, P. C., K. J. Chandler, R. L. Poulsen, W. E. Johnson, N. A. Speck, and B. J. Graves. 2009. DNA specificity determinants associate with distinct transcription factor functions. *PLoS genetics* 5: e1000778.

23. Eyquem, S., K. Chemin, M. Fasseu, M. Chopin, F. Sigaux, A. Cumano, and J. C. Bories. 2004. The development of early and mature B cells is impaired in mice deficient for the Ets-1 transcription factor. *Eur J Immunol* 34: 3187-3196.
24. Yokogawa, M., M. Takaishi, K. Nakajima, R. Kamijima, C. Fujimoto, S. Kataoka, Y. Terada, and S. Sano. 2014. Epicutaneous application of toll-like receptor 7 agonists leads to systemic autoimmunity in wild-type mice: a new model of systemic Lupus erythematosus. *Arthritis & rheumatology* 66: 694-706.

Appendix 1



Unleash what's possible.
The guava easyCyte™ flow cytometer is here.

EMD Millipore is a division of Merck KGaA, Darmstadt, Germany



This information is current as of July 16, 2014.

Interaction of Ets-1 with HDAC1 Represses IL-10 Expression in Th1 Cells

Choong-Gu Lee, Ho-Keun Kwon, Anupama Sahoo, Won Hwang, Jae-Seon So, Ji-Sun Hwang, Chang-Suk Chae, Gi-Cheon Kim, Jung-Eun Kim, Hong-Seob So, Eun Sook Hwang, Roland Grenningloh, I-Cheng Ho and Sin-Hyeog Im

J Immunol 2012; 188:2244-2253; Prepublished online 20 January 2012;
doi: 10.4049/jimmunol.1101614
<http://www.jimmunol.org/content/188/5/2244>

-
- Supplementary Material** <http://www.jimmunol.org/jimmunol/suppl/2012/01/20/jimmunol.1101614.DC1.html>
- References** This article **cites 62 articles**, 29 of which you can access for free at:
<http://www.jimmunol.org/content/188/5/2244.full#ref-list-1>
- Subscriptions** Information about subscribing to *The Journal of Immunology* is online at:
<http://jimmunol.org/subscriptions>
- Permissions** Submit copyright permission requests at:
<http://www.aai.org/ji/copyright.html>
- Email Alerts** Receive free email-alerts when new articles cite this article. Sign up at:
<http://jimmunol.org/cgi/alerts/etoc>
- Errata** An erratum has been published regarding this article. Please see [next page](#) or:
<http://www.jimmunol.org/content/189/12/5996.full.pdf>



Interaction of Ets-1 with HDAC1 Represses IL-10 Expression in Th1 Cells

Choong-Gu Lee,* Ho-Keun Kwon,* Anupama Sahoo,* Won Hwang,* Jae-Seon So,* Ji-Sun Hwang,* Chang-Suk Chae,* Gi-Cheon Kim,* Jung-Eun Kim,* Hong-Seob So,^{†,‡} Eun Sook Hwang,[§] Roland Grenningloh,^{¶,||} I-Cheng Ho,^{¶,||} and Sin-Hyeog Im*

IL-10 is a multifunctional cytokine that plays a crucial role in immunity and tolerance. IL-10 is produced by diverse immune cell types, including B cells and subsets of T cells. Although Th1 produce IL-10, their expression levels are much lower than Th2 cells under conventional stimulation conditions. The potential role of E26 transformation-specific 1 (Ets-1) transcription factor as a negative regulator for *Il10* gene expression in CD4⁺ T cells has been implicated previously. In this study, we investigated the underlying mechanism of Ets-1-mediated *Il10* gene repression in Th1 cells. Compared with wild type Th1 cells, Ets-1 knockout Th1 cells expressed a significantly higher level of IL-10, which is comparable with that of wild type Th2 cells. Upregulation of IL-10 expression in Ets-1 knockout Th1 cells was accompanied by enhanced chromatin accessibility and increased recruitment of histone H3 acetylation at the *Il10* regulatory regions. Reciprocally, Ets-1 deficiency significantly decreased histone deacetylase 1 (HDAC1) enrichment at the *Il10* regulatory regions. Treatment with trichostatin A, an inhibitor of HDAC family, significantly increased *Il10* gene expression by increasing histone H3 acetylation recruitment. We further demonstrated a physical interaction between Ets-1 and HDAC1. Coexpression of Ets-1 with HDAC1 synergistically repressed IL-10 transcription activity. In summary, our data suggest that an interaction of Ets-1 with HDAC1 represses the *Il10* gene expression in Th1 cells. *The Journal of Immunology*, 2012, 188: 2244–2253.

Many cell types, such as B cells, macrophages, mast cells, eosinophils, dendritic cells, and diverse subsets of T cells, produce IL-10, an immunoregulatory cytokine. IL-10 has anti-inflammatory properties and inhibits the function of macrophages and dendritic cells. IL-10 also plays critical roles in maintaining immune homeostasis and has diverse effects on numerous nonimmune cell populations, such as keratinocytes and endothelial cells (1, 2).

Naive CD4⁺ T cells can be differentiated into various effector populations, such as Th1, Th2, Th17, and regulatory T cells, when they are exposed to Ags with unique cytokine milieu. For example, Th1 cells produce IFN- γ and protect against intracellular pathogen such as virus and bacteria. Th2 cells produce IL-4, IL-5, and IL-13, and confer protection against multicellular parasitic infection (3, 4). Initially, IL-10 was reported as a typical Th2 cytokine (1). Recently, Th1 cells were also reported to produce IL-10, but only under specific circumstances (2, 5), such as in chronic and nonhealing infectious conditions (6, 7). In line with this, IL-12, IL-27, and Notch signals can also induce IL-10 production in Th1 cells (8–10). Nevertheless, the expression level of IL-10 in conventional Th1 cells still needs to be maintained in a repressed state to allow Th1 cells to exercise their effector function. Following the earlier notion, it was reported that the promoter and several putative regulatory elements within the *Il10* locus were silenced in Th1 cells (11, 12). Several studies have elucidated the role of specific transcription factors, such as GATA-3 and c-Jun, together with epigenetic mechanisms, in the regulation of *Il10* gene expression in Th2 cells (12–15). However, it is still unclear how the repressed state of *Il10* gene expression is maintained in conventional Th1 cells.

E26 transformation-specific 1 (Ets-1) is a member of the ETS family of transcription factors, and it binds to the conserved GGAA/T sequence (16, 17). Previous studies in Ets-1 knockout (Ets-1KO) mice have demonstrated the important functions of Ets-1 in development, proliferation, and survival of NK and T cells (18–20). Furthermore, Ets-1 acts as a cofactor of T-bet and is essential for Th1 effector function and differentiation by regulating IFN- γ expression (21). Ets-1 is a negative regulator of Th17 differentiation, and Th17 cells deficient of Ets-1 express increased IL-17 and IL-17-related cytokines (22). On the contrary, Ets-1 positively regulates several cytokine genes such as *Il2*, *Il5*, and *Gmcsf* (23). These studies suggest that Ets-1 may modulate the

*School of Life Sciences and Immune Synapse Research Center, Gwangju Institute of Science and Technology, Gwangju 500-712, The Republic of Korea; [†]Center for Metabolic Function Regulation, Wonkwang University School of Medicine, Iksan, Jeonbuk 570-749, The Republic of Korea; [‡]Department of Microbiology, Wonkwang University School of Medicine, Jeonbuk 570-749, The Republic of Korea; [§]Division of Life and Pharmaceutical Sciences, College of Pharmacy, Ewha Womans University, Seoul 120-750, The Republic of Korea; [¶]Division of Rheumatology, Immunology, and Allergy, Department of Medicine, Brigham and Women's Hospital, Boston, MA 02115; and ^{||}Harvard Medical School, Boston, MA 02115

Received for publication June 2, 2011. Accepted for publication December 15, 2011.

This work was supported by Grant A080588-20 from the Korea Healthcare Technology Research and Development Project, Ministry for Health, Welfare and Family Affairs; National Research Foundation Grant 2011-0028529 from the Korean government (Ministry of Education, Science and Technology); American Recovery and Reinvestment Act R03 Grant A1081052 from the National Institutes of Health (to I.-C.H.); a Pilot Project grant from the Alliance for Lupus Research (to I.-C.H.); and Grant Department of Defense W81XWH-11-1-0492 (to I.-C.H.).

Address correspondence and reprint requests to Dr. Sin-Hyeog Im, School of Life Sciences and Immune Synapse Research Center, Gwangju Institute of Science and Technology (GIST), 123 Cheomdan-gwagiro, Buk-gu, Gwangju 500-712, Republic of Korea. E-mail address: imsh@gist.ac.kr

The online version of this article contains supplemental material.

Abbreviations used in this article: ChIP, chromatin immunoprecipitation; CNS, conserved noncoding sequence; Ets-1, E26 transformation-specific 1; Ets-1KO, Ets-1 knockout; H3Ac, histone H3 acetylation; HDAC1, histone deacetylase 1; HPRT, hypoxanthine-guanine phosphoribosyl transferase; IB, immunoblotting; IP, immunoprecipitated; KO, knockout; NP-40, Nonidet P-40; PLA, proximity ligation assay; qRT-PCR, quantitative RT-PCR; TSA, trichostatin A; UTR, untranslated region; WT, wild type.

Copyright © 2012 by The American Association of Immunologists, Inc. 0022-1767/12/\$16.00

effector function of Th cells by acting as a positive or negative regulator in a context-dependent manner (24–26). In addition, Ets-1 deficiency leads to altered B cell differentiation, hyper-responsiveness to TLR9, and autoimmune disease (22, 27). Interestingly, Ets-1KO Th1 cells produce an abnormally high level of IL-10 (21). Despite these observations, it is still unclear how Ets-1 represses the *Il10* gene expression in Th1 cells.

In this study, we demonstrated that Ets-1KO Th cells showed elevated IL-10 expression upon *ex vivo* stimulation. Th1 cells from Ets-1KO mice showed increased histone H3 acetylation (H3Ac) recruitment but reduced histone deacetylase 1 (HDAC1) binding at the *Il10* regulatory regions compared with their wild type (WT) counterparts. We further tested and demonstrated that a physical interaction between Ets-1 and HDAC1 cooperatively downregulated *Il10* gene expression in Th1 cells.

Materials and Methods

Mice, cells, and reagents

C57BL/6 and BALB/c mice were purchased from Orient Bio (Gyeonggi-do, Korea). Ets-1-deficient (21), T-bet-deficient (28) and STAT4-deficient (29) mice were described previously. Mice were housed in specific pathogen-free barrier facilities and used in accordance with protocols approved by the Animal Care and Ethics Committees of the Gwangju Institute of Science and Technology. The HEK-293 cells were obtained from the Korean Cell Line Bank (Seoul National University, Seoul, Korea). Cells were cultured in DMEM supplemented with 10% FBS and penicillin-streptomycin. Recombinant human IL-2 and anti-IL-4 (11B11) were provided by the National Cancer Institute, Preclinical Repository (Bethesda, MD). IL-4 was purchased from PeproTech (Rocky Hill, NY), and IL-12 was purchased from Sigma-Aldrich (St. Louis, MO). Anti-CD3 (145.2C11), anti-CD28 (37.51), anti-IFN- γ (XMG1.2), and anti-IL-12 (C17.8) were purchased from BD Biosciences (San Jose, CA). Trichostatin acid A and DMSO were obtained from Sigma-Aldrich.

CD4⁺ T cell purification, differentiation, and ELISA

CD4⁺ T cells were purified from the lymph nodes and spleen of 8- to 10-wk-old mice using magnetic beads (L3T4; Miltenyi Biotec GmbH, Bergisch Gladbach, Germany). For Th1 differentiation, the cells (5×10^6 /ml) were stimulated with 1 μ g/ml plate-bound anti-CD3 and 2 μ g/ml soluble anti-CD28 under Th1-skewing (10 ng/ml IL-12 plus 10 μ g/ml anti-IL-4) or Th2-skewing (10 ng/ml IL-4, 10 μ g/ml anti-IFN- γ plus 10 μ g/ml anti-IL-12) conditions in RPMI 1640 medium (Welgene, Daegu, Korea) supplemented with 10% FBS, L-glutamine, penicillin-streptomycin, non-essential amino acids, sodium pyruvate, HEPES, and 2-ME. A total of 100 U/ml recombinant human IL-2 was added after 24 h, and the cells were expanded in complete medium containing IL-2 for 6 d. ELISA for IL-10 was performed using the mouse IL-10 ELISA kit (KOMA Biotech, Seoul, Korea) according to the manufacturer's protocol.

RNA isolation, cDNA synthesis, quantitative RT-PCR

Total RNA was extracted using TRI Reagent (MRC, Cincinnati, OH). For reverse transcription, cDNA was generated using 1 μ g total RNA, oligo (dT) primer (Promega, Madison, WI), and Improm-II Reverse Transcriptase (Promega) in a total volume of 20 μ l. One microliter of cDNA was amplified using the following RT-PCR primers sets: *HPRT* (5'-TTATG-GACAGGACTGAAAGAC-3' and 5'-GCTTTAATGTAATCCAGCAGGT-3'), *Il10* (5'-ATAACTGCACCCACTTCCCA-3' and 5'-TCATTTCGTAAGGCTTGG-3'), *Il24* (5'-GCCAGTAAGGACAATTCCA-3' and 5'-ATTTGTCATCCAGGTCAGG-3'), *Ccr8* (5'-GCTCAGATAATTGGTC-TTCT-3' and 5'-ACGAGACTAAGATGACCAG-3'), *Bcl2l1* (5'-GAC-AAGGAGATGCAGGTATTGG-3' and 5'-TCCCGTAGAGATCCACAA-AAGT-3'), *Irf3* (5'-GAGCCAGATTATCTTTCTACC-3' and 5'-GTT-GTTGACCTCAAACCTGG-3'), *Il4* (5'-CAACGAAGAACCACACAGAG-3' and 5'-GGACTTGACTCATTCATGG-3'). Mouse hypoxanthine-guanine phosphoribosyl transferase (HPRT) primer was used for quantitative RT-PCR (qRT-PCR) to normalize the amount of cDNA used for each condition.

Plasmids and luciferase reporter assays

Reporter constructs were generated by cloning the minimal promoter and conserved noncoding sequence (CNS) regions of the *Il10* locus from P1 clones into the pXPG reporter vector containing the luciferase gene described in the previous report (30). Flag-Ets-1 plasmid was described previously (21). The cDNA encoding Flag-Ets-1 was cloned into pLV-

CAG-EGFP vector (kindly provided by Dr. Masahito Ikawa, Osaka University, Osaka, Japan). HEK-293 cells were transfected using GeneEx-presso (Excellgen, Rockville, MD) according to the manufacturer's protocol. After 24 h, cells were harvested and luciferase activity was measured by the dual luciferase assay system (Promega). Data were normalized by the activity of *Renilla* luciferase, which was used as an internal control for transfection.

Chromatin immunoprecipitation assays

Chromatin immunoprecipitation (ChIP) assays were performed as described previously (30). In brief, cells were cross-linked with formaldehyde at a final concentration 1%, lysed, and sonicated to shear DNA. After immunoprecipitation with anti-Ets-1 (Santa Cruz Biotechnology, Santa Cruz, CA), anti-HDAC1 (Abcam, Cambridge, MA), anti-H3Ac (K9/14) (Millipore, Billerica, MA), or rabbit IgG (Vector Laboratories, Burlingame, CA) at 4°C overnight, Ab/DNA complexes were eluted and cross-linking was reversed by boiling with Chelex-100 (31). After reversal of cross-links, the presence of selected DNA sequences was assessed by real-time PCR using the following primers: CNS-0.12 (5'-TCTGTACATAGAACAGCTGTC-3' and 5'-CTGGTCGGAATGAACTTCTG-3'), CNS+1.65 (5'-GTCTC-TTGCTCATCTGTCTC-3' and 5'-GCTAATAACCCACAATGACTC-3'), CNS+2.98 (5'-ACTAGGTGTTGAGGAGAGTG-3' and 5'-GAATTCTG-CCTTCTGCTCGT-3'), CNS+6.45 (5'-GTGGTCATTTTTTCAGTAAGA-CC-3' and 5'-CCTAACCTTTCATCTCACAG-3'), IL-24 promoter (5'-TCATCTCACCTGAGGGACTG-3' and 5'-TCATGGTAGAGATCTT-CT-3'), CCR8 promoter (5'-GGTTTGAAGTCTGAGGTCCTCA-3' and 5'-GGCTGGAATTCAGTCGTGTC-3'), Bcl-XL 3' untranslated region (UTR) (5'-CTGAAGTCATTAACAGTCTGGG-3' and 5'-CTGAAAGTCCAC-CTTGCTAGAG-3'). As a loading control, the qRT-PCR was done directly on input DNA purified from chromatin before immunoprecipitation. Data are presented as the amount of DNA recovered relative to the input control. Result of ChIP with isotype IgG was confirmed as a background value and showed <0.001 of relative ratio to input. IgG level was shown only when it is necessary.

Chromatin accessibility by real-time PCR assay

Chromatin accessibility by real-time PCR assays were performed as described previously (32) with minor modifications. Cells were washed and lysed by resuspending pellets in ice-cold Nonidet P-40 (NP-40) lysis buffer (10 mM Tris-HCl [pH 7.4], 10 mM NaCl, 3 mM MgCl₂, 0.5% NP-40, 0.15 mM spermine, 0.5 mM spermidine) and incubating on ice for 5 min. Nuclei were collected by centrifuge at 3000 rpm for 5 min at 4°C. Isolated nuclei were washed with MNase digestion buffer without CaCl₂ (10 mM Tris-HCl [pH 7.4], 15 mM NaCl, 60 mM KCl, 0.15 mM spermine, 0.5 mM spermidine), collected by centrifuge at 3000 rpm for 5 min at 4°C, and resuspended in MNase digestion buffer supplemented with 1 mM CaCl₂. Nuclease treatment was achieved with or without MNase with various concentrations. Samples were divided as "cut" or "uncut" to identify MNase-treated and control untreated samples, respectively. Samples were then incubated at 37°C for 1 min. Reactions were stopped by addition of 20 μ l 100 mM EDTA/10 mM EGTA (pH 8.1) and 10 μ l of 10% SDS (w/v). Genomic DNA was isolated using Genomic DNA prep kit (Solgent, Daejeon, Korea). Concentrations of final eluted DNA were accessed by means of a BioSpec-nano spectrophotometer (Shimadzu, Kyoto, Japan), and 50 ng DNA was subsequently used as a template in real-time PCR to quantify target sequences in "cut" and "uncut" samples. Each eluate was also subject to agarose gel electrophoresis to visualize the extent of MNase digestion of genomic DNA. Primers used in the quantitative assays were validated by amplifying serially diluted genomic DNA as templates to create standard curve for each primer set and analyzed using the quantification method. Chromatin accessibility was calculated and expressed as the average fold difference of target template in "uncut" over "cut" samples. Thus, readily digested sequences (hypersensitive sites) were expected to be depleted in MNase-treated samples and give higher chromatin accessibility values than less accessible sequences.

Immunoprecipitation and immunoblotting

Immunoprecipitation was performed using a polyclonal Ab recognizing HDAC1 (Abcam), Ets-1 (Santa Cruz Biotechnology), or rabbit IgG (Vector Laboratories, Burlingame, CA) followed by protein A-Sepharose (Millipore) incubation from overexpressed HEK-293 or primary Th1 total lysates. To determine levels of HDAC1 proteins, we prepared total lysate from Th1 and Ets-1KO Th1 cells in RIPA buffer (50 mM Tris [pH 7.6], 150 mM NaCl, 1% NP-40) containing protease inhibitors mixture (Roche, Mannheim, Germany) for 30 min on ice. Samples were loaded together with a Page Ruler Prestained Protein ladder (Fermentas, Glen Burnie, MD) on a 10% SDS-PAGE gel. The proteins were electroblotted onto a nitro-

cellulose membrane (Bio-Rad, Richmond, CA). After blocking for 1 h in 5% skim milk, the membranes were incubated with mAb of Ets-1 (Santa Cruz Biotechnology), HDAC1 (Millipore), and β -actin (Abcam) in 3% blocking buffer overnight at 4°C. The blots were developed using a 1/5000 diluted anti-mouse HRP (Abcam) and visualized.

Intracellular cytokine staining

Cells were stimulated with 1 μ g/ml plate-bound anti-CD3 and 2 μ g/ml soluble anti-CD28 plus 10 μ g/ml brefeldin A (Sigma-Aldrich) for 6 h. Cells were harvested, washed with PBS, and fixed in fixation/permeabilization buffer (eBioscience, San Diego, CA) for 0.5 h. Cells were washed and resuspended in 100 μ l permeabilization buffer (eBioscience). For intracellular detection of IL-10, anti-IL-10-PE (eBioscience) or isotype control Ab (eBioscience) was added and incubated for 0.5 h at 4°C. After incubation, cells were washed, resuspended in 1 ml PBS, and analyzed by flow cytometry (Beckman Coulter, Brea, CA).

Proximity ligation assay

WT Th1 and Ets-1KO Th1 cells were differentiated and were incubated in 8S Multicell (CTRL Life Science, Gwangju, Korea) coated with Poly-L-Lys in PBS for overnight at 4°C. For fixation, 4% paraformaldehyde was added and incubated for 10 min. 0.25% Triton X-100 was used for permeabilization. Proximity ligation assay was performed using the Rabbit PLUS and Mouse MINUS Duolink in situ proximity ligation assay (PLA) kits with Ab of Ets-1 (rabbit) and HDAC1 (mouse) (OLINK Bioscience, Uppsala, Sweden) according to the manufacturer's protocol. Subsequently, slides were dehydrated, air-dried, and embedded in DAPI-containing mounting medium. Fluorescence was detected using a FluoView microscope (Olympus, Center Valley, PA).

Computational analysis

Genomic sequences spanning the *Il10* gene were analyzed using the Web-based alignment software, VISTA browser 2.0 (33), to identify CNSs.

Statistical analysis

Data are the mean \pm SD of at least three independent experiments, unless differently specified in the text. A Student *t* test was used to calculate the statistical significance of the experimental data. The level of significance was set at **p* < 0.05 and ***p* < 0.01. Significance was indicated only when appropriate.

Results

Increased IL-10 expression in Ets-1-deficient Th cells

To elucidate the molecular mechanism of Ets-1-mediated *Il10* gene repression in Th1 cells, we compared IL-10 expression in Th1 cells differentiated from WT or Ets-1KO mice. Cells were left without stimulation or stimulated with anti-CD3/anti-CD28; then IL-10 mRNA and protein levels were measured by qRT-PCR, ELISA, and flow cytometry. Th1 cells from Ets-1KO showed >8-fold increase in IL-10 mRNA expression compared with WT Th1 cells (Fig. 1A). Next, we measured the IL-10 protein level by ELISA to check whether protein level is also increased in Ets-1KO cells. Indeed, a significant increase of IL-10 (9-fold) was observed in Ets-1KO cells compared with WT Th1 cells (Fig. 1B). We further analyzed protein expression by performing intracellular cytokine staining. The IL-10⁺ cells constituted ~9% of Ets-1KO cells compared with 1.7% in WT Th1 (Fig. 1C). Similarly, Ets-1KO Th2 cells also expressed more IL-10 than WT Th2 cells even though WT cells already produced a high level of IL-10.

We further tested whether ex vivo isolated Ets-1KO CD4⁺ T cells also expressed higher levels of IL-10 transcript than WT cells. Like in Th1 cells, ex vivo CD4⁺ T cells isolated from Ets-1KO mice expressed a much higher level of IL-10 transcript compared with WT CD4⁺ T cells under unstimulated (>8-fold increase) and stimulated (>5-fold increase) conditions (Fig. 2A). A significant increase in IL-10 protein level (2-fold) was also observed in Ets-1KO cells compared with WT CD4⁺ T cells (Fig. 2B). Intracellular cytokine staining showed that ~0.5% of WT Th cells was stained positively for intracellular IL-10 ex vivo, whereas near 3% of Ets-1KO cells were positive for IL-10 (Fig. 2C). These results

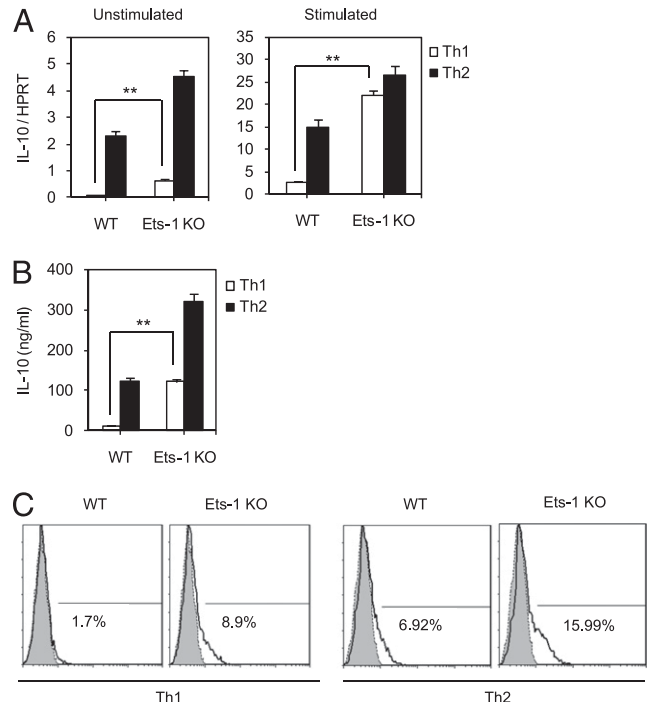


FIGURE 1. Enhanced IL-10 expression in Ets-1-deficient Th1 and Th2 cells. CD4⁺ T cells obtained from spleens and lymph nodes of WT and Ets-1KO mice were cultured under Th1- and Th2-skewing conditions, as described in *Materials and Methods*. **(A)** Total RNA was isolated from Th1 and Th2 cells unstimulated or restimulated with anti-CD3/anti-CD28 and subjected to real-time PCR (RT-PCR) analysis. Mouse *HPRT* was used as a control. **(B)** Differentiated Th1 and Th2 cells were restimulated using anti-CD3/anti-CD28 for 24 h. IL-10 levels in culture supernatant were analyzed by ELISA. All data are presented as means with SD from three to five independent experiments. **(C)** Intracellular IL-10 protein levels were measured by flow cytometry analysis after staining with IL-10 Ab or control isotype IgG. Data are representative of three separate experiments. ***p* < 0.01.

collectively indicate that Ets-1 plays a negative role in *Il10* gene regulation in both Th1 and Th2 cells.

Changes in histone modification and chromatin accessibility upon Ets-1 deficiency

To find out the underlying molecular mechanism of Ets-1-mediated *Il10* gene repression in Th1 cells, we analyzed whether Ets-1 deficiency caused any changes in chromatin architecture and epigenetic modifications around the *Il10* regulatory regions. We and others previously reported the involvement of epigenetic regulation in IL-10 expression (11–14). We have previously measured the levels of recruited H3Ac as a marker for transcriptionally active chromatin (34). We focused on four CNSs of the *Il10* locus identified with VISTA: promoter (−0.12), intron regions (+1.75 and +2.98), and 3' end (+6.45) (Fig. 3A). To measure the relative amount of H3Ac recruited to the promoter and intronic regions of the *Il10* locus, we performed ChIP with Ab specific for H3Ac. Consistent with the published data, a significant increase of H3Ac level was observed in WT Th2 cells compared with WT Th1 cells at the promoter (−0.12) and introns (+1.64 and +2.98) (Fig. 3B). However, the CNS+6.45 region did not show any difference in H3Ac levels between WT Th1 and Th2 cells. This observation is in agreement with the previous report showing no histone acetylation (H4Ac) in this region compared with other regions of the *Il10* locus (13). Interestingly, Ets-1KO Th1 cells displayed a pattern of H3Ac recruitment similar to that of WT Th2 cells. We further tested whether increased H3Ac recruitment and

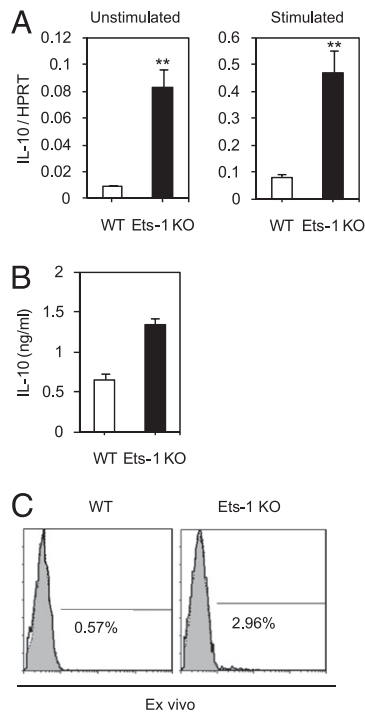


FIGURE 2. Enhanced ex vivo IL-10 expression in Ets-1-deficient CD4⁺ T cells. CD4⁺ T cells were obtained from spleens and lymph nodes of WT and Ets-1KO mice and stimulated directly with anti-CD3/anti-CD28 for 24 h or left unstimulated. **(A)** Total RNA was subjected to real-time PCR (RT-PCR) analysis. Mouse *HPRT* was used as a control. **(B)** IL-10 levels in culture supernatant were analyzed by ELISA. All data are presented as means with SD from three to five independent experiments. **(C)** Intracellular IL-10 protein levels were measured by flow cytometry analysis after staining with IL-10 Ab or control isotype IgG. Data are representative of three separate experiments. ***p* < 0.01.

higher IL-10 expression in Ets-1KO Th1 cells are associated with changes in the accessibility of chromatin architecture around the *Il10* locus. Nuclei were prepared from Th1 cells differentiated from WT and Ets-1KO CD4⁺ T cells and treated with MNase. The chromatin accessibility was measured by qRT-PCR. Ets-1KO Th1 cells showed a significantly increased chromatin accessibility than WT Th1 cells in the IL-10 promoter region, but not in CNS+1.65 and CNS+2.98 regions (Fig. 3C). The chromatin accessibility for the promoter region of *HPRT* and *H19* genes was also tested as control regions for open and closed accessibility, respectively. These results suggest that an increased IL-10 expression in Ets-1KO Th1 cells is correlated with enhanced chromatin accessibility and H3Ac enrichment.

Downregulation of HDAC1 recruitment in Ets-1-deficient Th1 cells

Acetylation of histone is regulated by HDACs (35). The class I deacetylase HDAC1 and HDAC2 are highly expressed in thymus and spleen, and HDAC1-associated factors, such as Ikaros, Aiolos, and Sin3A, play important roles during T cell development (36, 37). To examine whether the increased H3Ac recruitment and more accessible chromatin structure at the *Il10* locus in Ets-1KO Th1 cells are related with the loss of HDAC1 recruitment, we analyzed the level of in vivo HDAC1 binding to *Il10* regulatory loci by ChIP analysis. Previous studies including our own have showed that higher HDAC1 recruitment is inversely correlated to IL-10 expression (11, 12). In this study, we also confirmed the involvement of HDAC1 recruitment in differential IL-10 expression in Th1 and Th2 cells. Th1 cells expressing much lower IL-10

level than Th2 cells showed a preferential HDAC1 enrichment in promoter (−0.12) and intron regions (+1.65 and +2.98) (Fig. 4A). HDAC1 enrichment at the *Il10* regulatory regions, however, was significantly reduced in Ets-1KO Th1 cells to the comparable level of WT Th2 cells (Fig. 4A).

To further elucidate the role of HDAC in IL-10 repression, we tested the effect of HDAC inhibitor, trichostatin A (TsA), on IL-10 expression level and histone acetylation status in Th1 cells. CD4⁺ T cells obtained from WT and Ets-1KO were differentiated into Th1 cells. At day 4 of differentiation, cells were treated with TsA or DMSO (control) and then harvested 2 d later. TsA treatment significantly increased IL-10 expression up to 8-fold as measured by qRT-PCR (Fig. 4B). TsA treatment also increased IL-10 protein levels as measured by ELISA and intracellular cytokine staining (Fig. 4B, 4C). To test whether the increase of IL-10 expression by TsA treatment was also affected by changes in the recruitment of H3Ac to the regulatory elements of the *Il10* locus, we performed ChIP analysis. Indeed, TsA treatment significantly increased H3Ac recruitment at CNS−0.12, CNS+1.65, and CNS+2.98 (Fig. 4D). These results collectively suggest that Ets-1 deficiency reduced the recruitment of HDAC1 in *Il10* regulatory elements, which leads to increased histone acetylation and favorable chromatin architecture for upregulation of IL-10 expression.

Physical interaction between Ets-1 and HDAC1

We then set to determine how deficiency of Ets-1 led to a reduced level of HDAC1 recruitment in the *Il10* regulatory regions. We found that mRNA level of HDAC1 was not altered by Ets-1 deficiency (data not shown). However, HDAC1 protein level was slightly decreased in Ets-1KO Th1 cells compared with WT counterpart (Fig. 5A). However, this difference was subtle and could not account for the difference in HDAC1 recruitment shown in Fig. 4A. We therefore postulated that Ets-1 interacted directly with and recruited HDAC1 to the *Il10* locus. To test whether there is a physical interaction between Ets-1 and HDAC1, we performed coimmunoprecipitation experiment in HEK-293 cells that were transfected with Ets-1 and HDAC1 expression constructs. HDAC1 protein was detected by anti-HDAC1 immunoblotting (IB) in immunoprecipitate brought down by Ets-1 Ab (Fig. 5B, top panel). Conversely, immunoprecipitation with anti-HDAC1 Ab, but not control IgG, also pulled down Ets-1 protein (Fig. 5B, bottom panel). In addition, we were able to demonstrate a physical interaction between endogenous Ets-1 and HDAC1 proteins in vivo in primary Th1 cells by immunoprecipitation assay (Fig. 5C). To further confirm the colocalization of Ets-1 and HDAC1, we performed an in situ PLA (38). Because a PLA signal can be detected when the proteins of interest are in close proximity, this technique enabled us to detect direct protein–protein (Ets-1 and HDAC1) interaction in CD4⁺ T cells. Association of endogenous Ets-1 and HDAC1 in primary Th1 cells was observed and the interaction took place in the nucleus (Fig. 5D, upper row). The specificity of this interaction was confirmed by the absence of association between Ets-1 with HDAC1 in Ets-1KO Th1 cells (Fig. 5D, bottom row).

Functional synergism of Ets-1 and HDAC1 to repress IL-10 expression

To test the relationship between Ets-1 recruitment and the differential IL-10 expression profile, we performed an Ets-1 ChIP assay in Th1 (IL-10^{low}) and Th2 (IL-10^{high}) cells, using an Ets-1-specific Ab. Specific binding of Ets-1 to the IL-10 regulatory elements was confirmed using Ets-1KO mice as a negative control in Th1 cells (Fig. 6A). No significant difference was observed in

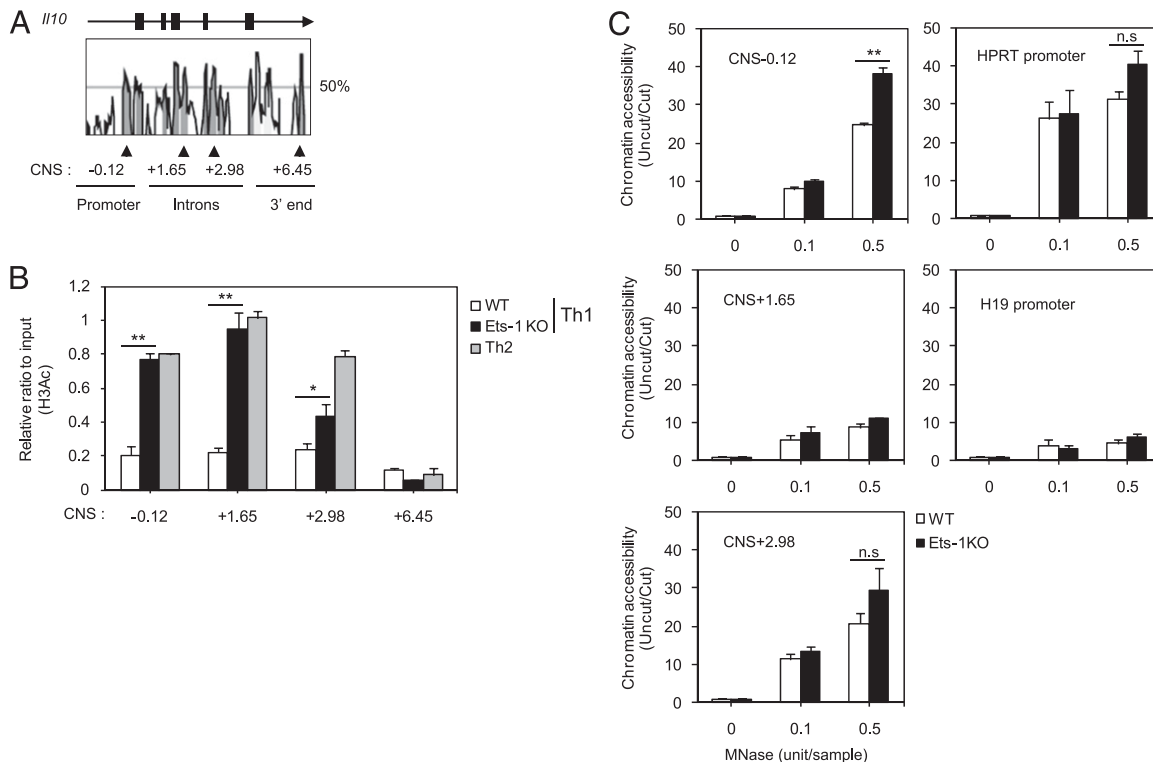


FIGURE 3. Accessible chromatin configuration at the *Il10* regulatory regions in Ets-1KO Th1 cells. **(A)** CNSs in the *Il10* loci of mouse and human are shown. The mouse genomic sequence is used as the base sequence on the *x*-axis. CNS regions are marked with arrowheads. CNS regions are named according to their distance in kilobases from the IL-10 transcription start site. **(B)** ChIP was performed using WT and Ets-1KO Th1 cells with anti-H3Ac or isotype IgG Ab, and the levels of precipitated DNA were measured by qRT-PCR with primers specific for each indicated CNS region. **(C)** Nuclei isolated from WT or Ets-1KO Th1 cells were left untreated or subjected to MNase treatment, as described in *Materials and Methods*. Extracted genomic DNA was then subjected to RT-PCR using specific primers for indicated regulatory regions. Graphs depict the relative chromatin accessibility normalized to undigested samples and show mean \pm SEM, $n = 3$. All data are presented as means with SD from three independent experiments. * $p < 0.05$, ** $p < 0.01$.

the level of Ets-1 enrichment between Th1 and Th2 cells (Fig. 6B). We further examined the functional significance of the interaction between Ets-1 and HDAC1 in the repression of *Il10* gene expression. We performed in vitro reporter assay using IL-10 re-

porter constructs containing a minimal IL-10 promoter and the diverse CNSs (30). Overexpression of Ets-1 alone failed to repress the IL-10 reporter activity of CNS-0.12 (Fig. 6C, upper panel, fourth bar). Interestingly, Ets-1 alone actually induced reporter

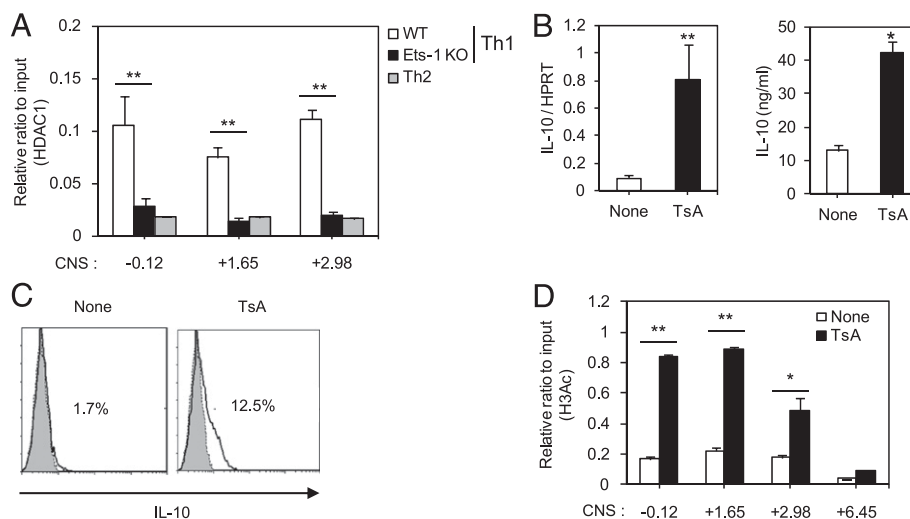


FIGURE 4. Increased IL-10 expression upon treatment of HDAC inhibitor, TsA. **(A)** ChIP was performed using WT and Ets-1KO Th1 cells with anti-HDAC1 or isotype IgG Ab, and levels of precipitated DNA were measured by qRT-PCR with primers specific for each indicated CNS region. All data are presented as means with SD from three independent experiments. **(B)** IL-10 mRNA and protein level were analyzed by qRT-PCR and ELISA. **(C)** Intracellular IL-10 protein level was measured by flow cytometry analysis after intracellular cytokine staining with IL-10 Ab or control isotype IgG. **(D)** ChIP was performed on nontreated or TsA-treated cells with anti-H3Ac or isotype IgG Ab, and levels of precipitated DNA were measured by qRT-PCR with primers specific for each indicated CNS region. All data are presented as means with SD from three independent experiments; intracellular cytokine staining data are representative of three separate experiments. * $p < 0.05$, ** $p < 0.01$.

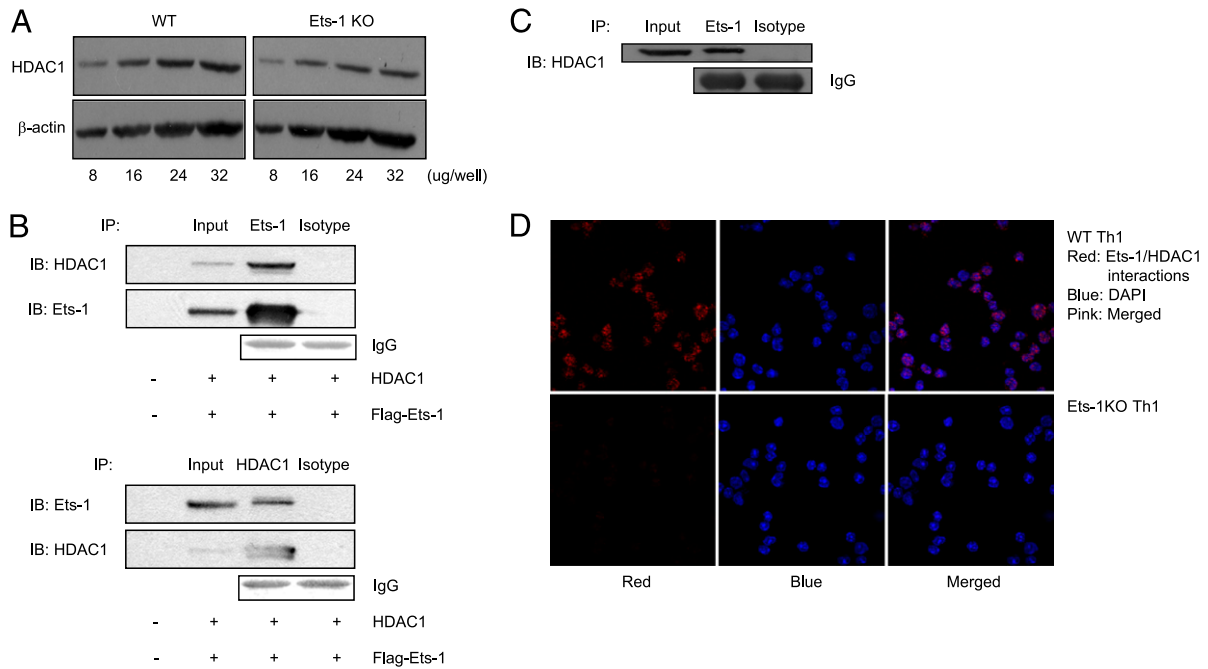


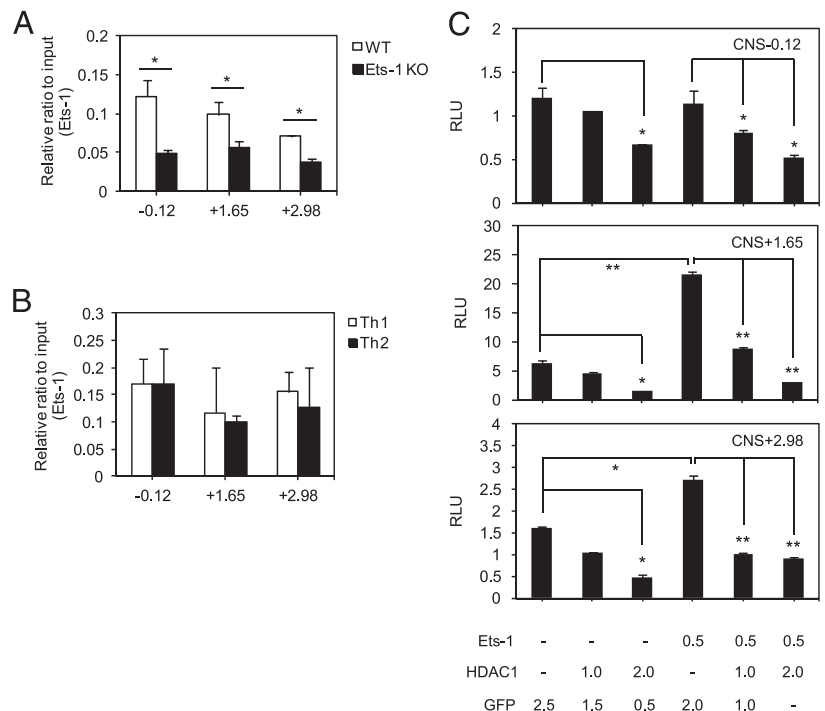
FIGURE 5. Physical interaction of Ets-1 with HDAC1. **(A)** Total cell lysates of WT or Ets-1KO Th1 cells were prepared and total HDAC1 levels were assayed by Western blot. Ab to β -actin was used as a loading control. **(B)** Flag-Ets-1 and HDAC1 constructs were transiently transfected into HEK-293 cells. Transfected cells were harvested after 24 h and lysates were IP with Ets-1 or isotype IgG Ab. Coprecipitated HDAC1 was analyzed by IB with HDAC1 Ab. IP of Ets-1 was confirmed by IB with Ets-1 Ab. Conversely, transfected cells were harvested after 24 h and lysates were IP with HDAC1 or isotype IgG Ab. Coprecipitated Ets-1 was analyzed by IB with Ets-1 Ab. IP of HDAC1 was confirmed by IB with HDAC1 Ab. **(C)** Primary Th1 cells were used for immunoprecipitation with Ets-1 Ab, then detected with HDAC1 Ab. Ponceau S-stained IgG H chain was shown as a loading control (IgG). Immunoprecipitation using rabbit IgG (isotype) was used as a negative control for coimmunoprecipitation. **(D)** Detection of Ets-1 and HDAC1 interaction in primary WT Th1 and Ets-1KO Th1 cells using Duolink with two primary Abs. Duolink signals are shown in red, and DAPI was used for staining of nuclei. Stained cells were examined by confocal microscopy (original magnification $\times 60$). Data were representative of three independent experiments.

activity of CNS+1.65 and CNS+2.98. However, dose-dependent overexpression of HDAC1 significantly decreased Ets-1-induced IL-10 reporter activity (Fig. 6C, fifth and sixth bars). These results suggest that Ets-1-mediated repression of IL-10 expression is dependent on HDAC1.

Role of T-bet or STAT4 in Ets-1-mediated IL-10 repression

A previous report showed that Ets-1 deficiency could decrease the level of STAT4 and T-bet expression (21). However, the exact role of T-bet or STAT4 in regulating IL-10 expression still remains undefined. Thus, we tested whether the increased IL-10 expression

FIGURE 6. Suppression of IL-10 expression by functional cooperation between Ets-1 and HDAC1. **(A)** ChIP was performed using WT and Ets-1KO Th1 cells with anti-Ets-1 or isotype IgG Ab, and the levels of precipitated DNA were measured by qRT-PCR with primers specific for each indicated CNS region. **(B)** Ets-1 recruitment in the *Il10* regulatory regions in Th1 and Th2 cells. ChIP assay was performed using primary Th1 and Th2 cells. Quantitative real-time PCR was performed on each CNS region as indicated. Data are presented as means with SD from three independent experiments. **(C)** HEK-293 cells were transfected with the indicated IL-10 CNS reporter constructs together with Ets-1 or HDAC1 alone, or Ets-1 plus HDAC1 in combination. Luciferase activity is expressed relative to the expression of a cotransfected *Renilla* luciferase plasmid (pRL-TK) as a control for transfection efficiency. Relative luciferase units are expressed as the fold difference relative to the control value. Data shown are the average of at least three independent experiments. * $p < 0.05$, ** $p < 0.01$.



in Ets-1-deficient Th1 cells is a result of a defect in Th1 cell differentiation and whether T-bet or STAT4 deficiency is linked to differential Ets-1 recruitment to the IL-10 regulatory sites. The effect of T-bet or STAT4 deficiency on IL-10 expression was analyzed. CD4⁺ T cells from T-betKO and STAT4KO were differentiated into Th1 cells, and IL-10 levels were measured by RT-PCR and ELISA. In vitro differentiated Th1 cells from T-betKO and STAT4KO did not show any significant differences in the levels of IL-10 production, mRNA (data not shown), and protein (Fig. 7A, 7D). As expected, T-betKO and STAT4KO T cells showed significantly reduced IFN- γ , whereas IL-4 level was up-regulated (Supplemental Fig. 1). Next, we performed Ets-1 ChIP analysis to test the effect of T-bet or STAT4 deficiency on the recruitment of Ets-1 and HDAC1 to the IL-10 regulatory sites. T-bet or STAT4 deficiency slightly increased Ets-1 binding to CNS-0.12 and CNS+1.65, but not CNS+2.98. However, no significant difference was observed in the level of HDAC1 recruitment to the IL-10 regulatory sites, which is well correlated with the similar level of IL-10 expression, regardless of T-betKO and STAT4KO deficiency (Fig. 7A, 7D). This result suggests that T-bet or STAT4 may not directly regulate Ets-1-mediated IL-10 repression in Th1 cells.

Increased IL-24 and CCR8 expression in Ets-1-deficient Th1 cells

We also tested whether the Ets-1 and HDAC1 interaction could also downregulate the expression of Th2 cell-associated molecules in Th1 cells. Similar to IL-10 expression in Th1 cells, IL-24 level is significantly lower in Th1 than Th2 cells (39). Chemokine receptor CCR8 is also preferentially expressed in Th2, but not Th1 cells (40). Because both targets have relatively low expression level in Th1 cells, we tested the effect of Ets-1 deficiency on the expression level of *Ii24* and *Ccr8* mRNA. Ets-1KO Th1 cells showed an increase in both *Ii24* and *Ccr8* expression level (Fig. 8A). To further confirm the physical association of Ets-1 and HDAC1 to the promoter of *Ii24* and *Ccr8* loci, we performed Ets-1 and HDAC1 ChIP experiments. *Bcl2l1* 3'UTR region was used as a negative binding region for Ets-1 and HDAC1 (41). Significant enrichment of Ets-1 and HDAC1 was observed in the promoter region of *Ii24* and *Ccr8* compared with the negative *Bcl2l1* locus (Fig. 8B, 8C). In addition, Ets-1 deficiency significantly increased the level of H3Ac recruitment to the *Ii24* and *Ccr8* promoter

regions (Fig. 8D). These results collectively suggest that interaction of Ets-1 with HDAC1 could repress the expression of Th2 cell-associated molecules, such as *Ii10*, *Ii24*, and *Ccr8*, in Th1 cells by affecting histone modification of regulatory elements.

Discussion

The main purpose of this study was to elucidate the molecular mechanism of Ets-1-mediated *Ii10* gene repression in Th1 cells. We demonstrated that Ets-1 negatively regulates IL-10 expression through functional and physical cooperation with HDAC1 in Th1 cells. Ets-1 deficiency resulted in increased H3Ac recruitment and chromatin accessibility, whereas decreasing HDAC1 recruitment in the *Ii10* regulatory regions. Physical interaction between Ets-1 and HDAC1 cooperatively repressed IL-10 transcription in Th1 cells.

Unlike subset-specific Th cytokines, such as IFN- γ and IL-4, IL-10 is relatively promiscuous and can be produced by both Th2 and Th1 cells. Although Th2 cells express a much higher amount of IL-10 (11, 12), Th1 cells also express IL-10 under certain conditions (2, 5–10) through unknown mechanisms. We have previously shown that Ets-1-deficient Th1 cells produced larger amounts of IL-10 than WT Th1 cells (21). In this study, we further confirmed a significant increase of IL-10 expression in ex vivo isolated Ets-1KO CD4 T cells (Fig. 2). Ets-1 is a transcription factor and has a dual function, acting as both a transcriptional activator and repressor (16, 42, 43). In most cases, Ets-1 positively regulates the expression of its target genes (23). However, Ets-1 can also suppress its target gene through interacting with repressive factors like EAP1/Daxx (44). Recently, Hollenhorst et al. (45) reported an enrichment of Ets-1 in regulatory elements of the *Ii10* locus through ChIP-seq analysis in human Jurkat T cell. We also found in vivo binding of Ets-1 in the regulatory regions of the *Ii10* gene including promoter, intron 3, and intron 4 regions (Fig. 6A). However, the amount of Ets-1 binding was similar in Th1 (IL-10^{low}) and Th2 (IL-10^{high}) cells (Fig. 6B). How does Ets-1 binding selectively repress IL-10 expression in Th1 cells? We assumed that Ets-1 may regulate IL-10 expression by altering the local chromatin architecture. Indeed, chromatin accessibility was significantly increased in Ets-1KO Th1 cells, mainly at the IL-10 promoter region (Fig. 3C), in comparison with WT Th1 cells. We also tested the H3Ac level in *Ii10* regulatory regions because H3Ac is one of the well-characterized active marks of histone

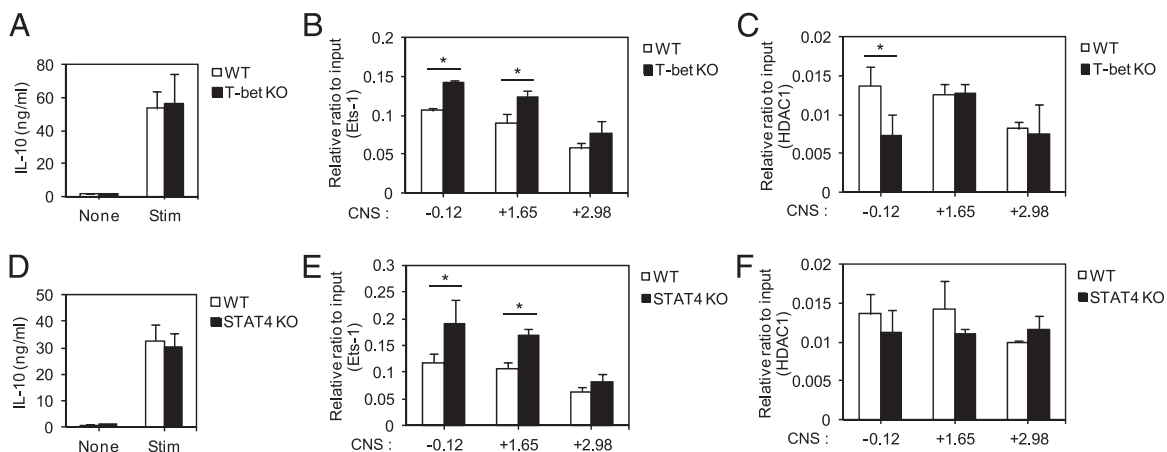
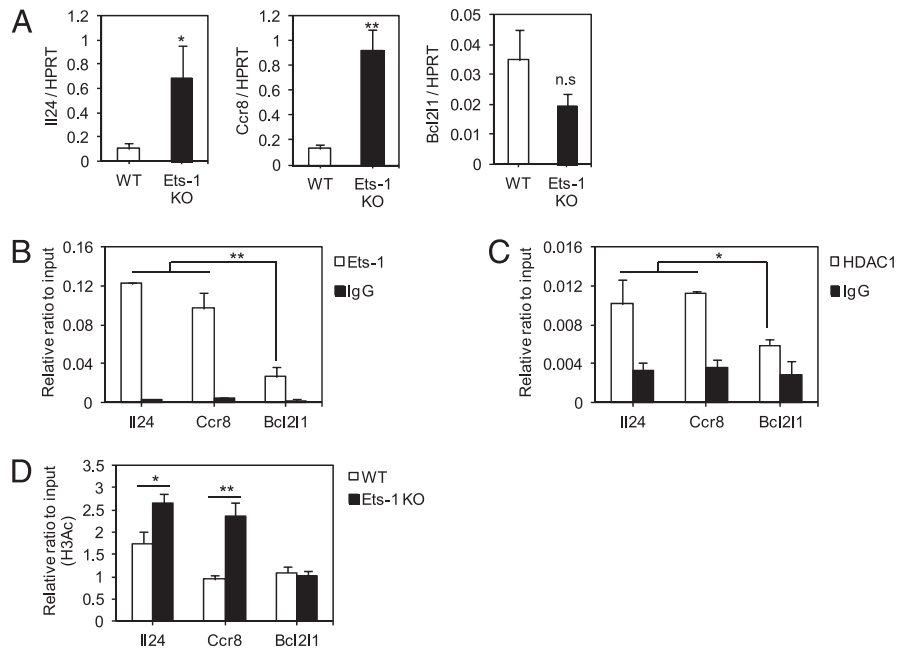


FIGURE 7. Role of T-bet or STAT4 on Ets-1-mediated IL-10 repression in Th1 cells. (A and D) CD4⁺ T cells were isolated from WT and T-betKO or STAT4KO mice. After 6 d of Th1 differentiation, cells were stimulated with anti-CD3/anti-CD28. IL-10 expression was analyzed by ELISA. (B and E) ChIP was performed using WT and T-betKO or STAT4KO Th1 cells with anti-Ets-1 or isotype IgG Ab. (C and F) ChIP was performed using WT and T-betKO or STAT4KO Th1 cells with anti-HDAC1 or isotype IgG Ab, and the levels of precipitated DNA were measured by qRT-PCR with primers specific for each indicated CNS region. Results showed mean \pm SEM, $n = 3$. All data are presented as means with SD from three independent experiments. * $p < 0.05$.

FIGURE 8. Repression of *Il24* and *Ccr8* expression by Ets-1 and HDAC1. **(A)** RNA was isolated from WT and Ets-1KO Th1 cells under unstimulated conditions after 6 d of differentiation. *Il24* and *Ccr8* mRNA were analyzed by qRT-PCR, and *Bcl2l1* was used as a negative control. **(B and C)** ChIP was performed using WT Th1 cells with anti-Ets-1 or anti-HDAC1 Ab. Promoter regions of *IL-24* and *Ccr8* were used for enrichment of Ets-1 and HDAC1, whereas *Bcl2l1* 3'UTR regions were regarded as a negative region. **(D)** ChIP was performed using WT and Ets-1KO Th1 cells with anti-H3Ac or isotype IgG Ab (and the levels of precipitated DNA were measured by qRT-PCR with primers specific for each indicated region). Results showed mean \pm SEM; $n = 3$. All data are presented as means with SD from three independent experiments. * $p < 0.05$, ** $p < 0.01$.



modification in gene expression (34, 35, 46, 47). Ets-1KO Th1 cells showed a significantly higher H3Ac level around the *Il10* regulatory regions (Fig. 3B). These results suggest that higher expression level of IL-10 in Ets-1KO Th1 cells is closely linked with enhanced histone acetylation status (11, 13).

DNA binding proteins often interact with and recruit HDAC proteins to exert their suppressive activity on target gene expression (46). The increased chromatin accessibility together with enriched H3Ac level in Ets-1KO Th1 cells suggest the involvement of differential recruitment of silencing complexes. HDAC proteins are the main regulators of histone deacetylation (35). Previously, we reported that HDAC1 was enriched in the promoter and introns 3 and 4 of the *Il10* gene in D5 cells (Th1 clone) (11). Recently, Villagra et al. (48) also reported that HDAC11 regulated IL-10 expression in APCs. In this study, we found a significant decrease of HDAC1 recruitment in *Il10* regulatory regions in Ets-1KO Th1 cells compared with WT Th1 cells (Fig. 4A). Treatment of TSA, an HDAC inhibitor, significantly enhanced IL-10 expression in Th1 cells by decreasing HDAC1 recruitment (Fig. 4B–D). These results suggest the involvement of histone deacetylase activity in the repression of *Il10* expression. The effects of TSA in this experimental system may be direct, because the TSA treatment did not affect Ets-1 expression level but increased the level of IL-10 expression. However, the effect of TSA might also be indirect, because TSA can affect the expression of other genes, which indirectly regulate IL-10 expression.

Ets-1 deficiency did not cause any significant differences in HDAC1 mRNA levels (data not shown), although a slight decrease of HDAC1 protein level was observed in Ets-1KO Th1 cells (Fig. 5A). However, this difference in the level of HDAC1 protein is subtle and, in our view, is insufficient to explain the marked reduction in HDAC1 recruitment to the *Il10* gene seen in Ets-1KO Th1 cells. Overexpression of Ets-1 alone failed to suppress IL-10 reporter activity rather than activate reporter activities of CNS+1.65 and CNS+2.98 (Fig. 6C). However, HDAC1 coexpression efficiently suppressed *Il10* reporter activity, suggesting the important role of HDAC1 as a composite repressor of the Ets-1 complex. Our data collectively suggest that Ets-1 negatively regulates IL-10 expression by affecting histone modification states and HDAC1

recruitment. Ets-1-mediated recruitment of HDAC1 likely is also subjective to regulation by yet to be characterized mechanisms.

It is known that IFN- γ can suppress the expression of Th2 cytokines, including IL-10, raising the possibility that overproduction of IL-10 by Ets-1KO Th1 cells may be a secondary effect, because of the reduced IFN- γ level. Upon Ets-1 deficiency, a decreased level of STAT4 and T-bet expression was also observed (21). In this study, we tested whether T-bet or STAT4 deficiency could mediate differential Ets-1 and HDAC1 recruitment to the IL-10 regulatory sites. However, no quantitative differences were observed in the level of IL-10 expression by T-bet or STAT4 deficiency in Th1 compared with WT Th1 cells (Fig. 7A, 7D). In addition, it has been reported that T-bet deficiency did not cause any effect on IL-10 production by NK cells (49). According to another report in Th1 cells, STAT4 may positively regulate IL-10 production, rather than repress it, under the control of IL-12 stimulation (10). Furthermore, T-bet or STAT4 deficiency did not cause statistically significant changes in the level of Ets-1 and HDAC1 recruitment to the IL-10 regulatory sites, suggesting that T-bet or STAT4 may not be directly involved in Ets-1-mediated IL-10 repression in Th1 cells.

Function of Ets-1 is mainly dependent upon its interaction with other binding partners (16, 42, 43, 50). For example, Ets-1 cooperates with transcriptional coactivator CREB binding protein and the related p300 protein to upregulate its target genes (51). In contrast, Ets-1 cooperates with EAP1/Daxx to repress its target genes (44). Therefore, Ets-1-mediated recruitment of HDAC1 might be heavily influenced by its binding partners. In this study, we demonstrated that HDAC1 is the major partner of Ets-1-mediated IL-10 repression (Fig. 5). However, other repressor proteins could also composite as an Ets-1 repressor complex. To identify the Ets-1 interacting protein partners, we have recently performed mass spectrometry using the Ets-1 immunoprecipitated (IP) protein complex. We confirmed the interaction of Ets-1 with HDAC1, mSin3a, and DNA methyltransferase 3a and 3b (C.G. Lee and S.-H. Im, unpublished data). Those molecules could form an Ets-1 repressor complex and affect the epigenetic status of DNA methylation (52, 53) and histone modifications, resulting in an inactive chromatin configuration at the Ets-1 target gene loci.

However, it is still unclear whether the formation of the Ets-1 and HDAC1 complex is a general mechanism to suppress Ets-1 target genes. To test this idea, we analyzed two target genes, *Il24* and *Ccr8*, that are known to have higher expression in Th2 compared with Th1 cells. Like IL-10, Ets-1 deficiency significantly increased the expression level of *Il24* and *Ccr8* mRNA in Th1 cells by increasing H3Ac levels in the promoter regions (Fig. 8D). Recently, we have performed an expression microarray to observe the transcriptional changes between WT Th1 and Ets-1KO Th1 cells. More than 800 genes were identified as potential Ets-1 target genes. Among them, 312 genes were upregulated (data not shown). Currently, we are investigating whether the formation of an Ets-1 and HDAC1 complex is also involved in the repression of these newly identified Ets-1 target genes.

Another possible scenario is that the ability of Ets-1 to recruit HDAC1 is regulated by its posttranslational modifications, which may differ in Th1 and Th2 cells. Phosphorylation is a well-known posttranslational modification of the ETS family of transcription factors (17). Phosphorylation of Ets-1 can enhance or attenuate its transcriptional activity (54–56). However, neither activating nor inhibitory phosphorylation of Ets-1 had much impact on Th cytokine production (57). Acetylation of Ets-1 often results in the upregulation of target gene expression because acetylated Ets-1 is preferentially associated with the p300/CREB binding protein complexes (58). However, the effect of acetylated Ets-1 in IL-10-expressing cells has yet to be reported so far and needs further investigation.

In summary, our work advances our understanding of how Ets-1 suppresses IL-10 expression. Our findings are also clinically relevant. Single nucleotide polymorphisms at the *Ets1* locus were recently shown to be associated with a greater risk for systemic lupus erythematosus (SLE) (59, 60). Patients with SLE often overproduce IL-10, the level of which correlates with disease activity (61, 62). However, the molecular mechanism mediating the overproduction of IL-10 is poorly understood. It will be of great interest to investigate whether the recruitment of Ets-1 and/or HDAC1 to the *Il10* locus is altered and whether the interaction between Ets-1 and HDAC1 is disrupted in SLE patients.

Acknowledgments

We thank our colleagues in the laboratory for valuable comments on the work and Dr. Darren Williams, Gwangju Institute of Science and Technology, for critical review of the manuscript.

Disclosures

The authors have no financial conflicts of interest.

References

- Moore, K. W., R. de Waal Malefyt, R. L. Coffman, and A. O'Garra. 2001. Interleukin-10 and the interleukin-10 receptor. *Annu. Rev. Immunol.* 19: 683–765.
- O'Garra, A., and P. Vieira. 2007. T(H)1 cells control themselves by producing interleukin-10. *Nat. Rev. Immunol.* 7: 425–428.
- Murphy, K. M., and S. L. Reiner. 2002. The lineage decisions of helper T cells. *Nat. Rev. Immunol.* 2: 933–944.
- Wilson, C. B., E. Rowell, and M. Sekimata. 2009. Epigenetic control of T-helper-cell differentiation. *Nat. Rev. Immunol.* 9: 91–105.
- Trinchieri, G. 2007. Interleukin-10 production by effector T cells: Th1 cells show self control. *J. Exp. Med.* 204: 239–243.
- Anderson, C. F., M. Oukka, V. J. Kuchroo, and D. Sacks. 2007. CD4(+)CD25(-) Foxp3(-) Th1 cells are the source of IL-10-mediated immune suppression in chronic cutaneous leishmaniasis. *J. Exp. Med.* 204: 285–297.
- Jankovic, D., M. C. Kullberg, C. G. Feng, R. S. Goldszmid, C. M. Collazo, M. Wilson, T. A. Wynn, M. Kamanaka, R. A. Flavell, and A. Sher. 2007. Conventional T-bet(+)Foxp3(-) Th1 cells are the major source of host-protective regulatory IL-10 during intracellular protozoan infection. *J. Exp. Med.* 204: 273–283.
- Batten, M., N. M. Kljavin, J. Li, M. J. Walter, F. J. de Sauvage, and N. Ghilardi. 2008. Cutting edge: IL-27 is a potent inducer of IL-10 but not FoxP3 in murine T cells. *J. Immunol.* 180: 2752–2756.
- Rutz, S., M. Janke, N. Kassner, T. Hohnstein, M. Krueger, and A. Scheffold. 2008. Notch regulates IL-10 production by T helper 1 cells. *Proc. Natl. Acad. Sci. USA* 105: 3497–3502.
- Saraiva, M., J. R. Christensen, M. Veldhoen, T. L. Murphy, K. M. Murphy, and A. O'Garra. 2009. Interleukin-10 production by Th1 cells requires interleukin-12-induced STAT4 transcription factor and ERK MAP kinase activation by high antigen dose. *Immunity* 31: 209–219.
- Im, S. H., A. Hueber, S. Monticelli, K. H. Kang, and A. Rao. 2004. Chromatin-level regulation of the IL10 gene in T cells. *J. Biol. Chem.* 279: 46818–46825.
- Jones, E. A., and R. A. Flavell. 2005. Distal enhancer elements transcribe intergenic RNA in the IL-10 family gene cluster. *J. Immunol.* 175: 7437–7446.
- Chang, H. D., C. Helbig, L. Tykocinski, S. Kreher, J. Koeck, U. Niesner, and A. Radbruch. 2007. Expression of IL-10 in Th memory lymphocytes is conditional on IL-12 or IL-4, unless the IL-10 gene is imprinted by GATA-3. *Eur. J. Immunol.* 37: 807–817.
- Shoemaker, J., M. Saraiva, and A. O'Garra. 2006. GATA-3 directly remodels the IL-10 locus independently of IL-4 in CD4+ T cells. *J. Immunol.* 176: 3470–3479.
- Wang, Z. Y., H. Sato, S. Kusam, S. Sehara, L. M. Toney, and A. L. Dent. 2005. Regulation of IL-10 gene expression in Th2 cells by Jun proteins. *J. Immunol.* 174: 2098–2105.
- Sharrocks, A. D. 2001. The ETS-domain transcription factor family. *Nat. Rev. Mol. Cell Biol.* 2: 827–837.
- Dittmer, J. 2003. The biology of the Ets1 proto-oncogene. *Mol. Cancer* 2: 29.
- Barton, K., N. Muthusamy, C. Fischer, C. N. Ting, T. L. Walunas, L. L. Lanier, and J. M. Leiden. 1998. The Ets-1 transcription factor is required for the development of natural killer cells in mice. *Immunity* 9: 555–563.
- Bories, J. C., D. M. Willerford, D. Grévin, L. Davidson, A. Camus, P. Martin, D. Stéhelin, and F. W. Alt. 1995. Increased T-cell apoptosis and terminal B-cell differentiation induced by inactivation of the Ets-1 proto-oncogene. *Nature* 377: 635–638.
- Muthusamy, N., K. Barton, and J. M. Leiden. 1995. Defective activation and survival of T cells lacking the Ets-1 transcription factor. *Nature* 377: 639–642.
- Grenningloh, R., B. Y. Kang, and I. C. Ho. 2005. Ets-1, a functional cofactor of T-bet, is essential for Th1 inflammatory responses. *J. Exp. Med.* 201: 615–626.
- Moisan, J., R. Grenningloh, E. Bettelli, M. Oukka, and I. C. Ho. 2007. Ets-1 is a negative regulator of Th17 differentiation. *J. Exp. Med.* 204: 2825–2835.
- Russell, L., and L. A. Garrett-Sinha. 2010. Transcription factor Ets-1 in cytokine and chemokine gene regulation. *Cytokine* 51: 217–226.
- Blumenthal, S. G., G. Aichele, T. Wirth, A. P. Czernilofsky, A. Nordheim, and J. Dittmer. 1999. Regulation of the human interleukin-5 promoter by Ets transcription factors. Ets1 and Ets2, but not Elf-1, cooperate with GATA3 and HTLV-1 Tax1. *J. Biol. Chem.* 274: 12910–12916.
- Romano-Spica, V., P. Georgiou, H. Suzuki, T. S. Papas, and N. K. Bhat. 1995. Role of ETS1 in IL-2 gene expression. *J. Immunol.* 154: 2724–2732.
- Thomas, R. S., M. J. Tymms, L. H. McKinlay, M. F. Shannon, A. Seth, and I. Kola. 1997. ETS1, NFκB and AP1 synergistically transactivate the human GM-CSF promoter. *Oncogene* 14: 2845–2855.
- Wang, D., S. A. John, J. L. Clements, D. H. Percy, K. P. Barton, and L. A. Garrett-Sinha. 2005. Ets-1 deficiency leads to altered B cell differentiation, hyperresponsiveness to TLR9 and autoimmune disease. *Int. Immunol.* 17: 1179–1191.
- Szabo, S. J., B. M. Sullivan, C. Stemmann, A. R. Satoskar, B. P. Sleckman, and L. H. Glimcher. 2002. Distinct effects of T-bet in TH1 lineage commitment and IFN-γ production in CD4 and CD8 T cells. *Science* 295: 338–342.
- Kaplan, M. H., Y. L. Sun, T. Hoey, and M. J. Grusby. 1996. Impaired IL-12 responses and enhanced development of Th2 cells in Stat4-deficient mice. *Nature* 382: 174–177.
- Lee, C. G., K. H. Kang, J. S. So, H. K. Kwon, J. S. Son, M. K. Song, A. Sahoo, H. J. Yi, K. C. Hwang, T. Matsuyama, et al. 2009. A distal cis-regulatory element, CNS-9, controls NFAT1 and IRF4-mediated IL-10 gene activation in T helper cells. *Mol. Immunol.* 46: 613–621.
- Nelson, J. D., O. Denisenko, and K. Bomsztyk. 2006. Protocol for the fast chromatin immunoprecipitation (ChIP) method. *Nat. Protoc.* 1: 179–185.
- Rao, S., E. Procko, and M. F. Shannon. 2001. Chromatin remodeling, measured by a novel real-time polymerase chain reaction assay, across the proximal promoter region of the IL-2 gene. *J. Immunol.* 167: 4494–4503.
- Mayor, C., M. Brudno, J. R. Schwartz, A. Poliakov, E. M. Rubin, K. A. Frazer, L. S. Pachter, and I. Dubchak. 2000. VISTA: visualizing global DNA sequence alignments of arbitrary length. *Bioinformatics* 16: 1046–1047.
- Kouzarides, T. 2007. Chromatin modifications and their function. *Cell* 128: 693–705.
- Berger, S. L. 2007. The complex language of chromatin regulation during transcription. *Nature* 447: 407–412.
- Koipally, J., A. Renold, J. Kim, and K. Georgopoulos. 1999. Repression by Ikaros and Aiolos is mediated through histone deacetylase complexes. *EMBO J.* 18: 3090–3100.
- Cowley, S. M., B. M. Iritani, S. M. Mendrysa, T. Xu, P. F. Cheng, J. Yada, H. D. Liggitt, and R. N. Eisenman. 2005. The mSin3A chromatin-modifying complex is essential for embryogenesis and T-cell development. *Mol. Cell Biol.* 25: 6990–7004.
- Fredriksson, S., M. Gullberg, J. Jarvius, C. Olsson, K. Pietras, S. M. Gústafsdóttir, A. Ostman, and U. Landegren. 2002. Protein detection using proximity-dependent DNA ligation assays. *Nat. Biotechnol.* 20: 473–477.
- Sahoo, A., C. G. Lee, A. Jash, J. S. Son, G. Kim, H. K. Kwon, J. S. So, and S. H. Im. 2011. Stat6 and c-Jun mediate Th2 cell-specific IL-24 gene expression. *J. Immunol.* 186: 4098–4109.
- Soler, D., T. R. Chapman, L. R. Poisson, L. Wang, J. Cote-Sierra, M. Ryan, A. McDonald, S. Badola, E. Fedyk, A. J. Coyle, et al. 2006. CCR8 expression

- identifies CD4 memory T cells enriched for FOXP3+ regulatory and Th2 effector lymphocytes. *J. Immunol.* 177: 6940–6951.
41. Hollenhorst, P. C., A. A. Shah, C. Hopkins, and B. J. Graves. 2007. Genome-wide analyses reveal properties of redundant and specific promoter occupancy within the ETS gene family. *Genes Dev.* 21: 1882–1894.
 42. Oikawa, T., and T. Yamada. 2003. Molecular biology of the Ets family of transcription factors. *Gene* 303: 11–34.
 43. Verger, A., and M. Duterque-Coquillaud. 2002. When Ets transcription factors meet their partners. *Bioessays* 24: 362–370.
 44. Li, R., H. Pei, D. K. Watson, and T. S. Papas. 2000. EAP1/Daxx interacts with ETS1 and represses transcriptional activation of ETS1 target genes. *Oncogene* 19: 745–753.
 45. Hollenhorst, P. C., K. J. Chandler, R. L. Poulsen, W. E. Johnson, N. A. Speck, and B. J. Graves. 2009. DNA specificity determinants associate with distinct transcription factor functions. *PLoS Genet.* 5: e1000778.
 46. Narlikar, G. J., H. Y. Fan, and R. E. Kingston. 2002. Cooperation between complexes that regulate chromatin structure and transcription. *Cell* 108: 475–487.
 47. Schübeler, D., D. M. MacAlpine, D. Scalzo, C. Wirbelauer, C. Kooperberg, F. van Leeuwen, D. E. Gottschling, L. P. O'Neill, B. M. Turner, J. Delrow, et al. 2004. The histone modification pattern of active genes revealed through genome-wide chromatin analysis of a higher eukaryote. *Genes Dev.* 18: 1263–1271.
 48. Villagra, A., F. Cheng, H. W. Wang, I. Suarez, M. Glogzak, M. Maurin, D. Nguyen, K. L. Wright, P. W. Atadja, K. Bhalla, et al. 2009. The histone deacetylase HDAC11 regulates the expression of interleukin 10 and immune tolerance. *Nat. Immunol.* 10: 92–100.
 49. Grant, L. R., Z. J. Yao, C. M. Hedrich, F. Wang, A. Moorthy, K. Wilson, D. Ranatunga, and J. H. Bream. 2008. Stat4-dependent, T-bet-independent regulation of IL-10 in NK cells. *Genes Immun.* 9: 316–327.
 50. Wasyluk, B., S. L. Hahn, and A. Giovane. 1993. The Ets family of transcription factors. *Eur. J. Biochem.* 211: 7–18.
 51. Yang, C., L. H. Shapiro, M. Rivera, A. Kumar, and P. K. Brindle. 1998. A role for CREB binding protein and p300 transcriptional coactivators in Ets-1 transactivation functions. *Mol. Cell. Biol.* 18: 2218–2229.
 52. Aalfs, J. D., and R. E. Kingston. 2000. What does 'chromatin remodeling' mean? *Trends Biochem. Sci.* 25: 548–555.
 53. Ng, H. H., and A. Bird. 2000. Histone deacetylases: silencers for hire. *Trends Biochem. Sci.* 25: 121–126.
 54. Cowley, D. O., and B. J. Graves. 2000. Phosphorylation represses Ets-1 DNA binding by reinforcing autoinhibition. *Genes Dev.* 14: 366–376.
 55. Pufall, M. A., G. M. Lee, M. L. Nelson, H. S. Kang, A. Velyvis, L. E. Kay, L. P. McIntosh, and B. J. Graves. 2005. Variable control of Ets-1 DNA binding by multiple phosphates in an unstructured region. *Science* 309: 142–145.
 56. Nelson, M. L., H. S. Kang, G. M. Lee, A. G. Blaszcak, D. K. Lau, L. P. McIntosh, and B. J. Graves. 2010. Ras signaling requires dynamic properties of Ets1 for phosphorylation-enhanced binding to coactivator CBP. *Proc. Natl. Acad. Sci. USA* 107: 10026–10031.
 57. Grenningloh, R., S. C. Miaw, J. Moisan, B. J. Graves, and I. C. Ho. 2008. Role of Ets-1 phosphorylation in the effector function of Th cells. *Eur. J. Immunol.* 38: 1700–1705.
 58. Czuwara-Ladykowska, J., V. I. Sementchenko, D. K. Watson, and M. Trojanowska. 2002. Ets1 is an effector of the transforming growth factor beta (TGF-beta) signaling pathway and an antagonist of the profibrotic effects of TGF-beta. *J. Biol. Chem.* 277: 20399–20408.
 59. Han, J. W., H. F. Zheng, Y. Cui, L. D. Sun, D. Q. Ye, Z. Hu, J. H. Xu, Z. M. Cai, W. Huang, G. P. Zhao, et al. 2009. Genome-wide association study in a Chinese Han population identifies nine new susceptibility loci for systemic lupus erythematosus. *Nat. Genet.* 41: 1234–1237.
 60. Yang, W., N. Shen, D. Q. Ye, Q. Liu, Y. Zhang, X. X. Qian, N. Hirankarn, D. Ying, H. F. Pan, C. C. Mok, et al; Asian Lupus Genetics Consortium. 2010. Genome-wide association study in Asian populations identifies variants in ETS1 and WDFY4 associated with systemic lupus erythematosus. *PLoS Genet.* 6: e1000841.
 61. Llorente, L., and Y. Richaud-Patin. 2003. The role of interleukin-10 in systemic lupus erythematosus. *J. Autoimmun.* 20: 287–289.
 62. Houssiau, F. A., C. Lefebvre, M. Vanden Berghe, M. Lambert, J. P. Devogelaer, and J. C. Renauld. 1995. Serum interleukin 10 titers in systemic lupus erythematosus reflect disease activity. *Lupus* 4: 393–395.

Corrections

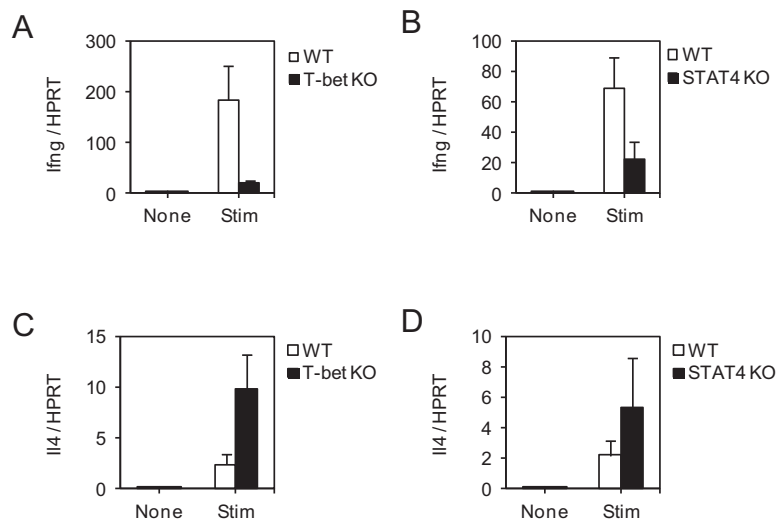
Lee, C.-G., H.-K. Kwon, A. Sahoo, W. Hwang, J.-S. So, J.-S. Hwang, C.-S. Chae, G.-C. Kim, J.-E. Kim, H.-S. So, E. S. Hwang, R. Grenningloh, I-C. Ho, and S.-H. Im. 2012. Interaction of Ets-1 with HDAC1 represses IL-10 expression in Th1 cells. *J. Immunol.* 188: 2244–2253.

An additional funding source has been added to the grant support footnote. The corrected footnote is shown below. The footnote has been corrected in the online version of this article, which now differs from the print version as originally published.

This work was supported by Grant A080588-20 from the Korea Healthcare Technology Research and Development Project, Ministry for Health, Welfare and Family Affairs; National Research Foundation Grant 2011-0028529 from the Korean government (Ministry of Education, Science and Technology); American Recovery and Reinvestment Act R03 Grant AI081052 from the National Institutes of Health (to I-C.H.); a Pilot Project grant from the Alliance for Lupus Research (to I-C.H.); and Grant Department of Defense W81XWH-11-1-0492 (to I-C.H.).

www.jimmunol.org/cgi/doi/10.4049/jimmunol.1290074

Lee *et al*, Supplementary Fig. 1



Supplementary Figure 1. Expression level of *Ifng* and *Il4* in WT and T-betKO or Stat4KO Th1 cells. Total RNA was isolated from cells either unstimulated or restimulated with aCD3/aCD28, and subjected to real time PCR (RT-PCR) analysis. The data are presented as means with SD from three independent experiments.

Appendix 2

Ets-1 facilitates nuclear entry of NFAT proteins and their recruitment to the IL-2 promoter

Hsiao-Wei Tsao^a, Tzong-Shyuan Tai^b, William Tseng^b, Hui-Hsin Chang^b, Roland Grenningloh^{b,1}, Shi-Chuen Miaw^{a,2}, and I-Cheng Ho^{b,c,d,2}

^aGraduate Institute of Immunology, National Taiwan University College of Medicine, Taipei 10051, Taiwan; ^bDivision of Rheumatology, Immunology, and Allergy, Department of Medicine, Brigham and Women's Hospital, Boston, MA 02115; ^cHarvard Medical School, Boston, MA 02115; and ^dSection of Rheumatology, VA Boston Healthcare System, Boston, MA 02130

Edited by Laurie H Glimcher, Weill Cornell Medical College, New York, NY, and approved August 9, 2013 (received for review March 5, 2013)

E26 transformation-specific sequence 1 (Ets-1), the prototype of the ETS family of transcription factors, is critical for the expression of IL-2 by murine Th cells; however, its mechanism of action is still unclear. Here we show that Ets-1 is also essential for optimal production of IL-2 by primary human Th cells. Although Ets-1 negatively regulates the expression of Blimp1, a known suppressor of IL-2 expression, ablation of B lymphocyte-induced maturation protein 1 (Blimp1) does not rescue the expression of IL-2 by Ets-1-deficient Th cells. Instead, Ets-1 physically and functionally interacts with the nuclear factor of activated T-cells (NFAT) and is required for the recruitment of NFAT to the IL-2 promoter. In addition, Ets-1 is located in both the nucleus and cytoplasm of resting Th cells. Nuclear Ets-1 quickly exits the nucleus in response to calcium-dependent signals and competes with NFAT proteins for binding to protein components of noncoding RNA repressor of NFAT complex (NRON), which serves as a cytoplasmic trap for phosphorylated NFAT proteins. This nuclear exit of Ets-1 precedes rapid nuclear entry of NFAT and Ets-1 deficiency results in impaired nuclear entry, but not dephosphorylation, of NFAT proteins. Thus, Ets-1 promotes the expression of IL-2 by modulating the activity of NFAT.

E26 transformation-specific sequence 1 (Ets-1) is the founding member of the ETS family of transcription factors (1, 2); it is expressed mainly in lymphoid cells and plays multiple roles in regulating the development and function of these cells. Ets-1-deficient (KO) Th1 cells produce very little IL-2 (3). However, it is still unclear whether Ets-1 is also critical for the expression of IL-2 in human Th cells and how Ets-1 promotes the expression of IL-2.

The transcriptional regulation of IL-2 has been characterized (4, 5). One of the positive regulators of IL-2 expression is the nuclear factor of activated T-cells (NFAT) family of transcription factors, which contains five members (6, 7). The promoter of the IL-2 gene contains five consensus binding sequences of NFAT (8). Deficiency of both NFATc1 and NFATc2 severely attenuates the expression of IL-2, confirming the critical role of NFATs in regulating IL-2 expression (9). In resting T cells, NFATs are phosphorylated and retained in cytoplasm by the NRON complex, which consists of a backbone of noncoding RNA called noncoding RNA repressor of NFAT (NRON) and several proteins, including Tnp1, Iqgap1, chromosome segregation 1-like (Cse11), protein phosphatase 2, regulatory subunit A, alpha (Ppp2r1a), and Psm11 (10–12). The NRON complex serves as a cytoplasmic trap of NFAT. T-cell antigen receptor (TCR) signals and dephosphorylation of NFAT lead to the release of NFAT from the NRON complex. Free dephosphorylated NFAT is then translocated into the nucleus and transactivates IL-2 and many other genes. However, the detailed mechanism regulating the assembly/disassembly of the NRON complex and cytoplasmic/nuclear translocation of NFAT is still not fully understood.

B lymphocyte-induced maturation protein 1 (Blimp1) is a transcription repressor that is known to negatively regulate the expression of IL-2 (13–15). Both Blimp1 and Ets-1 are also expressed in B cells and counterregulate each other during the

terminal differentiation of B cells to plasma cells (16, 17). These observations raise the possibility that Blimp1 and Ets-1 also counterregulate each other in T cells, and that Ets-1 regulates the expression of IL-2 indirectly by suppressing Blimp1.

We set out to investigate how Ets-1 regulates IL-2 expression. We found that Ets-1 was also required for the expression of IL-2 in human T cells. Although Ets-1 suppressed the expression of Blimp1 in T cells, the impaired IL-2 expression in the absence of Ets-1 was not due to aberrant expression of Blimp1. Instead, endogenous Ets-1 physically interacted with endogenous NFAT. Ets-1 and NFAT synergistically transactivated the IL-2 promoter. In the absence of Ets-1, the recruitment of NFAT to the IL-2 promoter was markedly impaired. We further found that nuclear Ets-1 exited the nucleus before rapid NFAT nuclear entry and that cytoplasmic Ets-1 interacted with protein components of the NRON complex. More importantly, deficiency of Ets-1 deterred nuclear entry but not dephosphorylation of NFAT. Our data collectively demonstrate that Ets-1 promotes the expression of IL-2 through NFAT-dependent mechanisms.

Results

Ets-1 Is Required for IL-2 Production by Human T Cells. One key feature of Ets-1KO Th1 cells is impaired IL-2 production. To determine whether Ets-1 was also required for IL-2 production by human Th cells, we suppressed the expression of Ets-1 by nearly 80% in primary human Th cells with siRNA (Fig. 1A). Th cells transfected with Ets-1 siRNA, but not scrambled siRNA, expressed a significantly lower level of IL-2 in response to anti-CD3 stimulation. In contrast, the expression of phosphatase

Significance

IL-2 plays critical roles in many immune responses. However, its transcriptional regulation is still not fully understood. Data described in this paper demonstrate that the transcriptional factor E26 transformation-specific sequence 1 (Ets-1) promotes the expression of IL-2 by nuclear factor of activated T-cells (NFAT)-dependent mechanisms. Nuclear Ets-1 synergizes with NFAT in the transcription of IL-2. Ets-1 is also translocated to the cytoplasm in response to calcium-induced signals and facilitates the release of NFAT from noncoding RNA repressor of NFAT complex, which traps NFAT in the cytoplasm. This paper not only advances our understanding of the transcriptional regulation of IL-2 but also depicts a unique mechanism of action of Ets-1.

Author contributions: H.-W.T., S.-C.M., and I.-C.H. designed research; H.-W.T., T.-S.T., W.T., H.-H.C., and R.G. performed research; H.-W.T., T.-S.T., W.T., H.-H.C., R.G., S.-C.M., and I.-C.H. analyzed data; and H.-W.T., S.-C.M., and I.-C.H. wrote the paper.

The authors declare no conflict of interest.

This article is a PNAS Direct Submission.

¹Present address: Merck Serono, Billerica, MA 01821.

²To whom correspondence may be addressed. E-mail: iho@partners.org or smiaw@ntu.edu.tw.

This article contains supporting information online at www.pnas.org/lookup/suppl/doi:10.1073/pnas.1304343110/-DCSupplemental.

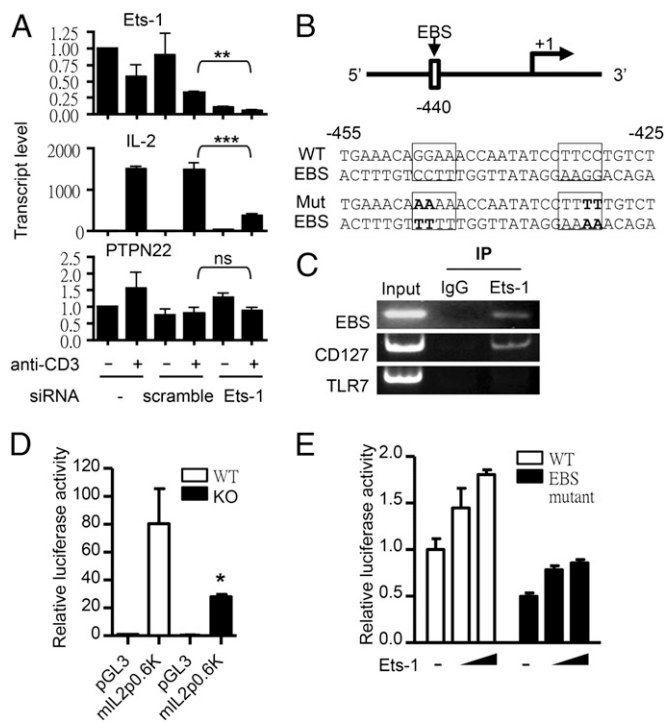


Fig. 1. Ets-1 regulates the expression of IL-2. (A) Primary human Th cells were either mock transfected or transfected with scrambled or Ets-1-specific siRNA. The transfected cells were stimulated with anti-CD3 for 24 h. The transcript levels of indicated genes were measured with real-time PCR. The transcript level was normalized against the level of mock-transfected, unstimulated cells. Statistical significance was calculated with one-way ANOVA followed by Tukey's test comparing stimulated scrambled and Ets-1 siRNA-transfected samples. (B) A schematic diagram and the DNA sequence of the promoter of the murine IL-2 gene. Conserved EBS is indicated. The boxed areas are wild-type and mutated EBS. (C) WT murine Th1 cells were stimulated with PMA/ionomycin for 1 h and subjected to ChIP with anti-Ets-1 antibody or control IgG. The recruitment of Ets-1 to the indicated genes was examined with PCR. The data shown is representative of two experiments. (D) WT and Ets-1KO Th1 cells were transfected with indicated reporters and stimulated with PMA/ionomycin for 3 h. Luciferase activity was first normalized against internal controls and then against the normalized value of pGL3-transfected WT cells. (E) EL4 cells were transfected with wild-type 0.6-kb IL-2 reporter or EBS mutant reporter along with increasing concentrations of Ets-1 expression vector. Relative luciferase activity was determined and shown. The data shown in A, D, and E are the averages and SDs of at least three independent experiments, which were performed in duplicate.

PTPN22, which is not a known Ets-1 target, was not affected by Ets-1 siRNA. This result confirms that Ets-1 is critical for the expression of IL-2 in both mouse and human T cells.

Ets-1 could regulate IL-2 production directly or indirectly. The murine IL-2 promoter contains several potential Ets-1 binding sites, including a region centering on -440 (Fig. 1B). This region, Ets binding sequence (EBS), actually contains two palindromic Ets-1 binding sites and has been shown to bind other Ets transcription factors, such as GABP α (18), and regulate the activity of the IL-2 promoter. We therefore conducted a ChIP assay and found that Ets-1 was recruited to EBS and also to a known Ets-1 binding site within the CD127 promoter in Th1 cells (19) (Fig. 1C). In contrast, we detected no recruitment of Ets-1 to TLR7, which is not regulated by Ets-1. We subsequently generated a 0.6-kb IL-2 promoter reporter (-574 to $+43$), encompassing the EBS. The activity of the 0.6-kb promoter was induced with phorbol myristate acetate (PMA)/ionomycin and was twice as active in WT Th1 cells than in Ets-1KO Th1 cells (Fig. 1D). However, overexpression of Ets-1 only modestly increased the activity of this promoter above baseline, and mutation of the

EBS did not affect the ability of Ets-1 to modestly enhance the activity of the 0.6-kb promoter (Fig. 1E). Similar results were obtained with an IL-2 promoter/reporter containing 7 kb of the genomic region upstream of the transcription start site (Fig. S1). We therefore theorized that Ets-1 indirectly controlled the expression of IL-2.

Ets-1 Deficiency Leads to Aberrant Expression of Blimp1. We then examined the expression of several transcription factors that are known to regulate the expression of IL-2 (4, 5). We found that the transcript level of Runx1, Oct1, and several NF- κ B members was slightly reduced in the absence of Ets-1, whereas the expression of Egr, NFAT, c-Jun, and c-Fos was unchanged (Fig. S2). Intriguingly, the transcript level of Blimp1 was substantially higher in Ets-1KO Th1 cells compared with WT cells. Because forced expression of Blimp1 strongly suppressed IL-2 production in Th cells (15), we postulated that Ets-1 indirectly regulated the production of IL-2 by suppressing the expression of Blimp1. We first compared the expression of Ets-1 and Blimp1 during the differentiation of WT Th1 cells. Under Th1-skewing conditions, Ets-1 levels gradually increased and reached a plateau ~ 3 –4 d after stimulation. Interestingly, Blimp1 was quickly induced within 12 h after stimulation; its expression reached a peak within 2–3 d after stimulation but started to fade away on day 4 when the expression of Ets-1 was at its peak (Fig. 2A). Fully differentiated WT Th1 cells expressed a low level of Blimp1. However, a significantly higher level of Blimp1 was detected in Ets-1KO Th1 cells, particularly in response to PMA/ionomycin (Fig. 2B). In contrast, Ets-1 levels were very comparable between WT and Blimp1KO Th1 cells. These results collectively indicate that Ets-1 directly or indirectly suppresses the expression of Blimp1 in Th1 cells but not vice versa. There are two conserved Ets-1 binding sites, EBS1 and EBS2, starting at -879 and -213 of the proximal promoter of Blimp1 (Fig. 2C). We found that Ets-1 was recruited to EBS2 but not EBS1 (Fig. 2D). Thus, Ets-1 very likely directly suppresses the expression of Blimp1 in Th1 cells by binding to the EBS2 of the Blimp1 promoter.

Ablation of Blimp1 Does Not Restore the Production of IL-2 by Ets-1KO Th Cells. To further test whether reduced IL-2 expression of Ets-1KO Th1 cells could be attributed to aberrant expression of Blimp1, we generated Ets-1/Blimp1 doubly deficient (DKO) mice. Given the low frequency of DKO mice, we were only able to obtain two DKO mice. We found that Blimp1 deficiency had a negligible impact on the development and homeostasis of Ets-1KO thymocytes (Fig. 2E). Both Ets-1KO and Blimp1KO mice had more memory/effector Th cells and less naive Th cells in their peripheral lymphoid organs compared with WT mice (Fig. 2E). This feature was even more prominent in DKO mice. Deficiency of Blimp1 did not lead to the expected increase in IL-2 production, which is probably due to the small sample size ($n = 3$) and the fact that WT Th1 cells already express a very high level of IL-2. Importantly, ablation of Blimp1 did not allow Ets-1KO Th1 cells to produce a normal level of IL-2 (Fig. 2F). Thus, the dysregulated IL-2 production seen in Ets-1KO Th1 cells was not due to heightened expression of Blimp1.

Ets-1 Physically and Functionally Interacts with NFAT. NFAT can physically interact with the ETS domain of Ets-1 when both proteins are translated in vitro (20). We theorized that Ets-1 and NFAT physically interact with each other in Th cells and synergistically transactivate the IL-2 gene. To test this theory, we first performed a coimmunoprecipitation assay with primary Th1 cells. We were able to coprecipitate NFATc2 and NFATc1 with anti-Ets-1 antibody but not with control IgG directly from nuclear extract of PMA/ionomycin-stimulated Th1 cells (Fig. 3A). Thus, endogenous Ets-1 does physically interact with endogenous NFAT proteins in the nucleus of Th cells. We used NFATc2 as an example of NFAT proteins in subsequent experiments. To examine the functional impact of the Ets-1/NFAT interaction on the transcription of IL-2, we transfected

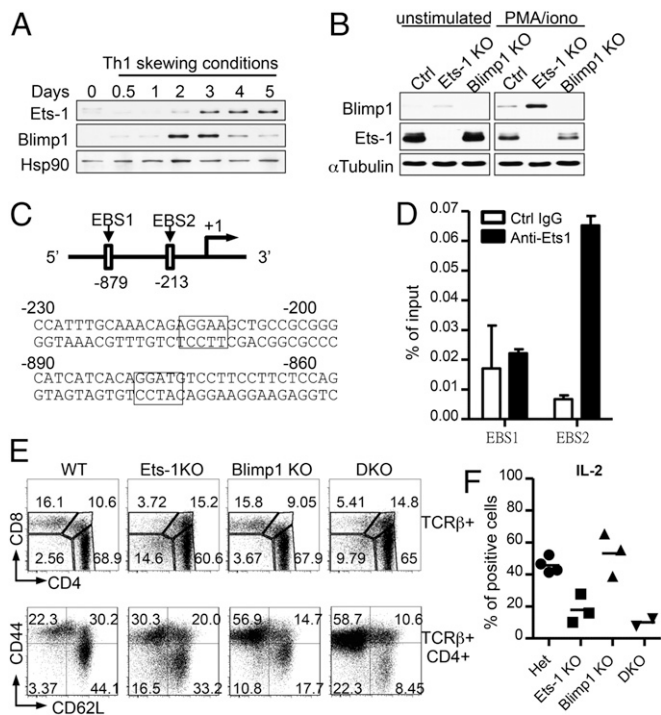


Fig. 2. Ets-1 suppresses Blimp1 expression in Th1 cells. (A) WT naive Th1 cells were stimulated under Th1 skewing conditions. At indicated time points, cell extract was harvested and subjected to Western blot analysis with indicated antibodies. (B) Th1 cells of indicated genotype were stimulated with PMA/ionomycin for 4 h. Cell extract was subjected to Western blot analysis with indicated antibodies. (C) Schematic diagram of the promoter of the *Prdm1* gene, which encodes Blimp1. The two putative EBS with arrows and boxes. (D) WT Th1 cells were subjected to ChIP with anti-Ets-1 or control IgG. The precipitated DNA was subjected to real-time PCR with primer specific to each EBS. (E) Thymocytes and lymph node cells obtained from 8-wk-old mice of indicated genotype were analyzed with FACS. The CD4/CD8 plots of TCR β thymocytes and CD62L/CD44 plots of CD4 $^{+}$ lymph node T cells are shown. (F) Th1 cells of indicated genotype were stimulated with PMA/ionomycin and subjected to intracellular cytokine staining with IL-2 antibody. The percentage of IL-2-positive cells is shown. Each dot represents one mouse. Data shown in A and B are representatives of two independent experiments. Data shown in D are the averages and SDs of three independent experiments done in duplicate.

EL4 T cells with expression vectors encoding Ets-1 and/or NFATc2 along with the IL-2 0.6-kb promoter/reporter. Again, Ets-1 alone only modestly transactivated the promoter, whereas overexpression of NFAT led to an approximately fourfold increase in luciferase activity (Fig. 3B). Coexpression of Ets-1 and NFAT resulted in an almost eightfold induction of luciferase activity, confirming the functional synergy between these two proteins.

We subsequently used ChIP to examine the recruitment of NFATc2 to the IL-2 promoter in the presence or absence of Ets-1. NFATc2 was recruited to the IL-2 promoter in WT Th1 cells after stimulation with PMA/ionomycin. However, the recruitment of NFATc2 was markedly reduced in the absence of Ets-1 (Fig. 3C). We then transduced Ets-1KO Th1 cells with bicistronic retroviral vectors expressing both Ets-1 and GFP or only GFP. The cells were then subjected to ChIP with anti-NFATc2 or control IgG, and the recruitment of NFATc2 to the IL-2 promoter was examined with semiquantitative PCR. We found that the recruitment of NFATc2 was restored by retroviral Ets-1 (Ets1 GFP $^{+}$ in Fig. 3D). In contrast, the recruitment of NFATc2 was still impaired in untransduced (GFP $^{-}$) or vector-transduced cells (vector GFP $^{+}$ in Fig. 3D). This observation suggests that Ets-1 facilitates the recruitment of NFATc2 to the IL-2 promoter.

Calcium-Dependent Signals Drive Nuclear Exit of Ets-1. Although Ets-1 is a DNA binding protein, we were surprised to see that Ets-1 was distributed in both the cytoplasm and nucleus of resting Th1 cells (Figs. 3A and 4A). There was an up-shift in the molecular weight of Ets-1 in stimulated cells due to phosphorylation of four serine residues located N-terminally to the ETS domain (21). Intriguingly, the level of nuclear Ets-1 decreased substantially within 15 min after stimulation (Fig. 4A). This decrease in the level of nuclear Ets-1 corresponded to an increase in the level of cytoplasmic Ets-1. However, by 90 min after stimulation, Ets-1 was dephosphorylated and the level of nuclear and cytoplasmic Ets-1 was restored to near prestimulation levels. This data strongly suggests that nuclear Ets-1 is translocated to the cytoplasm of activated Th1 cells. This presumable Ets-1 nuclear exit is driven by ionomycin but not PMA or other stimuli, such as IL-7, Tat, or dexamethasone (Fig. 4B).

The observation that nuclear exit of Ets-1 coincided with nuclear entry of NFAT prompted us to carefully examine the kinetics of these two events. There were significant variations in the nuclear/cytoplasmic distribution of NFATc2 in resting Th1 cells among experiments. To compensate for the interexperimental variations, we first normalized the level of NFATc2 against loading controls. We then calculated the percentage of nuclear NFATc2 at all time points and arbitrarily set the peak value as 1. We did the same normalization for cytoplasmic Ets-1. In resting Th1 cells, nearly all NFATc2 was phosphorylated and located in cytoplasm (Fig. 4C and D). Dephosphorylation and nuclear entry of NFATc2 started within 15 s after stimulation with PMA/ionomycin. This early phase of nuclear entry proceeded at a relatively slow pace, and its duration varied from 90 s

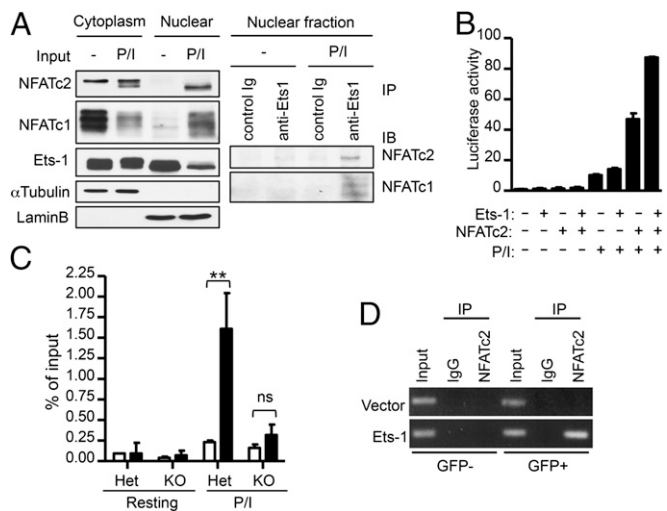


Fig. 3. Ets-1 physically and functionally interacts with NFAT proteins. (A) WT Th1 cells were stimulated with PMA/ionomycin (P/I) for 30 min. Cytoplasmic and nuclear extract were separately prepared and probed with indicated antibodies (Left). The nuclear extract was immunoprecipitated with anti-Ets-1 or control IgG and then probed with anti-NFATc1 and anti-NFATc2, respectively (Right). (B) EL4 cells were transfected with the 0.6-kb IL-2 promoter/reporter along with indicated expression vectors. The transfected cells were stimulated with P/I for 3 h. Relative luciferase activities are shown. (C) WT or Ets-1KO Th1 cells were stimulate with P/I for 1 h, and subjected to ChIP using anti-NFATc2 or control IgG. The recruitment of NFATc2 to the IL-2 promoter was quantified with real-time PCR. (D) Ets-1KO Th1 cells were transduced with bicistronic retroviral vectors expressing both Ets-1 and GFP or only GFP (vector). The transduced (GFP $^{+}$) and non-transduced (GFP $^{-}$) cells were sorted and stimulated with P/I, and subjected to ChIP with anti-NFATc2 or control IgG. The recruitment of NFATc2 to the IL-2 promoter was determined with semiquantitative PCR. The data shown in A and D are representative of two independent experiments. The data shown in B and C are the averages and SDs of three independent experiments done in duplicate.

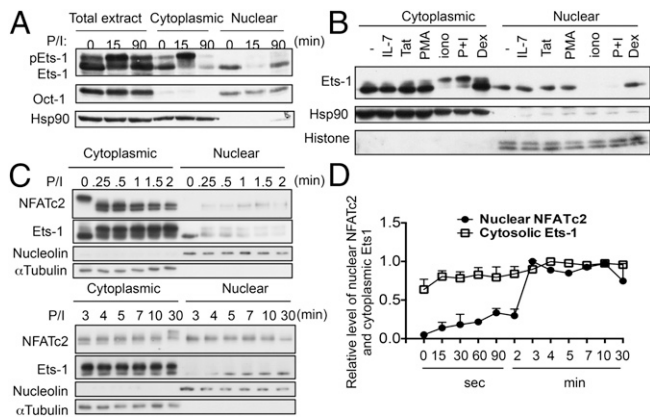


Fig. 4. Ets-1 exits nucleus in response to calcium-dependent signals. WT Th1 cells were stimulated with P/I (A and B) or other stimuli (B) for 15 min (B) or indicated periods of time (A). Whole-cell, nuclear, and cytoplasmic extracts were prepared at indicated time points and probed with indicated antibodies. (C) WT Th1 cells were stimulated with P/I. Cytoplasmic and nuclear extracts were separately prepared at indicated time points and probed with indicated antibodies. (D) The relative levels of nuclear NFATc2 and cytoplasmic Ets-1 were calculated in the way described in *Results*. The data shown in A–C are representative of at least two independent experiments, and the averages and SDs of three experiments are shown in D.

to 5 min. Only ~20% of total NFATc2 was translocated into the nucleus during the early phase. This early phase was followed by a phase of rapid translocation, during which 50–70% of total NFATc2 was translocated to the nucleus within a period of 1 min. Subsequently, nuclear NFATc2 was gradually rephosphorylated and translocated back to the cytoplasm. In contrast, ~60% of total Ets-1 was already located in the cytoplasm of resting Th1 cells. The level of cytoplasmic Ets-1 also started to increase within 15 s after stimulation. Instead of following biphasic kinetics similar to that of NFATc2 nuclear entry, this nuclear exit of Ets-1 proceeded at a steady rate and reached a plateau within 2–4 min.

Ets-1 Is Required for Efficient Nuclear Entry of NFAT. The observation that the nuclear exit of Ets-1 started before the onset of rapid nuclear entry of NFATc2 prompted us to question whether Ets-1 regulated nuclear entry of NFAT. We compared nuclear entry of NFATc2 between WT and Ets-1KO Th1 cells (Fig. 5A). We found that the level of total NFATc2 protein measured by combining cytoplasmic and nuclear pools was very comparable between WT and Ets-1KO cells, and that the level of total NFATc2 remained rather steady up to 60 min after stimulation (Fig. S3A). This result was consistent with the comparable level of NFAT transcript between WT and Ets-1KO Th cells (Fig. S2). Stimulation with PMA/ionomycin led to nearly complete and comparable dephosphorylation of NFATc2 within 10 min in both WT and KO cells (Fig. S3B). Thus, deficiency of Ets-1 did not affect calcium-induced dephosphorylation of NFATc2. We then examined the level of nuclear NFATc2 protein. As expected, the level of nuclear NFATc2 peaked ~5–10 min after stimulation. The level then gradually decreased, and only approximately a quarter of the peak level of nuclear NFATc2 was detected at 60 min after stimulation. Interestingly, the level of nuclear NFATc2 in Ets-1KO cells was only ~50% of that of WT cells at 10 min after stimulation (Fig. 5B). The level of nuclear NFATc2 in Ets-1KO cells also gradually decreased at a rate similar to that in WT cells. A similar defect in nuclear entry of NFATc1 was also observed in Ets-1KO Th1 cells (Fig. S3C). Thus, Ets-1 is required for efficient nuclear entry of NFAT but does not regulate its dephosphorylation and nuclear exit.

Thus far, our data suggest that Ets-1 not only facilitates nuclear entry of NFAT but also synergizes with NFAT in the transcription of IL-2. To further confirm that Ets-1 could influence NFAT

activity independently of its synergy with NFAT at the transcriptional level, we compared the activity of an NFAT-dependent artificial promoter/reporter between WT and Ets-1 KO Th1 cells. This reporter, 3xNFAT/activation protein 1 (AP-1)-Luc, is driven by three copies of a composite NFAT/AP-1 site derived from the IL-2 promoter but contains no consensus Ets-1 binding site (22); as expected, it was transactivated by NFATc2 but not Ets-1 (Fig. S4). Overexpression of both Ets-1 and NFATc2 did not yield a synergistic effect on this reporter. Instead, overexpression of Ets-1 attenuated the effect of NFATc2; mostly likely, the physical interactions between NFATc2 and Ets-1 resulted in the sequestration of NFATc2. Thus, 3xNFAT/AP-1 is ideal for determining whether Ets-1 can influence NFAT activity independently of its synergy with NFAT. In agreement with our hypothesis, this reporter was ~50% less active in Ets-1 KO Th1 cells than WT cells (Fig. 5C). In contrast, the activity of a reporter driven by three copies of a cyclic AMP-response element (CRE) site was comparable between WT and KO Th1 cells.

Ets-1 Interacts with Protein Components of the NRON Complex. One possible explanation for the impaired nuclear entry of NFAT was that Ets-1 suppressed the expression of the NRON complex. Alternatively, cytoplasmic Ets-1 could directly or indirectly facilitate the release of NFAT from the NRON complex. We found that the transcript levels of NRON RNA and the protein components of the NRON complex were unaltered in the absence of Ets-1 (Fig. 6A). We therefore examined whether Ets-1 physically interacted with the NRON complex. We found that Cse1l and Ppp2r1a, two protein components of the NRON complex, were coimmunoprecipitated by anti-Ets-1 antibody, confirming the physical interaction between Ets-1 and the NRON complex (Fig. 6B). We subsequently postulated that Ets-1 competed with NFAT for binding with NRON complex and that the increase in the level of cytoplasmic Ets-1 in activated Th1 cells led to the release of NFAT from the NRON complex. We generated 293T cells expressing a constant level of HA-NFATc2 but an increasing level of Flag-Ets-1 (Fig. 6C, top two panels). We then coimmunoprecipitated HA-NFATc2 with anti-Cse1l. The 293T cells expressed little endogenous Ets-1 (Fig. 6C, fourth

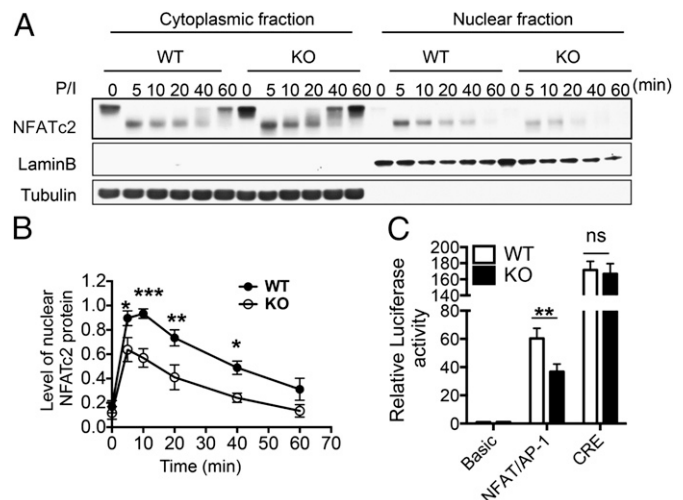
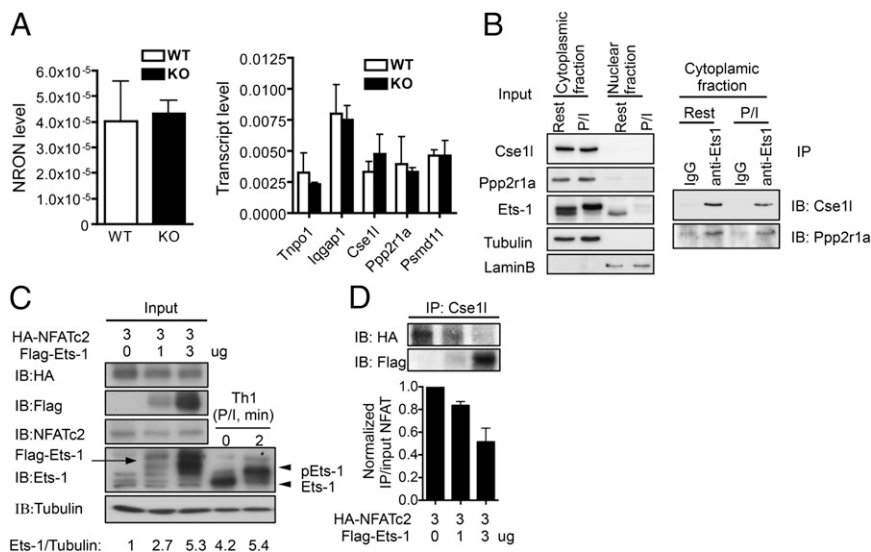


Fig. 5. Ets-1 facilitates nuclear entry of NFATs. (A and B) WT and Ets-1KO Th1 cells were stimulated with P/I for indicated periods of time. Nuclear and cytoplasmic extracts were separately prepared and probed with anti-NFATc2 and other indicated antibodies. A representative blot from four independent experiments is shown in A. The averages and SDs of the relative level of nuclear NFATc2 at different time points are shown in B. (C) WT and Ets-1KO Th1 cells were transfected with indicated luciferase reporters and stimulated with P/I for 6 h. The averages and SDs of relative luciferase activity from three independent experiments are shown.

Fig. 6. Ets-1 interacts with the NRON complex. (A) Transcript levels of NRON RNA and various protein components of the NRON complex of resting WT and Ets-1KO Th1 cells were quantified with real-time PCR. The data shown are the averages and SDs of three independent experiments done in duplicate. (B) WT Th1 cells were stimulated with P/I for 10 min. Cytoplasmic and nuclear extracts were probed with indicated antibodies (*Left*). Cytoplasmic extract was then immunoprecipitated with anti-Ets-1 or control IgG, and the immunoprecipitant was probed with anti-Cse11 and Ppp2r1a (*Right*). (C) The 293T cells were transfected with 3 μ g of HA-NFATc2 expression plasmid and an increasing amount of Flag-Ets-1 expression plasmid. Cytoplasmic extract from the transfected cells was probed with indicated antibodies. Cytoplasmic extract from resting and P/I-stimulated WT Th1 cells was included as references for endogenous Ets-1. The level of total Ets-1 (Flag-Ets-1 and endogenous Ets-1) was normalized against that of α -tubulin, and the relative values of total Ets-1 are shown at the bottom. (D) The cytoplasmic extract of 293T cells described in C was immunoprecipitated with anti-Cse11 and then probed with indicated antibodies (*Top and Middle*). The level of NFATc2 in immunoprecipitant (IP) was normalized against that of input shown in C. The averages and ranges of the normalized values of IP/input NFATc2 from two independent experiments are shown (*Bottom*).



panel). In the absence of exogenous Ets-1, HA-NFATc2 was readily coimmunoprecipitated with anti-Cse11 from 293T cells (Fig. 6D, *Top*). Exogenous Ets-1 was also coimmunoprecipitated with anti-Cse11 (Fig. 6D, *Middle*), a finding consistent with the data shown in Fig. 6B, and dose-dependently interfered with the interaction between HA-NFATc2 and Cse11 (Fig. 6D, *Top and Bottom*). Interestingly, a level of Flag-Ets-1 as high as that of endogenous Ets-1 seen in Th1 cells was needed to appreciably displace HA-NFATc2 from Cse11 (Fig. 6C, fourth panel, and D).

Discussion

The function of IL-2 is well established but the transcriptional regulation of IL-2 is still not fully understood. We found that Ets-1 critically regulated the expression of IL-2 by modulating the nuclear translocation of NFAT proteins and their recruitment to the IL-2 promoter. Ets-1, to the best of our knowledge, is the only transcription factor that has been shown to regulate nuclear entry of NFAT.

The role of Blimp1 in regulating the development and function of T cells has been characterized. The phenotype of Blimp1 KO T cells is the opposite of that of Ets-1KO cells in several aspects, such as the expression of IL-2 and IL-10 (14, 23). In addition, Ets-1 and Blimp1 play opposite roles during plasma cell differentiation, with Ets-1 suppressing but Blimp1 promoting the process. Accordingly, the expression of Ets-1 has to be shut down before the induction of Blimp1. We also found a pattern of mutually exclusive expression between these two proteins during Th1 differentiation. Our data indicate that Ets-1 suppresses the expression of Blimp1 in Th1 cells but not vice versa. The functional significance of this finding is still unknown. Ablation of Blimp1 did not rescue the developmental defect of T cells and the production of IL-2 resulting from Ets-1 deficiency. However, it is still possible that these two proteins counteract each other in yet-to-be-identified functional aspects of Th cells.

Our data indicate that nuclear entry of NFAT in response to calcium-dependent signals is a two-phase process. An early but slow phase takes place almost immediately after PMA/ionomycin stimulation and is followed by a rapid phase of nuclear entry, which occurs between 2 and 5 min after stimulation. In contrast, the nuclear exit of Ets-1, also taking place immediately after stimulation, is a relatively steady process and reaches its peak within 5 min. Ets-1 physically interacts with NRON-associated proteins, including Cse11 and Ppp2r1a, and competes with NFAT for binding to Cse11, thereby displacing NFAT from Cse11. This

later action of Ets-1 appears to require the high level of cytoplasmic Ets-1 that is seen in activated Th cells. Taken together, our data suggest the following scenario. During the activation of Th cells, calcium-dependent signals lead to rapid dephosphorylation of NRON-trapped NFAT, initiating the release of NFAT from NRON complex. This early release of NFAT is likely not very efficient and coincides with the early but slow phase of nuclear entry of NFAT. The calcium-dependent signals also induce a steady nucleus-to-cytoplasm translocation of Ets-1. Cytoplasmic Ets-1 eventually reaches a level that is sufficient to compete with NFAT for binding to NRON complex, thereby hastening the displacement of dephosphorylated NFAT from NRON complex. This Ets-1-assisted release of NFAT is partly responsible for the late but rapid phase of nuclear entry of NFAT. Additional experiments will be needed to confirm this scenario. Although Ets-1 physically interacts with NFAT, it is highly unlikely that the physical interaction between these two proteins is required for nuclear entry of NFAT, because they apparently move in opposite directions. Instead, their physical interaction is probably critical for residual nuclear Ets-1 to recruit NFAT to the IL-2 promoter. Thus, Ets-1 not only facilitates nuclear entry of NFAT but also recruits NFAT to the IL-2 promoter.

It was reported that Ets-1KO Th cells expressed a low level of inositol 1,4,5-triphosphate receptor, type 3 (IP₃R3) (24, 25), which can serve as a calcium channel, and that antagonists of IP₃R3 attenuated the expression of IL-2 and IFN- γ in T cells. Although the impaired expression of IP₃R3 may contribute to the defect in IL-2 production, stimulation with PMA/ionomycin, which should bypass the need of IP₃R3, did not correct this defect. Thus, the profound defect of IL-2 expression seen in Ets-1KO Th cells is probably not due to attenuated expression of IP₃R3.

Nuclear exclusion of Ets-1 has been reported and may play a regulatory role in erythropoiesis. Ets-1 is expressed in CD34+ erythroid-megakaryocytic progenitor cells (26). It is excluded from the nucleus during erythroid maturation but stays in the nucleus during megakaryocytic maturation. Why Ets-1 has to be excluded from nucleus and what signals drive its nuclear exit during erythroid maturation are still unknown. Because the role of NRON and NFAT in erythroid-megakaryocytic differentiation is rather limited, cytoplasmic Ets-1 may have NRON-independent functions. The nuclear exit of Ets-1 during erythroid maturation was mediated by a leucine-rich nuclear export signal (NES) located at the N terminus of Ets-1. However, we found that

mutation of this putative NES did not affect the nuclear exit of Ets-1 in T cells (Fig. S5), suggesting the presence of an additional NES that is required for the nuclear exit of Ets-1 in T cells. The identification of the additional NES will greatly facilitate future studies on the functional consequence of the nuclear exit of Ets-1 in T cells.

Material and Methods

Mice. Ets-1KO mice of N5 CH57BL/6 genetic background have been described previously (3). Heterozygous or wild-type littermates were used as controls. Blimp1FF mice were purchased from Jackson Laboratory and crossed to CD4-cre mice to generate Blimp1FF/CD4cre mice. All animals were housed under specific pathogen-free conditions, and experiments were approved by the Institutional Animal Care and Use Committee of Dana-Farber Cancer Institute and were performed in accordance with the institutional guidelines for animal care.

Purification and Differentiation of Th cells. Purification and differentiation of Th cells were performed according to a published protocol without modification (3).

Preparation of Cytoplasmic and Nuclear Extract of Th Cells, and Western Blot Analysis. Th cells were first suspended in hypotonic buffer [10 mM Tris-HCl (pH 7.4), 3 mM MgCl₂, 10 mM NaCl, 0.5% Nonidet P-40]. Nuclei were resuspended in lysis buffer [50 mM Tris-HCl (pH 7.4), 150 mM NaCl, 2 mM EDTA (pH 8), 0.5% Nonidet P-40, and 1% Triton-X 100] and lysed by sonication. The following antibodies were used in Western blotting: anti-Ets-1 [C-20; Santa Cruz Biotechnology, or EPR546(2); Epitomics], anti-Hsp90a/b (H-114; Santa Cruz Biotechnology), anti-NFATc2 (4G6-G5; Santa Cruz Biotechnology), anti-NFATc1 (7A6; Santa Cruz Biotechnology), anti-Lamin B (C-20; Santa Cruz Biotechnology), anti-Blimp-1 (ROS195G; BioLegend), anti-nucleolin (GTX30908; GeneTex), anti-HA (GTX115044; GeneTex), anti-Flag (M2; Sigma-Aldrich), and anti- α -tubulin (B-5-1-2; Sigma-Aldrich).

Cell Lines, Plasmid, Transfection, and Luciferase Assay. The promoter of mouse IL-2 (−574 to +43 and −7428 to +45) were amplified by PCR and cloned into pGL3-basic vector to become pGL3-IL-2. The 3xNFAT/AP-1-luc was obtained from Addgene (plasmid 17870). Full-length p51 Ets-1 and HA-tagged Nfatc2 were cloned into pcDNA3.1 and pcDNA3 expression vectors to generate

pcDNA3.1-Ets1 p51 and pcDNA3-HA-Nfatc2, respectively. pGL4.74-Renilla was purchased from Promega and included in all transfection experiments as a control of transfection efficiency. Transfection of EL4 cells was performed with Microporator MP-100 (Life Technologies) according to manufacturer protocols. Transfection of primary Th1 cells was performed with Amaxa nucleofection (Amaxa Biosystems) according to the manufacturer's instruction. Briefly, 5 million human CD4+ T cells were suspended in 100 μ L of Mouse T-cell Nucleofector Solution (VPA-1006) and transfected with 5 μ g of plasmid DNA. Luciferase activity was determined with Dual-Glo Luciferase Assay System (Promega).

Immunoprecipitation. Immunoprecipitation was performed as described previously (27). The following antibodies were used: anti-Ets-1 antibody (C-20; Santa Cruz), normal rabbit IgG (Santa Cruz), anti-CSE1L (N2N3; GeneTex), and anti-PPP2R1A (GTX102206; GeneTex).

Real-Time PCR and siRNA. Total RNA was extracted with TRIzol reagent and PureLink RNA Mini Kit (Life Technologies), and QuantiTect Reverse Transcription Kit (QIAGEN) was used for cDNA synthesis. Gene expression was determined by Brilliant II SYBR Green Kit and Mx3005P QPCR System (Agilent Technologies) according to the manufacturer's instructions. The sequences of primers are listed in Table S1. Human Ets-1 ON-TARGETplus SMARTpool siRNA (M-003887-00-0005) and ON-TARGETplus Nontargeting siRNA (D-001206-13-05) were purchased from Dharmacon/Thermo Scientific.

Chromatin Immunoprecipitation. CHIP assay was conducted as described previously with modifications (3). A detailed protocol is available upon request. Anti-Ets-1 (C20; Santa Cruz Biotechnology) and anti-NFATc2 (4G6-G5; Santa Cruz Biotechnology) were used for precipitation. The sequences of primers used in ChIP are listed in Table S2.

Statistical Analysis. Statistical analyses were performed with Student *t* test unless indicated otherwise. **P* < 0.05, ***P* < 0.01, ****P* < 0.001.

ACKNOWLEDGMENTS. This work is supported by National Institutes of Health Grant AI081052 (to I.-C.H.), US Department of Defense Grant W81XWH-11-1-0492 (to I.-C.H.), National Science Council of Taiwan Grant NSC 100-2320-B-002-090-MY3 (to S.-C.M.), and Graduate Students Study Abroad Program (H.-W.T.).

- Sharrocks AD (2001) The ETS-domain transcription factor family. *Nat Rev Mol Cell Biol* 2(11):827–837.
- Oikawa T, Yamada T (2003) Molecular biology of the Ets family of transcription factors. *Gene* 303:11–34.
- Grenningloh R, Kang BY, Ho IC (2005) Ets-1, a functional cofactor of T-bet, is essential for Th1 inflammatory responses. *J Exp Med* 201(4):615–626.
- Kim HP, Imbert J, Leonard WJ (2006) Both integrated and differential regulation of components of the IL-2/IL-2 receptor system. *Cytokine Growth Factor Rev* 17(5):349–366.
- Crispin JC, Tsokos GC (2009) Transcriptional regulation of IL-2 in health and autoimmunity. *Autoimmun Rev* 8(3):190–195.
- Rao A, Luo C, Hogan PG (1997) Transcription factors of the NFAT family: Regulation and function. *Annu Rev Immunol* 15:707–747.
- Müller MR, Rao A (2010) NFAT, immunity and cancer: A transcription factor comes of age. *Nat Rev Immunol* 10(9):645–656.
- Rooney JW, Sun YL, Glimcher LH, Hoey T (1995) Novel NFAT sites that mediate activation of the interleukin-2 promoter in response to T-cell receptor stimulation. *Mol Cell Biol* 15(11):6299–6310.
- Peng SL, Gerth AJ, Ranger AM, Glimcher LH (2001) NFATc1 and NFATc2 together control both T and B cell activation and differentiation. *Immunity* 14(1):13–20.
- Willingham AT, et al. (2005) A strategy for probing the function of noncoding RNAs finds a repressor of NFAT. *Science* 309(5740):1570–1573.
- Sharma S, et al. (2011) Dephosphorylation of the nuclear factor of activated T cells (NFAT) transcription factor is regulated by an RNA-protein scaffold complex. *Proc Natl Acad Sci USA* 108(28):11381–11386.
- Liu Z, et al. (2011) The kinase LRRK2 is a regulator of the transcription factor NFAT that modulates the severity of inflammatory bowel disease. *Nat Immunol* 12(11):1063–1070.
- Martins GA, Cimmino L, Liao J, Magnusdottir E, Calame K (2008) Blimp-1 directly represses Il2 and the Il2 activator Fos, attenuating T cell proliferation and survival. *J Exp Med* 205(9):1959–1965.
- Martins GA, et al. (2006) Transcriptional repressor Blimp-1 regulates T cell homeostasis and function. *Nat Immunol* 7(5):457–465.
- Gong D, Malek TR (2007) Cytokine-dependent Blimp-1 expression in activated T cells inhibits IL-2 production. *J Immunol* 178(1):242–252.
- John SA, Clements JL, Russell LM, Garrett-Sinha LA (2008) Ets-1 regulates plasma cell differentiation by interfering with the activity of the transcription factor Blimp-1. *J Biol Chem* 283(2):951–962.
- Bories JC, et al. (1995) Increased T-cell apoptosis and terminal B-cell differentiation induced by inactivation of the Ets-1 proto-oncogene. *Nature* 377(6550):635–638.
- Avots A, et al. (1997) GABP factors bind to a distal interleukin 2 (IL-2) enhancer and contribute to c-Raf-mediated increase in IL-2 induction. *Mol Cell Biol* 17(8):4381–4389.
- Grenningloh R, et al. (2011) Ets-1 maintains IL-7 receptor expression in peripheral T cells. *J Immunol* 186(2):969–976.
- Bassuk AG, Anandappa RT, Leiden JM (1997) Physical interactions between Ets and NF-kappaB/NFAT proteins play an important role in their cooperative activation of the human immunodeficiency virus enhancer in T cells. *J Virol* 71(5):3563–3573.
- Rabault B, Ghysdael J (1994) Calcium-induced phosphorylation of ETS1 inhibits its specific DNA binding activity. *J Biol Chem* 269(45):28143–28151.
- Macián F, García-Rodríguez C, Rao A (2000) Gene expression elicited by NFAT in the presence or absence of cooperative recruitment of Fos and Jun. *EMBO J* 19(17):4783–4795.
- Kallies A, et al. (2006) Transcriptional repressor Blimp-1 is essential for T cell homeostasis and self-tolerance. *Nat Immunol* 7(5):466–474.
- Nagaleekar VK, et al. (2008) IP3 receptor-mediated Ca²⁺ release in naive CD4 T cells dictates their cytokine program. *J Immunol* 181(12):8315–8322.
- Jayaraman T, Ondriasová E, Ondrias K, Harnick DJ, Marks AR (1995) The inositol 1,4,5-trisphosphate receptor is essential for T-cell receptor signaling. *Proc Natl Acad Sci USA* 92(13):6007–6011.
- Lulli V, et al. (2006) Overexpression of Ets-1 in human hematopoietic progenitor cells blocks erythroid and promotes megakaryocytic differentiation. *Cell Death Differ* 13(7):1064–1074.
- Lai CY, et al. (2012) Tyrosine phosphorylation of c-Maf enhances the expression of IL-4 gene. *J Immunol* 189(4):1545–1550.

Supporting Information

Tsao et al. 10.1073/pnas.1304343110

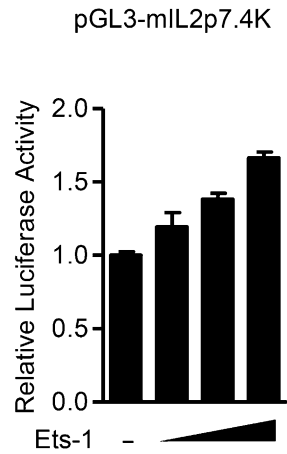


Fig. S1. E26 transformation-specific sequence 1 (Ets-1) weakly transactivates 7.4-kb IL-2 promoter/reporter. EL4 cells were transfected with the 7.4-kb IL-2 promoter/reporter along with escalating concentrations of Ets-1 expression vector. Cells were then stimulated with phorbol myristate acetate (PMA)/ionomycin, and relative luciferase activity was quantified and shown ($n = 3$).

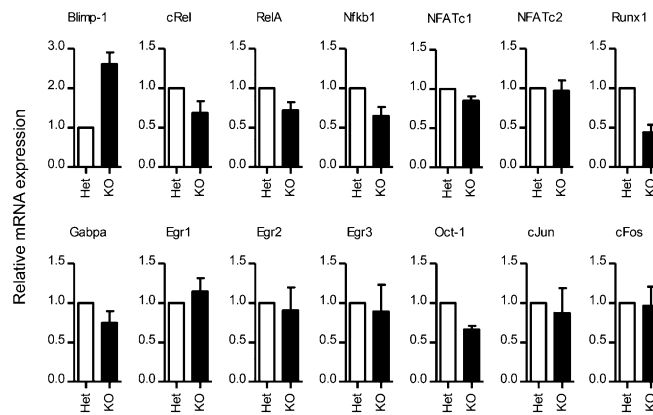


Fig. S2. Expression of transcription factors regulating the expression of IL-2. In vitro-differentiated WT and Ets-1KO Th1 cells were restimulated with PMA/ionomycin for 4 h. The transcript level of indicated genes was quantified with real-time PCR. The transcript level was first normalized against that of actin from the same sample. The normalized values obtained from WT Th1 cells were arbitrarily set as 1. The data shown are cumulative results of three independent experiments.

Appendix 3

RESEARCH ARTICLE

Open Access

Altered expression of protein tyrosine phosphatase, non-receptor type 22 isoforms in systemic lupus erythematosus

Hui-Hsin Chang^{1,2}, William Tseng¹, Jing Cui^{1,2}, Karen Costenbader^{1,2} and I-Cheng Ho^{1,2,3*}

Abstract

Introduction: A C-to-T single nucleotide polymorphism (SNP) located at position 1858 of human protein tyrosine phosphatase, non-receptor type 22 (PTPN22) complementary DNA (cDNA) is associated with an increased risk of systemic lupus erythematosus (SLE). How the overall activity of PTPN22 is regulated and how the expression of PTPN22 differs between healthy individuals and patients with lupus are poorly understood. Our objectives were to identify novel alternatively spliced forms of PTPN22 and to examine the expression of PTPN22 isoforms in healthy donors and patients with lupus.

Methods: Various human PTPN22 isoforms were identified from the GenBank database or amplified directly from human T cells. The expression of these isoforms in primary T cells and macrophages was examined with real-time polymerase chain reaction. The function of the isoforms was determined with luciferase assays. Blood samples were collected from 49 subjects with SLE and 15 healthy controls. Correlation between the level of PTPN22 isoforms in peripheral blood and clinical features of SLE was examined with statistical analyses.

Results: Human PTPN22 was expressed in several isoforms, which differed in their level of expression and subcellular localization. All isoforms except one were functionally interchangeable in regulating NFAT activity. SLE patients expressed higher levels of PTPN22 than healthy individuals and the levels of PTPN22 were negatively correlated with the Systemic Lupus International Collaborating Clinics/American College of Rheumatology Damage Index (SLICC-DI).

Conclusions: The overall activity of PTPN22 is determined by the functional balance among all isoforms. The levels of PTPN22 isoforms in peripheral blood could represent a useful biomarker of SLE.

Introduction

PTPN22 is a non-receptor type protein tyrosine phosphatase expressed mainly in hematopoietic cells [1]. It contains a basic bipartite nuclear localization signal (NLS) in its N-terminus, which is followed by a conserved protein tyrosine phosphatase (PTP) domain. An inhibitory domain inhibiting its phosphatase activity is located immediately after the PTP domain [2]. Its C-terminal half is relatively less conserved, with the exception of four proline-rich domains. Its physiological function is still not fully

understood. PTPN22 has been shown to attenuate the strength of T cell receptor (TCR) signals by interacting with Lck, Csk, and Vav [3-6]. PTPN22-deficient mice developed age-dependent splenomegaly due to hyperactivation of lymphocytes, and knockdown of PTPN22 in human T cells with small interfering RNA (siRNA) led to enhanced TCR-mediated nuclear factor-kappa B (NF- κ B) activity [7,8]. PTPN22 is present in both the cytoplasm and nucleus of macrophages [9]. Its nuclear localization requires the NLS proximal to the PTP domain. The expression of PTPN22 is further induced in alternatively activated macrophages through a STAT6-dependent mechanism. Cytoplasmic PTPN22 suppresses the polarization of classically activated macrophages, whereas nuclear PTPN22 promotes the differentiation of alternatively activated macrophages [9].

* Correspondence: iho@partners.org

¹Division of Rheumatology, Immunology, and Allergy, Department of Medicine, Brigham and Women's Hospital, One Jimmy Fund Way, Boston, MA 02115, USA

²Harvard Medical School, 25 Shattuck Street, Boston, MA 02115, USA
Full list of author information is available at the end of the article

Alternative splicing is an evolutionary conserved mechanism enabling a cell to produce proteins of different function from a single gene. A large body of evidence has indicated that the process of alternative splicing is correlated with disease activity or is even pathogenic in some autoimmune diseases [10-12]. At least two isoforms of PTPN22 have been reported. Lyp2, of which the sequence was deduced from two complementary DNA (cDNA) fragments, lacks the three most C-terminal proline-rich domains [1], whereas isoform 2, tentatively called PTPN22.2 for the purpose of discussion, splices out exons 10 and 11. However, it is unclear whether Lyp2 and PTPN22.2 are functionally distinct from the full-length PTPN22 (tentatively called PTPN22.1). We have also identified a novel isoform of PTPN22, called PTPN22.6, which lacks nearly the entire PTP domain [13]. Unlike PTPN22.1, overexpression of PTPN22.6 actually increased NFAT-dependent luciferase activity. More importantly, PTPN22.6 can act as a dominant negative mutant of PTPN22.1 in regulating cytokine production in Th cells, suggesting that the overall activity of PTPN22 can be influenced by the relative levels of its isoforms.

Several genome-wide association studies have linked PTPN22 to autoimmune diseases. A C-to-T single nucleotide polymorphism, which is located at position 1858 of PTPN22 cDNA and converts an arginine to a tryptophan, is associated with a higher risk of rheumatoid arthritis (RA), systemic lupus erythematosus (SLE), and type 1 diabetes but reduces the risk of Crohn's disease [7,14-17]. Despite these observations, it is still unclear whether the expression of PTPN22 in patients with autoimmune diseases differs from that of healthy individuals, and how this would occur. In addition, the functional impact of the C1858T SNP is still controversial and appears to be complicated. The conversion from arginine to tryptophan resulted in both gain and loss of function of PTPN22 in T cells in different studies [18,19]. We also found that the R-to-W conversion in the context of PTPN22.1 resulted in a gain of function of PTPN22 and a reduction of interleukin (IL)-2 production in T cells. In contrast, the R-to-W conversion in the context of PTPN22.6 led to a loss of function of PTPN22 and overproduction of IL-2 [13]. Thus, the functional impact of the C1858T SNP is isoform dependent. Furthermore, the C1858T SNP is associated with a loss-of-function phenotype in resting macrophages but a gain of function in classically activated macrophages [9]. How these C1858T SNP-associated functional changes affect the risk of autoimmune diseases is largely unknown. We have previously shown that the transcript level of PTPN22.6 but not total PTPN22 in peripheral blood is correlated with the 28-joint disease activity score with three variables including C-reactive protein (DAS28-CRP3) scores in patients with

RA [13]. However, it is unclear whether the expression of PTPN22 and its isoforms is altered in SLE patients and whether the level of PTPN22 isoforms also is correlated with disease activity of SLE.

Here we report the identification of additional isoforms of human PTPN22. We examined the expression of the PTPN22 isoforms in primary human T cells and macrophages. We further compared the expression of PTPN22 isoforms in the peripheral blood of 15 healthy donors and 49 SLE patients, and correlated the expression pattern of PTPN22 isoforms with clinical features of lupus.

Methods

Human samples

Forty-nine individuals with SLE fulfilling the 1997 American College of Rheumatology revised classification criteria [20] were previously recruited from the Lupus Center of the Brigham and Women's Hospital (BWH) for the Lupus Biobank. Fifteen control samples from healthy individuals without SLE or related connective tissue disease were obtained from the PhenoGenetic project at the same hospital. All study subjects consented to participate in studies conducted through the Lupus Biobank and the PhenoGenetic project, and agreed to the publication of results derived from such studies. Demographics were collected in addition to the following data from all SLE cases: 1) age at SLE onset; 2) SLE manifestations and organ involvement; 3) concurrent anti-double-stranded DNA antibody titer, C3 and C4. The treating rheumatologist performed a history and physical examination for SLE disease activity (Safety on Estrogens in Lupus Erythematosus National Assessment-SLE Disease Activity Index; SELENA-SLEDAI) [21], and history and chart review to complete an SLE organ damage assessment (SLICC-DI) [22]. Whole blood samples in PAX gene tubes (Qiagen, Germantown, MD, USA) were obtained from all subjects by standard antecubital venipuncture and stored at -80°C at the Broad Institute of MIT and Harvard as separated whole blood or extracted RNA. All aspects of the study were approved by the partners' Institutional Review Board.

Preparation of human peripheral blood mononuclear cells (PBMC) and helper T (Th) cells

PBMC were isolated from buffy coats. Th cells were enriched from PBMC with CD4 Microbeads (120-000-440, Miltenyi Biotec, Auburn, CA, USA). Macrophages were prepared from PBMC according to a published protocol [23].

Cell culture and medium

Human primary Th cells and Jurkat cells were cultivated in RPMI-1640. In some experiments, Th and Jurkat cells

were stimulated with 2.5 µg/ml of plate-bound anti-CD3 (Hit3a, Cat. # 300314, BioLegend, San Diego, CA, USA) and 2 µg/ml of soluble anti-CD28 (CD28.2, Cat. # 302914, BioLegend) in the presence of IL-2 (50 unit/ml) for an indicated amount of time. Human colonic adenocarcinoma cell line HT-29 cells (HTB38, ATCC) and human embryonic kidney cells 293 T were cultivated in McCoy's 5A medium (Gibco, Grand Island, NY, USA) and Dulbecco's modified Eagle's medium (DMEM), respectively. Primary human macrophages were stimulated with lipopolysaccharide (LPS) (1 µg/ml, InvivoGen, San Diego, CA, USA) along with human interferon-gamma (hIFN-γ) (50 ng/ml, PeproTech, Rocky Hill, NJ, USA) for 24 hours for M1 polarization or hIL-4 (25 ng/ml, PeproTech) along with hIL-13 (25 ng/ml, PeproTech) for 24 hours for M2 polarization.

Western blotting

Whole-cell extract was obtained by lysing cells with lysis buffer (50 mM Tris-HCl, pH 7.5, 150 mM NaCl, 1% TritonX-100, 0.5% DOC, 0.1% SDS, and 1 mM EDTA) containing 0.5 mM PMSF and complete protease inhibitor cocktail (Roche, Basel, Switzerland). Cytoplasmic and nuclear extracts were prepared by washing cells with cold phosphate-buffered saline (PBS) and resuspending them in hypotonic lysis buffer (10 mM HEPES, pH7.9, 1 mM MgCl₂, 10 mM KCl, 0.1% TritonX-100, 20% Glycerol, 0.5 mM PMSF, and protease inhibitors) on ice for 10 minutes. The supernatant, corresponding to cytoplasmic fraction, was collected by centrifugation at 12,000 g for 10 minutes. The nuclear pellet was washed with hypotonic lysis buffer and then resuspended in hypertonic lysis buffer (10 mM HEPES, pH7.9, 400 mM NaCl, 1 mM EDTA, 0.1% TritonX-100, 20% Glycerol, 1 mM PMSF, and protease inhibitors) and then incubated on ice for 20 minutes. Nuclear extract was collected by centrifugation. Protein extract was analyzed by immunoblot. The following antibodies were used: human PTPN22 antibody AF3428 (R & D Systems, Minneapolis, MN, USA), Hsp90 α/β (sc-7947) and Lamin B (sc-6216) antibody (Santa Cruz Biotechnology, Inc. Santa Cruz, CA, USA), Oct1 (sc-232, Santa Cruz Biotechnology, Inc.), and FLAG antibody (F3165, Sigma-Aldrich, St Louis, MO, USA).

Plasmid, transfection and luciferase assay

cDNAs encoding PTPN22.1 and PTPN22.8 were amplified directly from Jurkat cells with primers 5'-CGGGATCCTTGCTCTGCAGCATGGACCAAAGA-3' and 5'-GACGTCGACGCGTTTAAATATTCCAAGTTGGTGT-3'. cDNA clones BC071670 (PTPN22.2) and BC017785 (PTPN22.7) were purchased from Open Biosystems (Huntsville, AL, USA). cDNA clones AK3030124 (PTPN22.4), AK310698 (PTPN22.5), and AK310570

(PTPN22.6) were obtained from the NITE Biological Resource Center (Chiba, Japan). All cDNA fragments were cloned into an N-terminal FLAG-tag expression vector pCMV-Tag 2B (Stratagene, La Jolla, CA, USA). Transfection of 293 T cells was performed with Effectene Transfection Reagent (Cat. # 301427, Qiagen). Transfection of Jurkat cells was performed with electroporation with a Gene Pulser II (Bio-Rad, Hercules, CA, USA) set at 374 V/1050 µF. In all NFAT luciferase assays, Jurkat cells were transfected with 5 µg of 3xNFAT-Luc, 0.5 µg pTK-Renilla, and 10 µg of pCMV-Tag 2B expression vectors; rested for 48 hours; and then stimulated with anti-CD3 for 6 hours. Luciferase activity was determined with a Dual-Luciferase™ Reporter Assay System (Promega, Madison, WI, USA). Firefly luciferase activity was then normalized against Renilla luciferase activity obtained from the same sample. 3xNFAT-Luc and pTK-Renilla luciferase vectors were described previously [24].

Real-time PCR and non-quantitative PCR

Total RNA was prepared using a Trizol Plus kit (Invitrogen, Carlsbad, CA, USA). Reverse transcription was performed on 1 µg of total RNA using the QuantiTect Reverse Transcription kit (Qiagen). Real-time PCR analysis was performed using the Brilliant SYBR Green QPCR kit according to the manufacturer's protocol (Stratagene) on a MX-3000P apparatus (Stratagene). The cycling conditions are: one cycle of 95C for 10 minutes and 40 cycles of 95C for 30 seconds, 56C for 1 minute, and 72C for 1 minute. The following primer pairs were used: 'total' 5'-GCAGAAGTTCCTGGATGAG-3' and 5'-TCAGCCA CAGTTGTAGGATAG-3'; Lyp2 5'-GTGGAACATCTGA ACCAAAG-3' and 5'-AGCCAAGAGAAATTTTACCT G-3'; PTPN22.2 5'-CCAAGAGGATGACAGTGTTTC-3' and 5'-CTTTGCTTGACTCCCATCTTTTA-3'; PTPN 22.5/6 5'-ATCTGTAATTCTTGCCACC-3' and 5'-CTCTTCAGTAAAATAACACACATACC-3'; PTPN22.6 5'-TTTGCCCTATGATTATAGCCG-3' and 5'-GTTCTCA GGAATTATAAGGACACT-3'; PTPN22.7/8 5'-TCTACA ACCCTCCTGGACT-3' and 5'-TTTCAGCTTCCTTTC CCATT-3'; Ets-1(p51) 5'-CTCCTATGACAGCTTCGA CT-3' and 5'-ATCTCCTGTCCAGCTGATAA-3'; β-actin 5'-GTGACAGCAGTCGGTTGGAG-3' and 5'-AGGAC TGGGCCATTCTCCTT-3'. All real-time PCR reactions were done in duplicate and the transcript levels were normalized against those of β-actin.

siRNA transfection

One million Jurkat cells were resuspended with 400 µl Opti-mem I containing 400 pmole of siRNA and subjected to electroporation with a Gene Pulser II (Bio-Rad) set at 250 V/400 µF. Human PTPN22 ON-TARGETplus SMARTpool siRNA (L-008066-00-0005), ON-TARGETplus

non-targeting siRNA (D-001810-01-05), and siLyp2 (sense: 5'-UGGAAGAAUGGUUCGUAAAUU-3'; anti-sense: 5'-UUAACGAACCAUUCUCCAUAU-3') were purchased from Dharmacon/Thermo Scientific (Lafayette, CO, USA).

Statistical analysis

D'Agostino-Pearson omnibus normality test was used to examine the normality of the data. Statistical analysis was

performed with paired Student's *t* test (Figure 1C), one-way ANOVA (Figures 1D and 3B), the Mann-Whitney test (Figure 4), and Spearman correlation (Figure 5).

Results

Identification of additional PTPN22 isoforms

In addition to the published PTPN22 isoforms, we identified several cDNA sequences corresponding to three

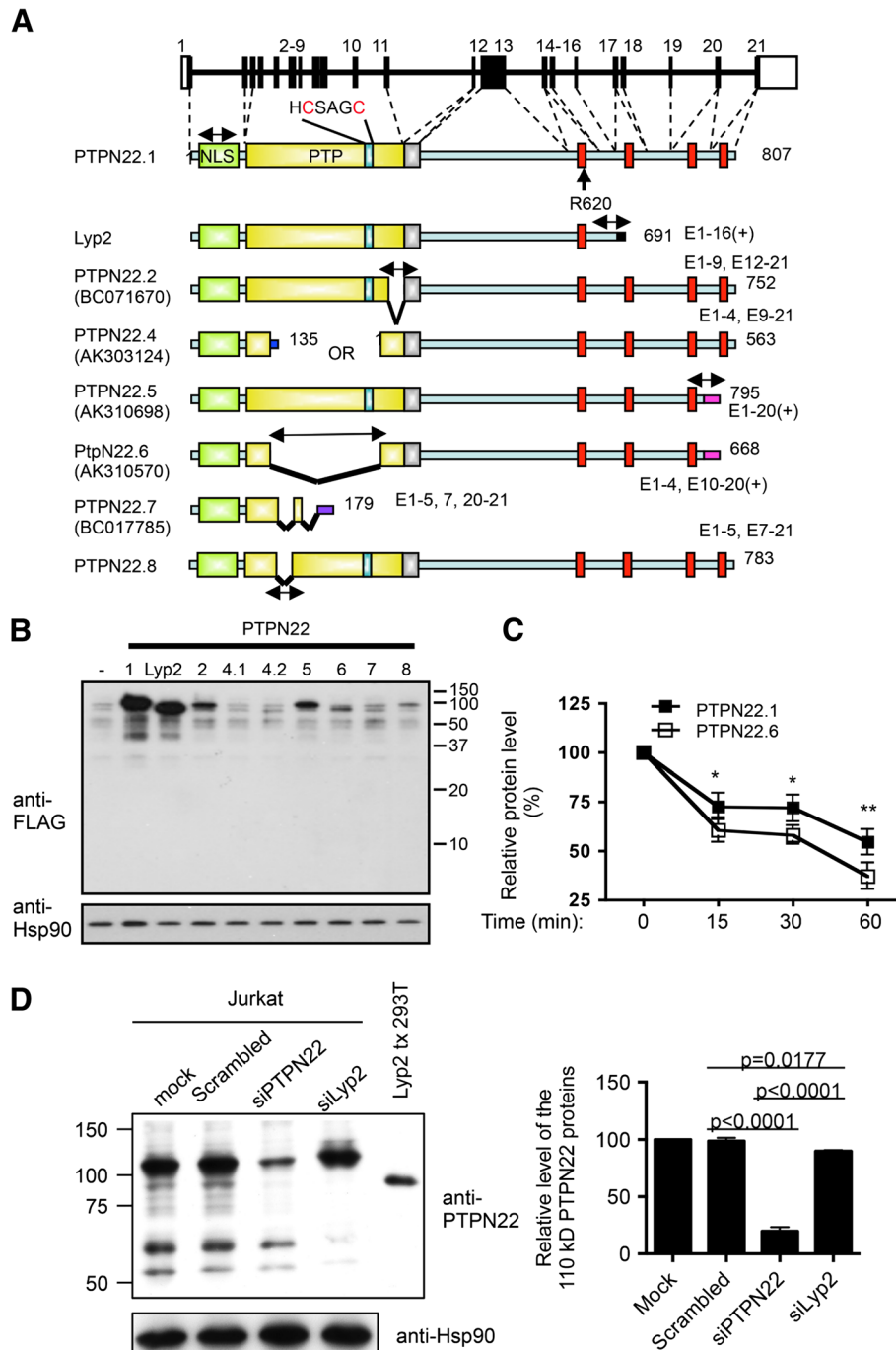


Figure 1 (See legend on next page.)

(See figure on previous page.)

Figure 1 Alternatively spliced forms of human protein tyrosine phosphatase, non-receptor type 22 (PTPN22). (A) Schematic diagrams of the human *ptn22* gene and putative protein products of each isoform. Exons are numbered, and white boxes represent untranslated exons. Green boxes represent nuclear localization signal (NLS). Yellow boxes represent the protein tyrosine phosphatase (PTP) domains. The key catalytic region (HCSAGC) and R620 are marked. Silver boxes are inhibitory domains. Red boxes represent proline-rich regions. Two-headed arrows indicate the real-time PCR products of the isoforms. The exons constituting each isoform are indicated. The GenBank accession numbers, if available, are listed in parentheses. (B) 293 T cells were transfected with 1 µg of an expression vector expressing indicated FLAG-PTPN22 isoforms. The protein levels of FLAG-PTPN22 isoforms and Hsp90 in the transfected cells were determined with Western blotting. (C) 293 T cells were transfected with a plasmid vector expressing FLAG-PTPN22.1 and FLAG-PTPN22.6. The transfected cells were treated with 20 µg/ml of cycloheximide. The levels of FLAG-PTPN22.1 and FLAG-PTPN22.6 were then determined with Western blotting and densitometry at indicated time points after the addition of cycloheximide. The level at time 0 for each protein was arbitrarily set as 100%. Statistical significance was determined with paired Student's *t* test. **P* < 0.05; ***P* < 0.005. (D) Jurkat cells were transfected with indicated siRNA. Cell extract of the transfected cells was then analyzed on Western blotting using anti-PTPN22 and anti-Hsp90 (the left panel). Extract from 293 T cells transfected with an expression vector of Lyp2 was included in the Western blotting (Lyp2 tx 293 T). The levels of the dominant 110 kD PTPN22 protein bands were quantified with a densitometer and normalized against the level of Hsp90 from the corresponding samples, and are shown in the right panel. The normalized level of the mock-transfected cells was arbitrarily set as 100%. Statistical analysis of three independent experiments was performed with one-way ANOVA followed by Tukey's test.

additional spliced variants of human PTPN22 in the NCBI Gene database (Figure 1A). AK303124 is the product of an out-of-frame splicing between exons 4 and 9. It contains two open reading frames: one of 135 amino acid residues and the other starting at a methionine of exon 9 and corresponding to the last 563 amino acid residues of the full-length PTPN22. AK310698 lacks exon 21 but includes at its C-terminus eight novel amino acid residues encoded by the genomic sequence immediately 3' to exon 20. BC017785 splices out exons 6 and 8 to 19. We tentatively named these three novel

isoforms PTPN22.4, PTPN22.5, and PTPN22.7. We also amplified a novel isoform PTPN22.8 (GenBank accession number JN084012), which lacks exon 6, directly from Jurkat T cells. We were able to confirm the presence of each of the unique or shared spliced junctions in human primary T cells with real-time PCR and DNA sequencing (Figure 1A and data not shown). In addition, we were able to amplify the transcript of each of the isoforms except Lyp2 in its entirety with PCR directly from Jurkat cells. Several attempts to amplify the entire Lyp2 were unsuccessful. The counterpart of PTPN22.2 is also

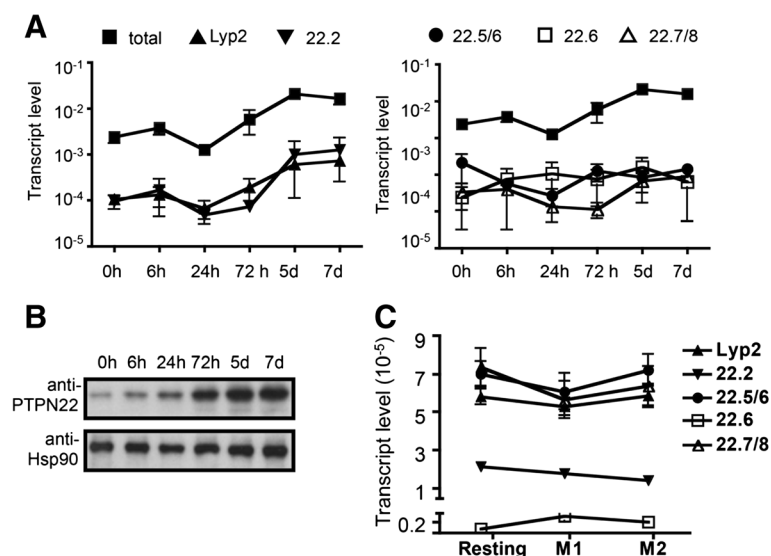


Figure 2 Expression of protein tyrosine phosphatase, non-receptor type 22 (PTPN22) isoforms in human helper T (Th) cells and macrophages. (A) RNA was prepared from human Th cells obtained from three healthy donors, which were stimulated *in vitro* with anti-CD3/anti-CD28 for indicated periods of time and subjected to real-time PCR analysis with isoform-specific primers. Each real-time PCR reaction was done in duplicate. The transcript levels thus obtained were normalized against those of β-actin from the same samples. The data shown are the means and standard deviations from three donors. (B) Protein extract prepared from human Th cells described in A was subjected to Western blotting and probed with PTPN22 antibody and Hsp90 antibody. (C) RNA was prepared from resting, M1, and M2 macrophages derived from peripheral blood of seven additional healthy donors and subjected to real-time PCR analysis with isoform-specific primers.

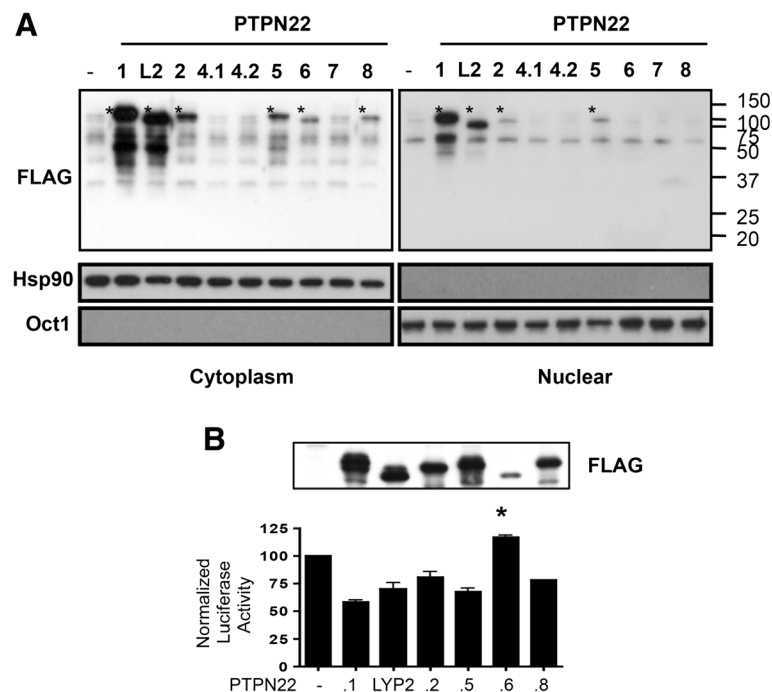


Figure 3 Subcellular localization and function of protein tyrosine phosphatase, non-receptor type 22 (PTPN22) isoforms. (A) 293 T cells were transfected with 1 μ g of plasmid vectors expressing indicated FLAG-tagged PTPN22 isoforms. Cytoplasmic and nuclear extract was separately prepared from the transfected cells and subjected to Western blotting with indicated antibodies. The protein product of each isoform is marked with '*'. **(B)** Jurkat cells were transfected with a NFAT-luc reporter, 10 μ g of pCMV2B expressing indicated FLAG-PTPN22 isoforms, and a TK-Renilla reporter. The transfected cells were then stimulated with anti-CD3 overnight. A fraction of the transfected cells was subjected to Western blotting with anti-FLAG (the top panel). The luciferase activity of the remaining cells was analyzed. Normalized firefly luciferase activity was calculated as described in Methods and is shown in the bottom panel. In each experiment, the normalized value from cells transfected with the empty expression vector was arbitrarily set as 100. The data shown are the means and standard deviations of three independent experiments. Statistical significance was calculated with one-way ANOVA followed by Dunn's test comparing non-full-length isoforms to PTPN22.1. * $P=0.0158$.

present in rhesus monkeys and chimpanzees, according to NCBI Gene database, suggesting that these alternative splicing events are evolutionarily conserved.

Not all of the isoforms can be expressed efficiently in mammalian cells. We replaced the initiating methionine of each isoform with a FLAG tag and expressed the FLAG-fused PTPN22 proteins in 293 T cells. We found that PTPN22.1 and Lyp2 were expressed more efficiently than PTPN22.2, PTPN22.5, PTPN22.6, and PTPN22.8 (Figure 1B). No protein product of PTPN22.4, either starting from the methionine in exon 1 (4.1) or exon 9 (4.2), or of PTPN22.7 was detected, suggesting that PTPN22.4 and PTPN22.7 are non-productive. We therefore excluded these two isoforms from subsequent functional analyses.

Despite the difference in the protein level, the transcript level of each isoform in transfected cells was very comparable when measured with real-time PCR using a pair of primers targeting the FLAG/PTPN22 fusion junction that is common to all isoforms (data not shown). As the transcripts of these FLAG-PTPN22 proteins contain the same Kozak sequence, initiating ATG, and 3' polyadenylation tail, which are embedded in the

expression vector, we postulated that the difference in the protein level was due to a difference in protein stability instead of translational efficiency. To test this hypothesis, we compared the protein stability between PTPN22.1 and PTPN22.6, which was chosen as an example because it was the least expressed but detectable isoform. We treated transfected cells with cycloheximide to stop protein synthesis and then compared the degradation rate of FLAG-PTPN22.1 and FLAG-PTPN22.6. PTPN22.1 protein was indeed more stable than PTPN22.6 (Figure 1C).

We previously used a PTPN22.6-specific antibody to demonstrate the presence of endogenous PTPN22.6 protein in human T cells. In addition, an anti-human polyclonal PTPN22 antibody, which was raised against S306-S684 of PTPN22.1 and should recognize all isoforms, detected one dominant broad protein band centering around 110 kD and several smaller protein species in Jurkat human T cells but not in HT-29 adenocarcinoma cells, which do not express PTPN22 (Figure 1D and [13]). The levels of almost all of the protein species were reduced by PTPN22 siRNA but not by scrambled siRNA. The commercially available PTPN22 siRNA

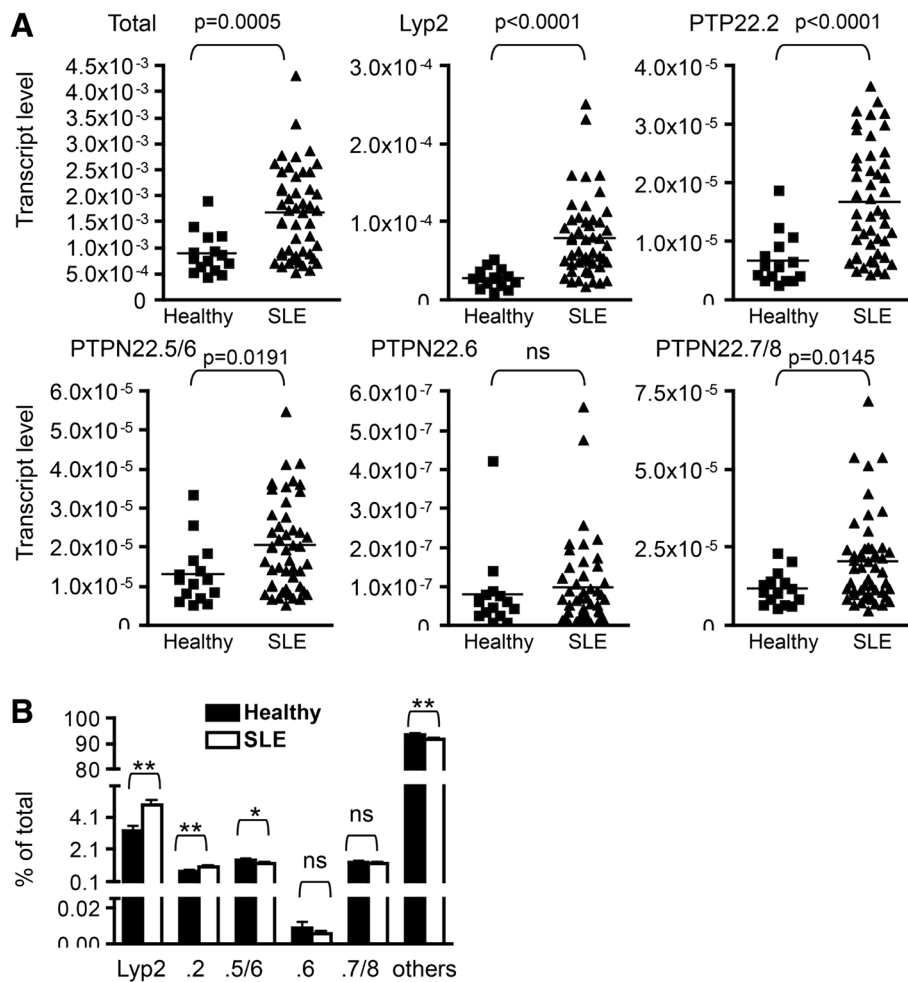


Figure 4 Expression of protein tyrosine phosphatase, non-receptor type 22 (PTPN22) isoforms in healthy donors and patients with lupus. (A and B) RNA was prepared from whole blood of healthy individuals (N = 15) and patients with lupus described in Table 1. The RNA was subjected to real-time PCR using PTPN22 isoform-specific primers. The transcript level thus obtained was normalized against that of β -actin obtained from the same sample and is shown in A. The relative level of PTPN22 isoforms is shown in B. Statistical significance was determined with Student's *t* test. ns stands for not significant. * $P < 0.05$; ** $P < 0.005$.

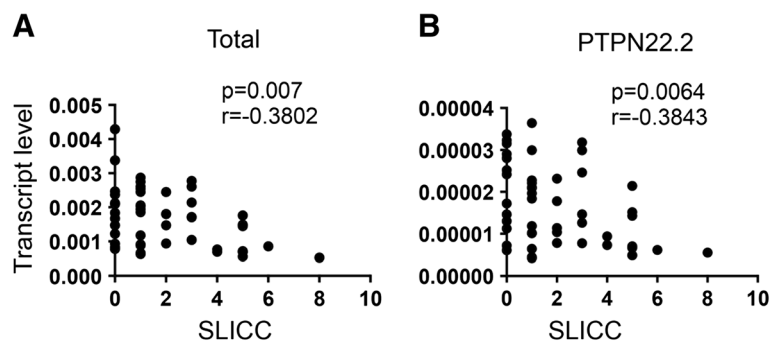


Figure 5 The level of protein tyrosine phosphatase, non-receptor type 22 (PTPN22) is negatively correlated with the Systemic Lupus International Collaborating Clinics/American College of Rheumatology Damage Index (SLICC). Transcript level of total PTPN22 (A) and PTPN22.2 (B) in peripheral blood of patients with lupus described in Figure 4 was plotted against SLICC. Correlation was analyzed with a non-parametric Spearman test and adjusted for covariates including gender, age, age of disease onset, duration of disease, and race (white or non-white).

recognizes four different RNA sequences of PTPN22 and very likely affects the expression of all isoforms. Therefore, the 110 kD broad protein band, which was reduced by approximately 80% by the PTPN22 siRNA, is very likely composed of PTPN22.1, PTPN2.2, PTPN22.5, and PTPN22.8, which have comparable molecular weight. The smaller protein species very likely include Lyp2 and/or yet-to-be-discovered isoforms. However, there is no other isoform-specific antibody, and it is still unclear whether the other non-full-length PTPN22 proteins also exist in human cells. To further confirm their existence, we designed a single siRNA targeting the 3' end of Lyp2. This siRNA is expected to suppress the expression of Lyp2 and any yet-to-be-discovered isoforms sharing the 3' end with Lyp2, but not the other isoforms shown in Figure 1A. Indeed, expression of the siLyp2 in Jurkat cells led to the disappearance of the smaller PTP22 protein species including one with a molecular weight comparable to that of Lyp2 (Figure 1D, the left panel), but had a negligible effect on the level of the dominant 110 kD protein band (Figure 1D, the right panel). This result strongly indicates that, in addition to PTPN22.6, endogenous Lyp2 protein is also present in human T cells.

Expression of PTPN22 isoforms in human PBMC

We set out to compare the expression kinetics of each isoform in human T cells. We isolated primary Th cells from the peripheral blood of healthy donors and stimulated the cells with anti-CD3/anti-CD28 for various periods of time. cDNA was prepared from the stimulated cells and subjected to real-time PCR. We designed three pairs of primers specific for PTPN22.2, Lyp2, and PTPN22.6. (Figure 1A). However, PTPN22.1, PTPN22.5, and PTPN22.8 do not have an isoform-specific splice junction. We therefore designed three additional pairs of primers. One pair targeted the 5' region shared by all isoforms and was used to represent 'total' PTPN22 expression. The second pair of primers (PTPN22.5/6) recognized both PTPN22.5 and PTPN22.6 but not other isoforms. The third pair of primers (PTPN22.7/8) was specific to the splice junction shared only by PTPN22.7 and PTPN22.8. We measured the level of PTPN22 isoforms in Th cells obtained from three healthy donors. The data on the level of total PTPN22 and PTPN22.6 were previously reported but were included here for the purpose of comparison. We found that the level of 'total' transcript dropped by approximately 50% 24 hours after stimulation and then gradually increased and eventually peaked 5 days after stimulation (Figure 2A). The level of the total PTPN22 transcript was approximately 10 to 50 times more than that of the non-full-length isoforms. The expression kinetics of the non-full-length PTPN22 isoforms can be roughly divided into two groups. The first group including Lyp2 and PTPN22.2 displayed a

kinetics similar to that of the total transcript (Figure 2A). In contrast, the transcript level of the second group including PTPN22.5/6, PTPN22.6, and PTPN22.7/8 was not induced throughout the whole course. None of the PTPN22 transcripts were detected at any significant level in HT-29 cells, which expressed no PTPN22 (data not shown). As the transcript levels of the non-full-length isoforms were much lower than that of the total PTPN22 transcript, we believe that the full-length PTPN22 (that is PTPN22.1) is the main contributor to the level of the total PTPN22 transcript. Indeed, the molecular weight of a dominant protein band detected with anti-PTPN22 on Western blotting corresponded to that of PTPN22.1 (Figure 2B). The level of PTPN22.1 protein in primary Th cells also gradually increased after stimulation, a kinetics similar to that of the total transcript of PTPN22 with the exception of no reduction in the levels at 24 hours.

PTPN22 is also expressed in myeloid cells including macrophages. Macrophages can be divided into two major functional subsets: classically activated macrophages (M1 cells) and alternatively activated macrophages (M2 cells). We have recently shown that resting macrophages expressed a basal level of total PTPN22 and that the level stayed relatively unchanged in M1 cells [9]. In contrast, the expression of total PTPN22 was induced in M2 cells to a level three to four times higher than that of resting or M1 cells. To examine the expression of PTPN22 isoforms in macrophages, we quantified the transcript level of PTPN22 isoforms in macrophages from seven healthy donors. We found that the levels of Lyp2, PTPN22.2, PTPN22.5/6, PTPN22.6, and PTPN22.7/8 were very comparable among resting, M1, and M2 macrophages (Figure 2C). Thus, the increase in total PTPN22 observed in M2 cells mainly comes from PTPN22.1. Taken together, our data indicate that the level of PTPN22 isoforms varies significantly among cells types and in response to different stimuli.

Subcellular localization and function of PTPN22 isoforms

PTPN22 contains a NLS at its N-terminus and is also present in the nucleus of macrophage and T cells [9]. This NLS is present in all isoforms. To further examine the subcellular localization of PTPN22 isoforms, we expressed each isoform in 293 cells and separately examined the cytoplasmic and nuclear extract of the transfected cells with Western blotting. As expected, PTPN22.1 was detected in both the cytoplasm and the nuclei of the transfected cells (Figure 3A). A similar pattern of subcellular localization was observed for Lyp2, PTPN22.2, and PTPN22.5. Interestingly, we detected PTPN22.6 and PTPN22.8 only in the cytoplasm but not in the nucleus of the transfected cells, suggesting the presence of an additional and essential NLS

encoded by exon 6, which is spliced out in these two isoforms.

PTPN22.6 can act as a dominant negative variant of PTPN22.1. But the function of the other isoforms is still unclear. We therefore examined the effect of the other isoforms on NFAT-driven luciferase activity. As expected, overexpression of PTPN22.1 in Jurkat cells suppressed NFAT-dependent luciferase activity by approximately 50%. Interestingly, Lyp2, PTPN22.2, PTPN22.5, and PTPN22.8, despite missing parts of the PTP domain, also had the same effect (Figure 3B). There was no statistically significant difference among these isoforms even after adjustment for the protein level. In addition, a catalytic dead mutant of mouse PTPN22, which contains D195A and C227S mutations [4], had no impact on NFAT activity (Additional file 1), further indicating that these isoforms are still catalytic active. In contrast, expression of PTPN22.6 resulted in a subtle but statistically significant increase in NFAT activity. This result was reported before but was included for comparison [13].

Expression of PTPN22 isoforms in healthy and SLE populations

To determine whether the expression of PTPN22 isoforms was altered in SLE patients and whether the level of PTPN22 isoforms was correlated with clinical features of SLE, we quantified the transcript level of each isoform in the peripheral blood of 15 healthy donors and 49 patients with SLE. The demographic characteristics of the study subjects are shown in Table 1. All healthy individuals were female, but two of the 49 patients with lupus were male. The average ages were 46.2 years and 48.8 years for the healthy and SLE groups, respectively.

We found that the transcript level of all isoforms except PTPN22.6 was approximately two to three times higher in the SLE group compared to that of the healthy group (Figure 4A). The level of PTPN22.6 was low but comparable in both groups. In addition, the transcript level of Ets-1, a gene that is associated with SLE in Asians [25-27], was also comparable between the two groups (Additional file 2), indicating that the aberrant expression of PTPN22 is not a non-specific event. To determine whether there was preferential expression of any one of the isoforms in SLE patients, we calculated the percentage of each isoform against the total PTPN22 transcript. After deducing the percentage of Lyp2, PTPN22.2, PTPN22.5/6, PTPN22.6, and PTPN22.7/8,

the remainder was designated as 'others,' which we believe was made up of mainly PTPN22.1. We found that SLE patients, compared to healthy individuals, had a modest but statistically significant increase in the percentage of Lyp2 and PTPN22.2 but a reciprocal decrease in the percentage of PTPN22.5/6 and the 'others' (Figure 4B). There was no difference in the percentage of PTPN22.6 and PTPN22.7/8. Thus, patients with SLE had not only overexpression of PTPN22 but also an alteration in the relative level of PTPN22 isoforms.

We subsequently examined whether there was any correlation between the transcript level of PTPN22 and clinical parameters of lupus. We found no correlation between total PTPN22 level and SLEDAI, level of anti-nuclear antibody, or level of anti-double-stranded DNA. However, a significant negative correlation between SLICC-DI and the total transcript level of PTPN22 was observed (Figure 5A). We then examined whether any of the non-full-length isoforms was also negatively correlated with SLICC-DI. We found that the level of PTPN22.2 but not other non-full-length isoforms also showed a negative correlation with SLICC-DI even after adjustment for covariates including gender, age, age of disease onset, duration of disease, and race (white or non-white) (Figure 5B).

Discussion

The collection of PTPN22 isoforms has expanded significantly over the past few years. During the preparation of this manuscript, another isoform lacking exon 15 was deposited in the NCBI database as isoform 3 (tentatively called PTPN22.3), which is also present in chimpanzees [28]. The expression of PTPN22.3 in different types of hematopoietic cells and its effect on NFAT activity have yet to be examined. Despite the publication of the cloning of Lyp2, we would like to cautiously point out that the existence of this transcript has yet to be confirmed. The conclusion that this isoform exists is based on the identification of a cDNA fragment corresponding to its unique 3' end. This isoform was then deduced from several overlapping cDNA fragments [1]. However, there is no full-length cDNA clone in the NCBI database matching Lyp2. In addition, we were unable to amplify the entire transcript of Lyp2 from Jurkat cells. Instead, we recently amplified an intact and novel transcript from Jurkat cells that shares the 3' end with Lyp2 but contains a deletion in the PTP domain (data not shown). It

Table 1 Demographic characteristics of the study subjects

	Healthy	With systemic lupus erythematosus
Number and gender	15 F	47 F and 2 M
Age (years)	46.2 ± 5.2	48.8 ± 12.5
Ethnicity	9 Caucasians, 4 blacks, 1 Asians, and 1 Asian/Caucasian	36 Caucasians, 4 blacks, 4 Asians, and 5 Hispanics

is very likely that there are other yet-to-be-discovered isoforms sharing the 3' end with Lyp2. This scenario is consistent with the observation that the siLyp2 suppresses the expression of several PTPN22 protein species (Figure 1D). Ultimately, mass spectrometry and/or isoform-specific antibodies will be needed to confirm the presence of non-full-length PTPN22 proteins in different types of immune cells.

With the exception of PTPN22.6, all isoforms examined in this study are functionally interchangeable in suppressing NFAT activity. However, the function of PTPN22 is still poorly understood. For example, we recently found that cytoplasmic PTPN22 suppresses M1 polarization, whereas nuclear PTPN22 promotes M2 polarization of macrophages [9]. PTPN22 is also expressed in neutrophils and NK cells, and its function in these cells is largely unknown. It is possible that the non-full-length isoforms, each missing a part (or parts) of the PTPN22 protein and some excluded from the nucleus, can also act as dominant negative mutants of PTPN22.1 in other functional readouts or immune cells. Thus, the overall activity of PTPN22 is determined by not only the total level of PTPN22 but also by the functional balance among all isoforms.

The functional balance of PTPN22 isoforms may critically influence the impact of the C1858T SNP. It is still poorly understood how the C1858T SNP increases the risk of SLE and RA but lowers the risk of Crohn's disease. There are conflicting data on the impact of this SNP on the responsiveness of human T cells to stimulation. We have previously shown that the effect of the C1858T SNP on cytokine production in Th cells is isoform dependent [13]. The R-to-W conversion in the context of PTPN22.1 further weakened NFAT activity and IL-2 production. In contrast, the R-to-W conversion in the context of PTPN22.6 enhanced IL-2 production. If the other non-full-length PTPN22 isoforms also have a function different from that of PTPN22.1, then the cumulative impact of the C1858T SNP can be complicated and highly dependent on the portfolio of PTPN22 isoforms. This scenario may explain the conflicting data described above.

Why do SLE patients express a higher level of PTPN22? The expression of PTPN22 is induced in activated T cells and M2 macrophages. Th and macrophages of patients with lupus are likely activated and express a higher level of PTPN22. The whole blood samples stored in the BWH Lupus Biobank did not allow separate quantification of PTPN22 levels in each type of blood cells. Some types of blood cells, such as T cells, may express more PTPN22 than other types of blood cells, such as macrophages. An expansion of the high PTPN22-expressing cells, but not necessarily an increase in their status of activation, may also contribute to the high level of PTPN22 observed in

the whole blood of patients with SLE. Identifying the PTPN22-expressing cells responsible for the higher PTPN22 level in the peripheral blood of patients with SLE may shed light on the pathogenesis of this disease. It is also intriguing to notice that patients with SLE not only have a high level of PTPN22 but also have an altered portfolio of PTPN22 isoforms. They express more Lyp2 and PTPN22.2 at the expense of PTPN22.1 compared to healthy individuals. The clinical significance of such an alteration in the portfolio of PTPN22 isoforms has yet to be determined.

A recent paper by Ronninger *et al.* reported a trend suggesting that the combined transcript level of long PTPN22 isoforms including PTPN22.1, PTPN22.2, and PTPN22.3 was higher in PBMC of patients with RA than healthy controls [29]. Although this trend is consistent with the data shown in Figure 4, their data also showed a trend of lower Lyp2 in patients with RA. In addition, the ratio of long PTPN22 to Lyp2 was significantly higher in patients with RA. We, however, found that the level of Lyp2 was higher while the ratio of long PTPN22 to Lyp2 was lower in our patients with lupus. This discrepancy may originate from fundamental differences in the pathogenesis between RA and lupus. In addition, the primers and probe used to detect long PTPN22 isoforms in Ronninger's paper target their 3' end and will not detect PTPN22.5, PTPN22.6, and other yet-to-be-discovered isoforms sharing the 3' end with PTPN22.5 and PTPN22.6. The difference in primers used may also explain why the ratio of long PTPN22 to Lyp2 is much lower in Ronninger's study (1 to 1.5) than ours (20 to 30). Our calculated ratio is more consistent with the data shown in Figure 1D.

McKinney *et al.* recently showed that a higher level of PTPN22, along with a low level of ITGA and Notch1 in CD8 + T cells but not PBMC, was associated with a poor prognosis in SLE and anti-neutrophil cytoplasmic antibody (ANCA)-associated vasculitis [30]. The molecular explanation for this correlation is still lacking. The level of PTPN22 in McKinney's study was indirectly determined by gene chip, which is not specific to any of the PTPN22 isoforms. It will be interesting to know whether such an association could be observed in PBMC if the expression of each of the PTPN22 isoforms was measured. Given the McKinney's report, it is surprising to find in our study that the level of PTPN22 in peripheral blood was not correlated with SLE disease activity (SLEDAI), but actually was negatively correlated with SLICC-DI. SLICC-DI is usually associated with disease duration. However, we found no correlation between PTPN22 level and disease duration in our SLE population. It is possible that the negative correlation is attributed to damage to one organ. The SLICC-DI in our SLE population was relatively low. However, we did

notice a trend suggesting a negative association between PTPN22 levels and damage to the musculoskeletal system (data not shown). More patients will be needed to establish such a negative association.

We do not have a biological explanation for the negative correlation between PTPN22 level and SLICC-DI at this moment. There was a substantial drop in the level of PTPN22 in patients with a SLICC-DI equal to or higher than three. We saw no obvious difference in the portfolio of PTPN22 isoforms in this small group of patients (N = 12) compared to the other patients with SLE. Deficiency of PTPN22 has been shown to lead to hyperactivation of lymphocytes and overexpression of inflammatory cytokines in macrophages [8,9]. Thus, a reduction in the level of PTPN22 as detected in those 12 patients can be proinflammatory, thereby resulting in more organ damage. This hypothesis remains to be confirmed.

Conclusions

This paper is the first to examine and compare the expression, subcellular localization, and function of various isoforms of PTPN22, a gene that is strongly associated with several rheumatic diseases. Human PTPN22 can be expressed in several isoforms, and some of the isoforms are also present in the nucleus due to at least two essential nuclear localization signals. The expression profile of PTPN22 isoforms varies among cell types, and is altered in patients with lupus. In addition, the levels of total PTPN22 and one of the isoforms are negatively correlated with SLICC-DI scores. Future studies investigating the molecular basis of this negative correlation will provide important insight into the pathogenesis of SLE.

Additional files

Additional file 1: Suppression of NFAT activity by protein tyrosine phosphatase, non-receptor type 22 (PTPN22). Description of data: the data show that a catalytic dead mutant of PTPN22 is not able to suppress NFAT activity.

Additional file 2: Expression of Ets-1 in healthy individuals and patients with systemic lupus erythematosus (SLE). Description of data: the data show that the expression of Ets-1 is comparable between healthy individuals and patients with SLE.

Abbreviations

cDNA: complementary DNA; DAS28-CRP3: 28-joint disease activity score with three variables including C-reactive protein; DMEM: Dulbecco's modified Eagle's medium; IFN: interferon; IL: interleukin; NF- κ B: nuclear factor-kappa B; NLS: nuclear localization signal; PBMC: peripheral blood mononuclear cells; PBS: phosphate-buffered saline; PCR: polymerase chain reaction; PTP: protein tyrosine phosphatase; RA: rheumatoid arthritis; SELENA-SLEDAI: safety on estrogens in lupus erythematosus national assessment-SLE disease activity index; siRNA: small inhibitory RNA; SLE: systemic lupus erythematosus; SLICC-DI: Systemic Lupus International Collaborating Clinics/American College of Rheumatology Damage Index; SNP: single nucleotide polymorphism; TCR: T cell receptor; Th: helper T.

Competing interests

The authors declare that they have no competing interests.

Authors' contributions

HHC identified the isoforms of PTPN22, examined their expression, and performed the Western and luciferase assays. WT examined the expression of PTPN22 isoforms in the peripheral blood of healthy donors and patients with lupus. JC performed the statistical analysis of Figure 5. KC recruited patients with lupus and participated in the design and draft of this manuscript. ICH conceived the study and participated in the design and draft of this manuscript. All authors read and approved the final manuscript.

Acknowledgements

We thank Tabatha Norton for her help in organizing the clinical samples and data. The statistical analyses of this work was conducted partly with support from Harvard Catalyst | The Harvard Clinical and Translational Science Center (National Center for Research Resources and the National Center for Advancing Translational Sciences, National Institutes of Health Award 8UL1TR000170-05 and financial contributions from Harvard University and its affiliated academic health care centers). The content is solely the responsibility of the authors and does not necessarily represent the official views of Harvard Catalyst, Harvard University and its affiliated academic health care centers, or the National Institutes of Health.

This work is supported by a grant from the Within Our Reach campaign of the American College of Rheumatology and an award from the Department of Defense (W81XWH-11-1-0492).

Author details

¹Division of Rheumatology, Immunology, and Allergy, Department of Medicine, Brigham and Women's Hospital, One Jimmy Fund Way, Boston, MA 02115, USA. ²Harvard Medical School, 25 Shattuck Street, Boston, MA 02115, USA. ³Section of Rheumatology, VA Boston Healthcare System, 150 South Huntington Avenue, Boston, MA 02130, USA.

Received: 28 June 2013 Accepted: 3 January 2014

Published: 17 January 2014

References

1. Cohen S, Dadi H, Shaoul E, Sharfe N, Roifman CM: Cloning and characterization of a lymphoid-specific, inducible human protein tyrosine phosphatase, *Lyp*. *Blood* 1999, **93**:2013-2024.
2. Liu Y, Stanford SM, Jog SP, Fiorillo E, Orru V, Comai L, Bottini N: Regulation of lymphoid tyrosine phosphatase activity: inhibition of the catalytic domain by the proximal interdomain. *Biochem* 2009, **48**:7525-7532.
3. Gyorloff-Wingren A, Saxena M, Williams S, Hammi D, Mustelin T: Characterization of TCR-induced receptor-proximal signaling events negatively regulated by the protein tyrosine phosphatase PEP. *Eur J Immunol* 1999, **29**:3845-3854.
4. Hill RJ, Zozulya S, Lu YL, Ward K, Gishizky M, Jallal B: The lymphoid protein tyrosine phosphatase *Lyp* interacts with the adaptor molecule *Grb2* and functions as a negative regulator of T-cell activation. *Exp Hematol* 2002, **30**:237-244.
5. Ghose R, Shekhtman A, Goger MJ, Ji H, Cowburn D: A novel, specific interaction involving the Csk SH3 domain and its natural ligand. *Nat Struct Biol* 2001, **8**:998-1004.
6. Wu J, Katrekar A, Honigberg LA, Smith AM, Conn MT, Tang J, Jeffery D, Mortara K, Sampang J, Williams SR, Buggy J, Clark JM: Identification of substrates of human protein-tyrosine phosphatase PTPN22. *J Biol Chem* 2006, **281**:11002-11010.
7. Begovich AB, Carlton VE, Honigberg LA, Schrodi SJ, Chokkalingam AP, Alexander HC, Ardlie KG, Huang Q, Smith AM, Spoerke JM, Conn MT, Chang M, Chang SY, Saiki RK, Catanese JJ, Leong DU, Garcia VE, McAllister LB, Jeffery DA, Lee AT, Batliwalla F, Remmers E, Criswell LA, Seldin MF, Kastner DL, Amos CI, Sninsky JJ, Gregersen PK: A missense single-nucleotide polymorphism in a gene encoding a protein tyrosine phosphatase (PTPN22) is associated with rheumatoid arthritis. *Am J Hum Gen* 2004, **75**:330-337.
8. Hasegawa K, Martin F, Huang G, Tumas D, Diehl L, Chan AC: PEST domain-enriched tyrosine phosphatase (PEP) regulation of effector/memory T cells. *Science (New York, NY)* 2004, **303**:685-689.

9. Chang HH, Miaw SC, Tseng W, Sun YW, Liu CC, Tsao HW, Ho IC: **PTPN22 modulates macrophage polarization and susceptibility to dextran sulfate sodium-induced colitis.** *J Immunol* 2013, **191**:2134–2143.
10. Croft DR, Dall P, Davies D, Jackson DG, McIntyre P, Kramer IM: **Complex CD44 splicing combinations in synovial fibroblasts from arthritic joints.** *Eur J Immunol* 1997, **27**:1680–1684.
11. Tolboom TC, Huidekoper AL, Kramer IM, Pieterman E, Toes RE, Huizinga TW: **Correlation between expression of CD44 splice variant v8-v9 and invasiveness of fibroblast-like synoviocytes in an in vitro system.** *Clin Exp Rheumatol* 2004, **22**:158–164.
12. Do HT, Baars W, Borns K, Windhagen A, Schwitzer R: **The 77C->G mutation in the human CD45 (PTPRC) gene leads to increased intensity of TCR signaling in T cell lines from healthy individuals and patients with multiple sclerosis.** *J Immunol* 2006, **176**:931–938.
13. Chang HH, Tai TS, Lu B, Iannaccone C, Cernadas M, Weinblatt M, Shadick N, Miaw SC, Ho IC: **PTPN22.6, a dominant negative isoform of PTPN22 and potential biomarker of rheumatoid arthritis.** *PloS one* 2012, **7**:e33067.
14. Orozco G, Sanchez E, Gonzalez-Gay MA, Lopez-Nevot MA, Torres B, Caliz R, Ortego-Centeno N, Jimenez-Alonso J, Pascual-Salcedo D, Balsa A, de Pablo R, Nuñez-Roldan A, González-Escribano MF, Martín J: **Association of a functional single-nucleotide polymorphism of PTPN22, encoding lymphoid protein phosphatase, with rheumatoid arthritis and systemic lupus erythematosus.** *Arthritis Rheum* 2005, **52**:219–224.
15. Gregersen PK, Lee HS, Batliwalla F, Begovich AB: **PTPN22: setting thresholds for autoimmunity.** *Sem Immunol* 2006, **18**:214–223.
16. Barrett JC, Hansoul S, Nicolae DL, Cho JH, Duerr RH, Rioux JD, Brant SR, Silverberg MS, Taylor KD, Barnada MM, Bitton A, Dassopoulos T, Datta LW, Green T, Griffiths AM, Kistner EO, Murtha MT, Regueiro MD, Rotter JJ, Schumm LP, Steinhardt AH, Targan SR, Xavier RJ, NIDDK IBD Genetics Consortium, Libioulle C, Sandor C, Lathrop M, Belaiche J, Dewit O, Gut I, *et al*: **Genome-wide association defines more than 30 distinct susceptibility loci for Crohn's disease.** *Nat Gen* 2008, **40**:955–962.
17. Chung SA, Criswell LA: **PTPN22: its role in SLE and autoimmunity.** *Autoimmunity* 2007, **40**:582–590.
18. Rieck M, Arechiga A, Onengut-Gumuscu S, Greenbaum C, Concannon P, Buckner JH: **Genetic variation in PTPN22 corresponds to altered function of T and B lymphocytes.** *J Immunol* 2007, **179**:4704–4710.
19. Zhang J, Zahir N, Jiang Q, Miliotis H, Heyraud S, Meng X, Dong B, Xie G, Qiu F, Hao Z, McCulloch CA, Keystone EC, Peterson AC, Siminovitch KA: **The autoimmune disease-associated PTPN22 variant promotes calpain-mediated Lyp/Pep degradation associated with lymphocyte and dendritic cell hyperresponsiveness.** *Nat Gen* 2011, **43**:902–907.
20. Hochberg MC: **Updating the American College of Rheumatology revised criteria for the classification of systemic lupus erythematosus.** *Arthritis Rheum* 1997, **40**:1725.
21. Petri M, Buyon J, Kim M: **Classification and definition of major flares in SLE clinical trials.** *Lupus* 1999, **8**:685–691.
22. Gladman DD, Goldsmith CH, Urowitz MB, Bacon P, Fortin P, Ginzler E, Gordon C, Hanly JG, Isenberg DA, Petri M, Nived O, Snaith M, Sturfelt G: **The systemic lupus international collaborating clinics/American college of rheumatology (SLICC/ACR) damage index for systemic lupus erythematosus international comparison.** *J Rheumatol* 2000, **27**:373–376.
23. Gan H, Lee J, Ren F, Chen M, Kornfeld H, Remold HG: **Mycobacterium tuberculosis blocks crosslinking of annexin-1 and apoptotic envelope formation on infected macrophages to maintain virulence.** *Nat Immunol* 2008, **9**:1189–1197.
24. Kang BY, Miaw SC, Ho IC: **ROG negatively regulates T-cell activation but is dispensable for Th-cell differentiation.** *Mol Cell Biol* 2005, **25**:554–562.
25. Han JW, Zheng HF, Cui Y, Sun LD, Ye DQ, Hu Z, Xu JH, Cai ZM, Huang W, Zhao GP, Xie HF, Fang H, Lu QJ, Xu JH, Li XP, Pan YF, Deng DQ, Zeng FQ, Ye ZZ, Zhang XY, Wang QW, Hao F, Ma L, Zuo XB, Zhou FS, Du WH, Cheng YL, Yang JQ, Shen SK, Li J, *et al*: **Genome-wide association study in a Chinese Han population identifies nine new susceptibility loci for systemic lupus erythematosus.** *Nat Genet* 2009, **41**:1234–1237.
26. Yang W, Shen N, Ye DQ, Liu Q, Zhang Y, Qian XX, Hirankarn N, Ying D, Pan HF, Mok CC, Chan TM, Wong RW, Lee KW, Mok MY, Wong SN, Leung AM, Li XP, Avihingsanon Y, Wong CM, Lee TL, Ho MH, Lee PP, Chang YK, Li PH, Li RJ, Zhang L, Wong WH, Ng IO, Lau CS, Sham PC, *et al*: **Genome-wide association study in Asian populations identifies variants in ETS1 and WDFY4 associated with systemic lupus erythematosus.** *PLoS Gen* 2010, **6**:e1000841.
27. Wang C, Ahlford A, Jarvinen TM, Nordmark G, Eloranta ML, Gunnarsson I, Svenungsson E, Padyukov L, Sturfelt G, Jonsen A, Bengtsson AA, Truedsson L, Eriksson C, Rantapää-Dahlqvist S, Sjöwall C, Julkunen H, Criswell LA, Graham RR, Behrens TW, Kere J, Rönnblom L, Sväven AC, Sandling JK: **Genes identified in Asian SLE GWASs are also associated with SLE in Caucasian populations.** *EJHG* 2012, **21**:994–999.
28. Wang S, Dong H, Han J, Ho WT, Fu X, Zhao ZJ: **Identification of a variant form of tyrosine phosphatase LYP.** *BMC Mol Biol* 2010, **11**:78.
29. Ronninger M, Guo Y, Shchetynsky K, Hill A, Khademi M, Olsson T, Reddy PS, Seddighzadeh M, Clark JD, Lin LL, O'Toole M, Padyukov L: **The balance of expression of PTPN22 splice forms is significantly different in rheumatoid arthritis patients compared with controls.** *Gen Med* 2012, **4**:2.
30. McKinney EF, Lyons PA, Carr EJ, Hollis JL, Jayne DR, Willcocks LC, Koukoulaki M, Brazza A, Jovanovic V, Kemeny DM, Pollard AJ, Macary PA, Chaudhry AN, Smith KG: **A CD8+ T cell transcription signature predicts prognosis in autoimmune disease.** *Nat Med* 2010, **16**:586–591.

doi:10.1186/ar4440

Cite this article as: Chang *et al.*: Altered expression of protein tyrosine phosphatase, non-receptor type 22 isoforms in systemic lupus erythematosus. *Arthritis Research & Therapy* 2014 **16**:R14.

Submit your next manuscript to BioMed Central and take full advantage of:

- Convenient online submission
- Thorough peer review
- No space constraints or color figure charges
- Immediate publication on acceptance
- Inclusion in PubMed, CAS, Scopus and Google Scholar
- Research which is freely available for redistribution

Submit your manuscript at
www.biomedcentral.com/submit



Appendix 4

ProbeSet_ID	Gene_Symbol	Gene_Description	NCBI_ID	FC	P.Value	adj.P.Val	DP	thymocyt stage	2NKT
10552406	Nkg7	natural killer	72310	0.313	0.00261906	0.13285808	218	697	
10606058	Cxcr3	chemokine (C	12766	0.37	5.15E-05	0.03000792	805	2173	
10540679	Il17re	interleukin 1	57890	0.399	6.90E-06	0.01431994	82	206	
10375973	Taf13	TAF13 RA pol	99730	0.404	0.00335518	0.14318114	65	162	
10494978	Ptpn22	protein tyros	19260	0.425	2.10E-05	0.0194828	387	911	
10362275	Samd3	sterile alpha	268288	0.432	0.00129819	0.10956681	96	222	
10475782	Dusp2	dual specifici	13537	0.446	0.00010914	0.04362461	512	1148	
10429114	Tmem71	transmembr:	213068	0.449	0.00017148	0.05409805	143	318	
10361234	Hsd11b1	hydroxysterc	15483	0.45	0.00182601	0.11924606	54	120	
10456378	Chmp1b	chromatin m	67064	0.451	0.00356183	0.14576007	142	315	
10464572	Ndufv1	ADH dehydr	17995	0.468	0.00049841	0.08491749	205	438	
10585599	Imp3	IMP3, U3 sm	102462	0.47	0.00146881	0.11193312	382	813	
10542981	Gmfg	glia maturati	63986	0.488	0.00101795	0.10458232	707	1448	
10532819	Kctd10	potassium ch	330171	0.503	0.00027563	0.06869334	210	418	
10429128	Sla	src-like adapt	20491	0.508	0.00023238	0.06480287	641	1263	
10538126	Gimap4	GTPase, IMA	107526	0.525	8.46E-05	0.03979411	2018	3843	
10538138	Gimap1	GTPase, IMA	16205	0.529	0.00203052	0.12299343	345	651	
10407192	Slc38a9	solute carrier	268706	0.533	0.00199259	0.12291894	89	167	
10439583	Sidt1	SID1 transme	320007	0.536	0.00051007	0.08491749	230	429	
10596119	Cep63	centrosomal	28135	0.544	0.00144795	0.11193312	88	161	
10493435	Gba	glucosidase,	14466	0.562	0.0063323	0.1751537	312	556	
10438109	Ube2l3	ubiquitin-cor	22195	0.567	0.00147781	0.11193312	566	999	
10353475	Eif3m	eukaryotic tr	98221	0.568	0.00505071	0.16442468	324	571	
10573217	Ddx39	DEAD (Asp-G	68278	0.569	0.00151326	0.11254465	272	478	
10570764	Alg11	asparagine-li	207958	0.57	0.00105881	0.10458232	72	126	
10533633	Diablo	diablo homol	66593	0.574	0.00279358	0.13682738	79	138	
10589929	Cmtm6	CKLF-like MA	67213	0.576	0.00143988	0.11193312	630	1094	
10454831	Paip2	polyadenylat	67869	0.582	0.00408822	0.1532128	291	499	
10347193	Atic	5-aminoimid:	108147	0.583	0.00167286	0.11580822	881	1510	
10425461	Adsl	adenylosucci	11564	0.584	0.0052654	0.16747141	482	826	
10503218	Chd7	chromodom:	320790	0.589	0.0003196	0.0735555	537	913	
10506870	Txnbc12	thioredoxin c	66073	0.59	0.00527069	0.16747141	283	480	
10407907	Rala	v-ral simian l	56044	0.603	0.0022663	0.12684229	208	345	
10472846	Pdk1	pyruvate deh	228026	0.604	0.00099687	0.10458232	261	433	
10524668	Coq5	coenzyme Q:	52064	0.605	0.00689663	0.17710181	124	204	
10584835	Mpzl3	myelin prote	319742	0.608	0.00349446	0.14490671	64	106	
10401958	Naca	nascent poly	17938	0.61	0.00292921	0.13783444	1810	2965	
10382300	Map2k6	mitogen-acti	26399	0.618	0.00159959	0.11556987	140	226	
10492997	Etv3	ets variant ge	27049	0.62	0.00444526	0.15788573	311	501	
10488892	Trpc4ap	transient rec	56407	0.625	0.00287947	0.13752875	600	960	
10419073	Tspan14	tetraspanin 1	52588	0.633	0.00236738	0.12826079	511	807	
10427628	Il7r	interleukin 7	16197	0.64	0.00091629	0.10384379	2092	3269	
10431872	Slc38a1	solute carrier	105727	0.651	0.00249876	0.13124764	520	799	
10489004	Nfs1	nitrogen fixa	18041	0.653	0.00593332	0.17194221	222	340	
10403604	Lyst	lysosomal tra	17101	0.654	0.00294659	0.13783444	263	401	
10420413	Lats2	large tumor s	50523	0.655	0.00272935	0.13523036	189	289	
10390691	Nr1d1	nuclear rece	217166	0.663	0.00445582	0.15788573	140	212	
10376312	Larp1	La ribonuclec	73158	0.667	0.00257923	0.13285808	535	801	
10353167	Tram1	translocating	72265	0.676	0.00715937	0.17842582	2212	3273	
10544976	Kbtbd2	kelch repeat	210973	0.682	0.00690016	0.17710181	354	520	
10360794	Fbxo28	F-box proteir	67948	0.687	0.00577022	0.17054356	314	457	
10418247	Pde12	phosphodies	211948	0.689	0.00442243	0.157451	159	231	
10443319	Def6	differentially	23853	0.691	0.00496215	0.16336428	487	705	
10452556	Rab12	RAB12, mem	19328	0.696	0.00406683	0.15284891	104	149	
10481540	Fnbp1	formin bindir	14269	0.724	0.00663847	0.17694121	1075	1485	